Studies on entry events of porcine epidemic diarrhea virus (PEDV)

by

Changin Oh

D.V.M., Konkuk University, Republic of Korea, 2010
M.S., Konkuk University, Republic of Korea, 2015

AN ABSTRACT OF A DISSERTATION

submitted in partial fulfillment of the requirements for the degree

DOCTOR OF PHILOSOPHY

Department of Diagnostic Medicine and Pathobiology
College of Veterinary Medicine

KANSAS STATE UNIVERSITY
Manhattan, Kansas

2020

# Abstract

Coronaviruses are currently the most serious public health concern. The new outbreak of coronavirus disease 2019 (COVID 19) represents a pandemic threat, which led to being declared a Public Health Emergency of International Concern (PHEIC) by the World Health Organization (WHO). The first US outbreak of porcine epidemic diarrhea virus (PEDV) in 2013 and its subsequent spreading to European and Asian countries raised significant economic and public health concerns worldwide. Thus, the development of coronavirus vaccines and therapeutics are urgently needed. Detailed studies on the entry event of coronaviruses may contribute to developing novel therapeutic targets for coronavirus infection.

Most cell culture adapted PEDV replication requires the addition of protease in the medium, but the mechanism of protease in PEDV infection is not well demonstrated. Thus, we examined the role of protease during the entry of PEDV using two different proteases-adapted PEDV US strains, PEDV KD and AA. Our study showed that the activity of protease was required at an early stage of PEDV KD replication, particularly after virus binding to cells. The addition of protease facilitated the escape of viruses from the endosome to the cytoplasm leading to a successful replication. The host endosomal protease and endosomal maturation were also shown to be important in the endosomal escape of PEDV by demonstrating endosomal retention of PEDV KD or AA in the presence of inhibitors of cathepsins or endosomal acidification.

We also explored the roles of the acid sphingomyelinase (ASM)/ceramide pathway in the entry of PEDV. The infection of PEDV 8aa in Vero cells induced ceramide formation mediated by ASM activation. The inhibition of ASM significantly reduced the replication of 8aa by inhibiting viral endosomal escape. These results demonstrated the importance of interactions among viruses, host cells, and proteases during coronavirus entry for successful replication.

During further examination of PEDV and host cell interaction, we observed that protease independent PEDV 8aa infection in Vero cells led to apoptotic cell death. Caspase 6 or 7 cleaved viral nucleocapsid(N) protein at the late stage of the replication while the cells were undergoing the apoptotic process. The caspase-mediated cleavage occurred between $D^{424}$ and $G^{425}$ near the C-terminal of N protein. Addition of a pan-caspase inhibitor to prevent the N protein cleavage significantly increased 8aa replication.

In conclusion, the achievement of endosomal escape is a crucial step in the PEDV life cycle. The addition of the exogenous protease facilitates the endosomal escape of protease adapted PEDV

strains. Activation of ASM/ ceramide pathway led to the efficient replication of protease independent PEDV by facilitating the endosomal escape of the virion. During protease independent PEDV replication, host cells activate caspase-mediated apoptosis as a defense mechanism. These in-depth understandings will provide clues for developing potential PEDV and coronavirus therapeutic targets.

Studies on entry events of porcine epidemic diarrhea virus (PEDV)


by


Changin Oh



D.V.M., Konkuk University, Republic of Korea, 2010
M.S., Konkuk University, Republic of Korea, 2015


A DISSERTATION


submitted in partial fulfillment of the requirements for the degree



DOCTOR OF PHILOSOPHY



Department of Diagnostic Medicine and Pathobiology
College of Veterinary Medicine



KANSAS STATE UNIVERSITY
Manhattan, Kansas



2020



Approved by:

Major Professor
Dr. Kyeong-Ok Chang

# Copyright

# Abstract

Coronaviruses are currently the most serious public health concern. The new outbreak of coronavirus disease 2019 (COVID 19) represents a pandemic threat, which led to being declared a Public Health Emergency of International Concern (PHEIC) by the World Health Organization (WHO). The first US outbreak of porcine epidemic diarrhea virus (PEDV) in 2013 and its subsequent spreading to European and Asian countries raised significant economic and public health concerns worldwide. Thus, the development of coronavirus vaccines and therapeutics are urgently needed. Detailed studies on the entry event of coronaviruses may contribute to developing novel therapeutic targets for coronavirus infection.

Most cell culture adapted PEDV replication requires the addition of protease in the medium, but the mechanism of protease in PEDV infection is not well demonstrated. Thus, we examined the role of protease during the entry of PEDV using two different proteases-adapted PEDV US strains, PEDV KD and AA. Our study showed that the activity of protease was required at an early stage of PEDV KD replication, particularly after virus binding to cells. The addition of protease facilitated the escape of viruses from the endosome to the cytoplasm leading to a successful replication. The host endosomal protease and endosomal maturation were also shown to be important in the endosomal escape of PEDV by demonstrating endosomal retention of PEDV KD or AA in the presence of inhibitors of cathepsins or endosomal acidification.

We also explored the roles of the acid sphingomyelinase (ASM)/ceramide pathway in the entry of PEDV. The infection of PEDV 8aa in Vero cells induced ceramide formation mediated by ASM activation. The inhibition of ASM significantly reduced the replication of 8aa by inhibiting viral endosomal escape. These results demonstrated the importance of interactions among viruses, host cells, and proteases during coronavirus entry for successful replication. During further examination of PEDV and host cell interaction, we observed that protease independent PEDV 8aa infection in Vero cells led to apoptotic cell death. Caspase 6 or 7 cleaved viral nucleocapsid(N) protein at the late stage of the replication while the cells were undergoing the apoptotic process. The caspase-mediated cleavage occurred between $D^{424}$ and $G^{425}$ near the C-terminal of N protein. Addition of a pan-caspase inhibitor to prevent the N protein cleavage significantly increased 8aa replication.

In conclusion, the achievement of endosomal escape is a crucial step in the PEDV life cycle. The addition of the exogenous protease facilitates the endosomal escape of protease adapted PEDV

strains. Activation of ASM/ ceramide pathway led to the efficient replication of protease independent PEDV by facilitating the endosomal escape of the virion. During protease independent PEDV replication, host cells activate caspase-mediated apoptosis as a defense mechanism. These in-depth understandings will provide clues for developing potential PEDV and coronavirus therapeutic targets.

# Table of Contents

# List of Figures

# Acknowledgements

# Dedication

I would like to dedicate this dissertation to my wife, Heeyoung, my daughter and son,

Jungwon and Junghyun, and my parents for all their love and support.

# Chapter 1 - Literature Review and Significance

## 1.1 General introduction and historical perspective of coronavirus

The coronaviruses, enveloped viruses with a positive-strand RNA genome, are within the *Nidovirales* order. The name of order, *Nidovirales*, is derived from the Latin '*nido*' (nest) for their most significant shared feature, the production of multiple 3'co-terminal nested subgenomic messenger RNAs(Brian & Baric, 2005; de Vries, Horzinek, Rottier, & de Groot, 1997).

Coronaviruses were isolated in the early 20th century as the causative agents of several animal diseases such as infectious bronchitis in poultry (Schalk, 1931), transmissible gastroenteritis in swine (Doyle & Hutchings, 1946), and severe hepatitis and neurologic disease in mice(Bailey, Pappenheimer, Cheever, & Daniels, 1949). Later, they were grouped and named by their shapes under electron microscopy, surface protrusions that morphologically resemble the solar corona (Tyrell, 1968). Until 2002, coronaviruses were considered mostly animal viruses although human coronaviruses are responsible for the common cold in the winter season. However, the emergence of two highly pathogenic human coronaviruses changed this perception dramatically. The outbreak of severe acute respiratory syndrome (SARS) in 2002, which was caused by a novel coronavirus, resulted in more than 8000 cases(Stohr & Coll, 2003) with 774 deaths in 27 countries(WHO, 2004). The emergence of SARS coronavirus recognized the first human introduction of a highly pathogenic coronavirus from the animals, related to Himalayan palm civets, raccoon dogs, and wild bats. This SARS outbreak has advanced coronavirus researches and led to a progression of understanding coronavirus epidemiology and pathogenesis. After 10 years, the second zoonotic transmission of coronavirus has occurred. A new coronavirus was isolated from a man in Saudi Arabia who died of acute pneumonia and renal failure(Zaki, van

Boheemen, Bestebroer, Osterhaus, & Fouchier, 2012) and was named Middle East respiratory syndrome coronavirus(MERS-CoV). Currently, the Dromedary camel is considered as a major reservoir host for MERS-CoV and an animal source of human MERS infection. The ongoing MERS epidemic in the Middle East is related to the failure to control camel-to human transmission. Because of the potential healthcare-associated outbreak and the high case-fatality rate, MERS-CoV is a significant public health concern. (Haagmans et al., 2014)

The outbreak of Porcine Epidemic Diarrhea Virus (PEDV) was first reported in England in 1971 and isolated in Belgium in 1978(M. B. Pensaert & de Bouck, 1978; Wood, 1977). Since then it has become an economic concern for the swine industry in Asian countries(C.-h. Kweon et al., 1993; Takahashi, Okada, & Ohshima, 1983). In late 2010, new highly pathogenic PEDV strains emerged in China with high mortality in infected piglets (D. Sun, Wang, Wei, Chen, & Feng, 2016). In April 2013, the first confirmed outbreak of PEDV was reported in the US and subsequently, it spread to most states, Canada and Mexico(Stevenson et al., 2013). Within a year, PEDV caused significant economic problems with approximately 7 million death of piglets(Jung & Saif, 2015) and up to $1.8 million economic loss(Paarlberg, 2014).

The outbreaks of SARS-CoV, MERS-CoV, and Coronavirus disease 2019 (COVID 19) are good examples demonstrating the significance of the Coronaviridae as emerging human viruses. Besides, the introduction of PEDV to the US in 2013 with the huge economic impact demonstrates the importance of the agriculture defense against animal coronaviruses. Therefore, there is a need to study mechanisms of coronaviruses entry, replication and its interaction with the host in order to develop countermeasures for current and future coronavirus outbreaks.
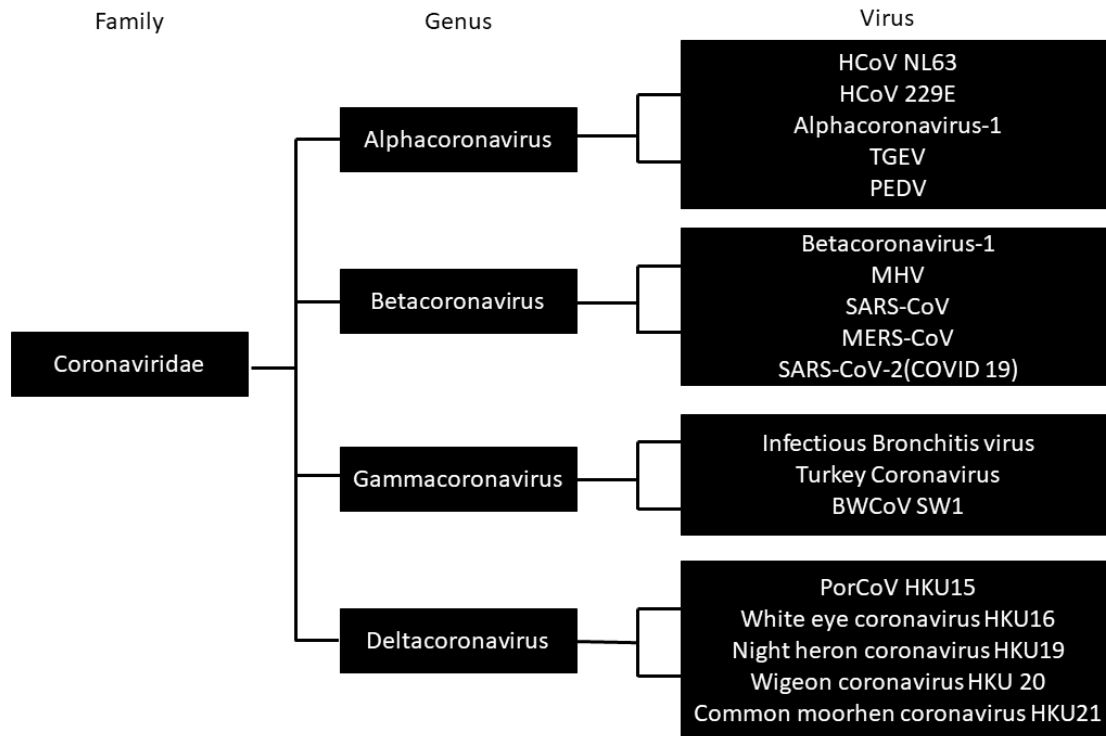
**Figure 1-1. Coronavirus classification according to the ICTV.**

Classification of the Coronaviridae family(R. J. De Groot et al., 2011). Abbreviations: HCoV, human coronavirus, FIPV, feline infectious peritonitis virus, TGEV, transmissible gastroenteritis virus, PEDV, porcine epidemic diarrhea virus, MHV, murine hepatitis virus, SARS-CoV, severe acute respiratory syndrome coronavirus, MERS-CoV, middle east respiratory syndrome virus, BWCoV SW1, beluga whale coronavirus, PorCoV, porcine coronavirus.

## 1.2 Coronavirus taxonomy

The coronaviruses are in the largest group within the *Nidovirales* order including *Coronaviridae*, *Arteriviridae*, and *Rnoiviridae* families. Currently, the subfamily *Coronavirinae* in the family *Coronaviridae* is classified into four genera, *Alphacoronavirus*, *Betacoronavirus*, *Gammacoronavirus*, and *Deltacoronavirus* by phylogenetic clustering (Raoul J de Groot et al., 2012) (Figure 1-1). Based on the evolution model study of coronaviruses, bats are the gene source of *Alpha-*and *Betacoronavirus* and birds are the gene source of *Gamma-* and *Deltacoronavirus* (Woo et al., 2012). The genus *Alphacoronavirus* comprises Alphacoronavirus-1(Feline

coronavirus, Canine coronavirus), Transmissible Gastroenteritis Virus (TGEV), Porcine Epidemic Diarrhea Virus (PEDV) and two human coronaviruses (HCoV 229E and NL63). The genus *Betacoronavirus* contains three highly pathogenic human coronaviruses (SARS-CoV, SARS-CoV-2, and MERS-CoV), Betacoronaivurs-1, Murine coronavirus (Mouse hepatitis virus and Rat coronavirus). The genus *Gammacoronavirus* has been isolated from avian hosts including Avian coronavirus(IBV and Turkey coronavirus) and Beluga whale coronavirus SW1. The genus *Deltacoronavirus* has recently been classified by genomic sequence analysis of both pig and avian isolates including Coronavirus HKU15(Porcine coronavirus HKU15),White-eye coronavirus HKU16, Night heron coronavirus HKU19, Wigeon coronavirus HKU20, and Common moorhen coronavirus HKU21.
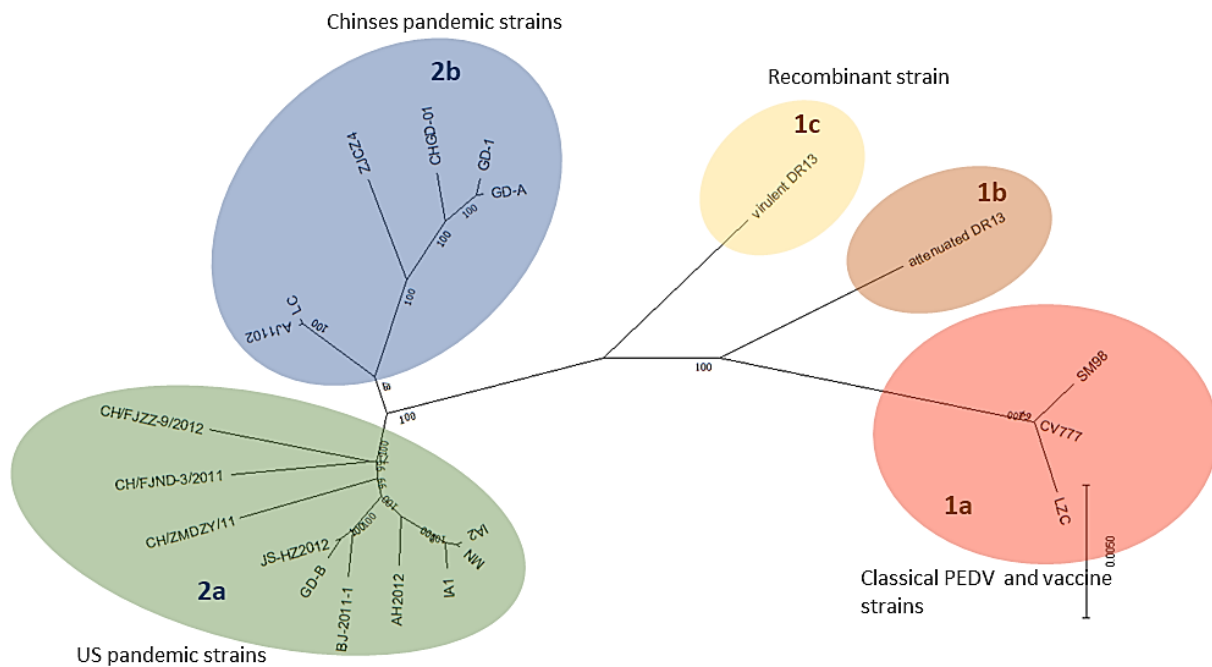


**Figure 1-2. Genotyping of PEDV strains.**

The tree was constructed by the neighbor-joining method, based on full-length genomic nucleotide sequences(Y.-W. Huang et al., 2013).

The PEDV strains are classified into two distinct genogroups, labeled genogroup 1(G1) and genogroup 2(G2), based on the phylogenetic analysis of the full-length of S gene or full PEDV genome(Y. W. Huang et al., 2013; tian, Lv, Xiao, & Li, 2016) (Figure 1-2). The G1 PEDV divides into three subgroups, G1a, G1b, and G1c. The first subgroup G1a contains the prototype CV777 strain, the Chinese LZC strain, and the Korean SM98 strain. Subgroup G1b contains DR13, which is an attenuated vaccine strain from South Korea, and the strains from China, and they share the same genetic signatures including the 8 amino acid deletion in nonstructural protein 3 (nsp3) and the large ORF deletion at the C terminus. Subgroup 1c consists of the virulent DR13 strain isolated in South Korea and CH/S strain isolated in China. The G2 PEDV divides into two subgroups designated G2a and G2b. PEDV strains isolated in the U.S. in 2013 and China in 2011 to 2012 are grouped in the G2a. Interestingly, The U.S. strains share over 99% nucleotide homology with AH2012 (China isolate) suggesting a closed connection between the US and China PEDV strains. The G2b represents the pandemic strains in China. In Asian countries, modified live attenuated vaccines for PEDV genogroup 1 have been widely used to control PEDV(C. H. Kweon, Kwon, Lee, Kwon, & Kang, 1999; Sato et al., 2011; D. Song, Moon, & Kang, 2015; D. S. Song et al., 2007)and are considered an effective control measure due to their ability to prime the immune system in the vaccinated saw. These vaccines, however, may not effectively control subgroup G2a PEDV because of the low genetic homology (10%) of the S1 gene between the G1a and G2a.

## 1.3 Coronavirus genome organization

Coronavirus has a single-stranded positive-sense RNA genome of ~30kb in length, which is the largest among all RNA viruses. It has a standard eukaryotic 5' terminal cap and 3' poly-A tail(D. Yang & Leibowitz, 2015) allowing it to act as an mRNA. The genome contains the basic

genes including the replicase (Rep 1a and 1b), the spike (S), the envelope(E), the membrane (M), and the nucleocapsid protein (N). At the beginning of each structural or accessory genes resides transcriptional regulatory sequences (TRSs) that are necessary for transcription of each subgenomic RNAs. In addition to the basic genes, there are a variable number of genes (up to 8 genes) encoding nonstructural proteins (Masters, 2006). These nonstructural proteins are usually not essential for replication in tissue culture but some have been reported to have important functions in viral pathogenesis(L. Zhao et al., 2012).

## 1.4 Coronavirus structure and structural proteins

Cryo-electron tomography and cryo-electron microscopy studies revealed that coronavirus is a spherical virion with a diameters of approximately 125nm (Barcena et al., 2009; Neuman et al., 2006). The most striking feature of coronavirus virion is the projections of a club-shaped S protein from the surface of the virion (Figure 1-3). Coronavirus contains four major structural proteins including spike (S), membrane (M), envelope (E), and nucleocapsid (N)(Gorbalenya, Enjuanes, Ziebuhr, & Snijder, 2006). The S protein is a large type I transmembrane protein of 150 kDa in size. A single coronavirus particle has about 200 spikes in homotrimer form (Davies & Macnaughton, 1979; Kirchdoerfer et al., 2016a). Coronavirus S protein contains three segments: a large ectodomain, a single-pass transmembrane anchor, and a short intracellular tail. The ectodomain consists of a receptor-binding subunit S1 and a membrane-fusion subunit S2. The S1 subunit is highly variable whereas the S2 subunit is most conserved. N-terminal S1 subunit has glycan-binding domain (N-terminal domain, S1-NTD) and receptor-binding domain (C-terminal domain, S1-CTD) interacting with host receptors. S2 subunit comprises the fusion peptide, heptad repeat 1 and 2 , which is responsible for viral-cellular

membrane fusion(Kirchdoerfer et al., 2016b). Protease cleavage sites are located between S1 and S2 subunits.
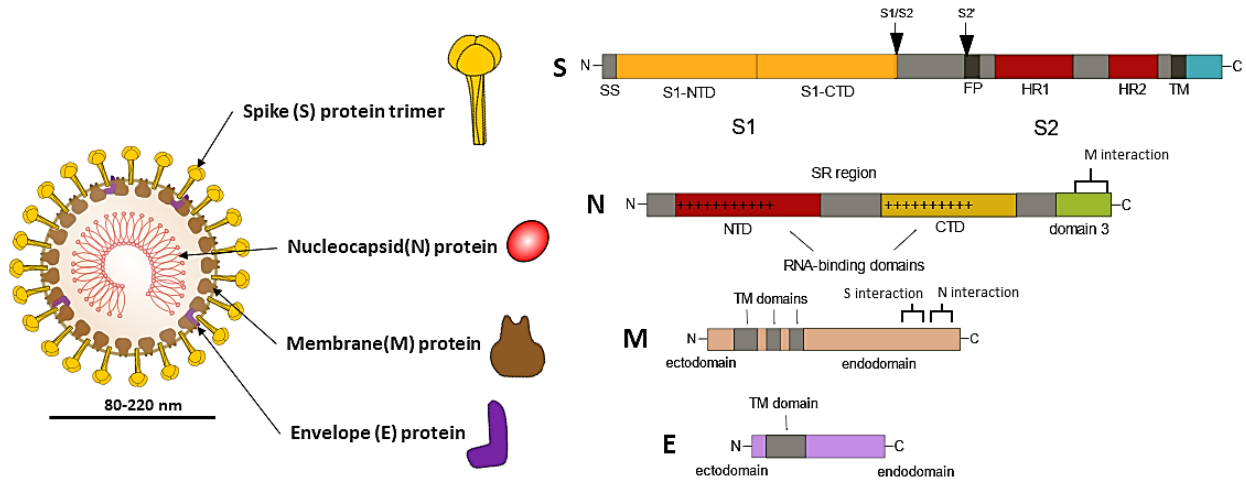


**Figure 1-3. PEDV virion structure.**

Illustration of PEDV virion structure (left) and linear representations of structural proteins(right). N proteins associated with viral RNA genome form ribonucleoprotein (RNP) inside the virion. The RNP is enfolded by viral envelope that is consist of S, E, and M. Abbreviation; SS, signal sequence; NTD, N-terminal domain; CTD, C-terminal domain; S1/S2, S1/S2 cleavage site; S2', S2' cleavage site; FP, fusion peptide; HR, heptad repeat; transmembrane domain, SR region, serine-and arginine-rich tract.

The M protein ranging from 25 to 30 kDa is the most abundant structural protein in coronavirus. The M protein is embedded in the viral envelope by its three transmembrane domains and maintains the shape of the virion envelope. The N-terminal of M protein is a small ectodomain whereas the C-terminal is a larger endodomain that extends 6-8nm into the interior of the virion(Nal et al., 2005) and interacts with S and N proteins. M protein exists as a dimer in the virion in two different conformations: a compact form that promotes greater membrane curvature and an elongated form(Neuman et al., 2011).

The E protein, a small protein of 8 to 12 kDa, is found in a small amount within the virion envelope(Ruch & Machamer, 2012). Even though E protein has a highly diverse sequence, it has

a common architecture: a short N-terminal hydrophilic ectodomain, followed by a large transmembrane region and hydrophilic C-terminal tail. The role of the E protein is the facilitation of viral assembly and release. Ion channel activity of SARS-CoV E protein is not required for viral replication but is required for pathogenesis(Nieto-Torres et al., 2014).

The N protein, 43 to 50 kDa in size, forms the nucleocapsid of coronavirus by binding the RNA genome in a bead-on-a-string configuration(Nelson, Stohlman, & Tahara, 2000). N protein mainly contains two domains, an N-terminal domain (NTD) and a C-terminal domain (CTD). Each domain can bind RNA separately but it has been suggested that interactions of both domains are required for the optimal RNA binding ability (K. R. Hurst, Koetzner, & Masters, 2009). Domain 3, which is located at the C-terminal of N protein, is another functionally distinct region (Kelley R. Hurst et al., 2005). The domain 3 mainly interacts with the carboxy tail of the M protein, and this N-M interaction plays an important role during coronavirus replication(Narayanan, Maeda, Maeda, & Makino, 2000). The N protein also interacts with two specific RNA substrates, the TRSs(Stohlman et al., 1988) and the genomic packaging signal(Molenkamp & Spaan, 1997) and also binds nsp3(K. R. Hurst et al., 2009). These N protein-RNA interactions help package the encapsidated genome into virion by localizing the viral genome to the replicase-transcriptase complex(RTC).

The hemagglutinin-esterase (HE) is encoded in only a subset of the beta-coronaviruses, including murine coronavirus, betacoronavirus 1, and HCoV-HKU1. The HE monomer of 48kDa consists of large N-terminal ectodomain and a very short C-terminal endodomain. This protein binds sialic acids on surface glycoproteins and removes acetyl groups from O-acetylated sialic acid (Desforges, Desjardins, Zhang, & Talbot, 2013). These activities are thought to enhance S protein-mediated cell entry and virus release (Cornelissen et al., 1997).

## 1.5 Coronavirus epidemiology

### 1.5.1 Human coronavirus epidemiology

In humans, coronaviruses cause the common cold and severe respiratory infections (M. Berry, Gamieldien, & Fielding, 2015). Up to now, seven human coronavirus species are identified to infect humans: OC43, 229E, NL63, HKU1, SARS-CoV, MERS-CoV, and SARS-CoV-2 (Fehr & Perlman, 2015; Pyrc, Berkhout, & van der Hoek, 2007; N. Zhu et al., 2020). HCoV-OC43 and HCoV-229E were reported nearly 50 years ago, whereas HCoV-NL63 and HCoV-HKU1 were recently identified after the SARS-CoV outbreak. HCoV-NL63 was first isolated form a 7-month-old baby in early 2004{van der Hoek, 2004 #1360} and HCoV-HKU1 was first identified from 71-year-old man in Hong Kong in 2005{Woo, 2005 #977}. Four viruses (229E, OC43, NL63, and HKU1) mainly cause mild, self-limiting respiratory infection in humans and are endemic in human populations. Based on the study on human coronavirus outbreaks, they can efficiently transmit in human populations through droplets. Serological studies suggest that neutralizing antibodies against HCoV-OC43 or 229E have been detected in about 50% of school-age children and up to 80% of adults(Kenneth McIntosh, 1974).

SARS-CoV initially emerged in 2002-2003 in Guangdong province in the southern part of China and caused severe lower respiratory tract infections with high morbidity and mortality. SARS-CoV was isolated from several exotic animals, including Himalayan palm civets and raccoon dogs in the wet market(Guan et al., 2003). Severe acute respiratory syndrome-related coronaviruses(SARSr-CoV) were also isolated from wild horseshoe bats in China(S. K. Lau et al., 2005; W. Li et al., 2005). These reports suggested that bats are the original source for the virus and the virus adapted to animals sold in the wet market accidentally spilled over to human

9

populations. Human-to-human transmission appeared to occur through direct person to person contact, fomites, droplets and probably aerosols in some instances (Peiris, Guan, & Yuen, 2004). Substantial patient-to-patient variation in the efficiency of transmission was reported. Most patients spread the virus to only one or a few susceptible persons suggesting that virus spread was relatively inefficient. However, through superspreading events, a single patient infected multiple people, but only a few infected individuals were involved in this type of spread(Lipsitch et al., 2003; Riley et al., 2003).

In September 2012, a novel human CoV was first reported from a patient with severe pneumonia and acute kidney injury in the Arabian Peninsula. The etiological agent of the series of highly pathogenic respiratory tract infections was identified and named Middle East Respiratory Syndrome Coronavirus (MERS-CoV) (Zaki et al., 2012). MERS-CoV found in various natural hosts such as the dromedary camels(*Camelus dromedaries*), bats(*Vespertilio superans* and *Neoromicia capensis*), and European hedgehog (*Erinaceus europaeus*)(S. K. P. Lau, Wong, Lau, & Woo, 2017; Z. Zhang, Shen, & Gu, 2016). Human MERS-CoV is considered to be originated from bats because several genetically close coronaviruses were isolated from bats (De Benedictis et al., 2014). Dromedary camels are also considered a natural host and reservoir of MERS-CoV for the following reasons. More than 90% of adult dromedaries in the middle east and Africa are seropositive for MERS-CoV(Mackay & Arden, 2015). The spike protein of the virus isolated from dromedaries has conserved receptor-binding domains for the human DPP4 receptor(Hemida et al., 2014). The serum samples from camel shepherds and slaughterhouse workers showed 15-23 times higher seroprevalence than the general population(M. A. Muller et al., 2015).

The largest MERS outbreak outside of the Middle East occurred in South Korea in May 2015 by a 68-year-old male who was infected during a business trip to Middle East countries. A

total of 186 cases were confirmed, with 38 deaths and 16,752 suspected cases. Similar to the SARS-CoV outbreak, MERS outbreak was mostly nosocomial and super-spreaders played a significant role in the spread of the virus. Furthermore, other problems contribute to the outbreak including late diagnosis, inadequate hospital infection management, and poor communication of the Government(K. H. Kim, Tandi, Choi, Moon, & Kim, 2017). MERS CoV still repeatedly introduced to the human population via direct or indirect contact with infected dromedary camels in the Arabian Peninsula. There is a probability of the MERS-CoV epidemic at any time in any place. All countries should be aware of it and prepare for potential introduction of MERS to prevent a large outbreak.

## 1.5.2 Animal coronavirus epidemiology

In animals, a variety of coronaviruses have been reported since the early 1970s. Infectious bronchitis virus (IBV) causes avian infectious bronchitis in chickens(Cavanagh, 2007). In dogs, canine coronavirus (CCoV) causes respiratory or enteric infection(Erles, Toomey, Brooks, & Brownlie, 2003). Murine hepatitis virus (MHV) can generally cause wide range of diseases in mouse and rat, including hepatitis, enteritis, respiratory infection, and progressive demyelinating encephalitis(Weiner, 1973){Wege, 1982 #1362}. Other animal coronaviruses infect gastrointestinal tract of their respective hosts, for example, transmissible gastroenteritis coronavirus (TGEV) and Porcine epidemic diarrhea (PEDV) in pigs(M. Pensaert, Haelterman, & Burnstein, 1970; M. B. Pensaert & de Bouck, 1978), bovine coronavirus (BCV), and feline coronavirus (FCoV).

### 1.5.3 PEDV epidemiology worldwide and the US

After first isolation of PEDV in 1977(M. B. Pensaert & de Bouck, 1978), PED has remained sporadic or locally endemic in the Netherlands(Pijpers, van Nieuwstadt, Terpstra, & Verheijden, 1993), Hungary(Nagy, Nagy, Meder, & Mocsari, 1996), England(Pritchard, Paton, Wibberley, & Ibata, 1999), and South Korea(S. J. Park, Song, & Park, 2013). In Thailand during 2007 -2008, PEDV outbreaks with a new genotype of PEDV, which is the same clade with the Chinese strain JS-2004-2 was reported (Puranaveja et al., 2009). In 2010, There were reports of severe PED outbreaks in seropositive pigs in different regions of China(W. Li et al., 2012; R.-Q. Sun et al., 2012; J. Wang et al., 2013). These outbreaks were caused by both classical and new PEDV variant strains that are genetically different from the prototype CV777 (W. Li et al., 2012).

In 2013, the first PEDV outbreak o was reported in the US with high mortality in neonatal piglets(Jung & Saif, 2015). The US PEDV strains were closely related to the Chinese strains (China/2012/AH2012) genetically(Y. W. Huang et al., 2013). Other PEDV variants with multiple or a large deletion in S gene were also isolated in the US: PEDV OH/OH851 strains contain multiple deletions and insertions in the S gene, which is close to Chinese strain HBQX-2010 or CH/ZMZKY/11(Vlasova et al., 2014). PEDV TC-PC22A strains have a large 197 amino acid deletion in the N-terminal of the S protein (Oka et al., 2014).

### 1.5.4 Recent coronavirus outbreak – COVID 19

Recently, a novel human coronavirus outbreak was reported in the city of Wuhan, China, on 31 December 2019, with severe respiratory disease possibly associated with exposures to animals in a seafood market (ProMED-mail, 2020). The person-to-person transmission was reported(J. F.-W. Chan et al., 2020). Based on the report of the World Health Organization (WHO)

on April 14th, 2020(WHO, 2020), 1844863 cases were confirmed and on 117021 deaths were reported globally. The official name for the disease the new coronavirus causes is coronavirus disease 2019 (COVID-19). The official name for the new coronavirus is severe acute respiratory syndrome coronavirus 2(SARS-CoV-2), which was named by the International Committee on Taxonomy of Virus. Based on its genetic classification. SARS-CoV-2 forms a sister clade to the SARS-CoV and bat coronaviruses of the species Severe acute respiratory syndrome-related coronavirus, and designated it as SARS-CoV-2{Gorbalenya, 2020 #1359}.

Two probable animal sources of the coronavirus were suggested: a horseshoe bat ( *Rhinolophus affinins*)(P. Zhou et al., 2020) and a Malayan pangolin ( *Manis javanica*)(M. C. Wong, Javornik Cregeen, Ajami, & Petrosino, 2020). The genome of the bat coronavirus (RaTG13) isolated from a horseshoe bat shares a 96% amino acid sequence identity to the SARS-CoV-2 genome. Since this bat coronavirus is known to be most closely related virus genome to COVID 19 virus, it is suggested that SARS-CoV-2 possibly originated from a bat (P. Zhou et al., 2020). However, further analysis of the S protein in RaTG13 and SARS-CoV-2 showed that lower homology (75% nucleotide and 78% amino acid identity) was observed at the receptor binding motif (RBM, 435 to 510), which is responsible for receptor binding. Wong et al. demonstrated that Malayan pangolin is the possible alternate source for the new coronavirus because the RBM of pangolin coronaviruses share an 89% nucleotide and 98% amino acid homologies to SARS-CoV-2(M. C. Wong et al., 2020). However, further researches will be needed with pangolin coronaviruses because this study used two partial pangolin coronavirus genomes instead of a full genome and this partial pangolin coronavirus shows lower sequence identity than RaTG13 bat coronavirus in whole genome level (90.5% amino acid similarity to SARS-CoV-2).

SARS-CoV-2 seem to be easily transmitted from human to human compared to SARS-CoV(N. Chen et al., 2020; Q. Li et al., 2020). Two interesting studies that may be able to explain this easy human to human transmission of the new coronavirus. Recent studies reported that SARS-CoV-2, like SARS-CoV, uses angiotensin-converting enzyme 2(ACE2) as a functional receptor(Hoffmann et al., 2020; P. Zhou et al., 2020) and the virus can use ACE2 of various hosts including human, Chinese horseshoe bat civet, and pig for virus entry(P. Zhou et al., 2020). Interestingly, based on the interaction kinetics of SARS-CoV or SARS-CoV-2 and ACE2, The ectodomain of S protein of SARS-CoV-2 binds ACE2 with approximately 10 to 20 fold higher efficiency than SARS-CoV S binding to ACE2(Wrapp et al., 2020). In addition, the multiple sequence alignment on the S protein of SARS-CoV-2 and closely related coronaviruses showed a "PRRS" region in the S1/S2 cleavage site in the S protein of SARS-CoV-2, which creates a furin recognition site. This PRRS site is not present in SARS-CoV and other three closely-related bat CoV, and pangolin CoV genomes. It has been reported that the presence of the cleavage site in the viral envelop glycoprotein may attribute to pathogenesis as shown in the influenza virus and IBV. (J. Chen et al., 1998; J. Cheng et al., 2019).

The World Health Organization (WHO) has declared the outbreak of COVID 19 a global pandemic(Cucinotta & Vanelli, 2020). This is a typical example of a CoV spillover from animals to the human population and that can repeatedly occur due to the increasing interaction of humans and wild animals (de Wit, van Doremalen, Falzarano, & Munster, 2016).


## 1.6 Immune responses and pathogenesis in coronavirus infections

Coronaviruses can cause  respiratory, enteric, or central nerve system (CNS) infection in humans and many species of animals. In humans, coronaviruses are the etiological agent of the

common cold. The prototype human coronaviruses, 229E and OC43 usually cause mild respiratory infection with sneezing, sore throat, malaise, headache, and nasal discharge with 2-5 days of incubation period (Monto, 1974; Tyrrell, Cohen, & Schlarb, 1993). However, there is no serological cross-reactivity between them(K. McIntosh, Dees, Becker, Kapikian, & Chanock, 1967). Because of the lesser impact on society and the economy, little is known about the pathogenesis of these four human coronaviruses.

### 1.6.1 SARS-CoV pathogenesis

SARS-CoV was the first human coronavirus that caused serious illness(Rota et al., 2003). SARS-CoV infects both alveolar epithelial cells to cause a severe lower respiratory tract infection and other organs (kidney, liver, and small intestine) (Y. L. Lau & Peiris, 2005). Patients who died from SARS-CoV infection had nonspecific pathological findings. Initially, cells in the upper airway were infected, leading to destroying cells but relatively little epithelial cell damage. After the virus rapidly spread to the alveoli, however, diffuse alveolar damage characterized by pneumocyte desquamation, alveolar edema, inflammatory cell infiltration, and hyaline membrane formation were observed. Eventually, pathologic signs of acute lung injury (ALI) and, in the most severe cases, acute respiratory distress syndrome (ARDS) were developed(N. Lee et al., 2003). Importantly, SARS-CoV infects macrophages and dendritic cells causing an abortive infection in these cells(Law et al., 2005; Spiegel, Schneider, Weber, Weidmann, & Hufert, 2006). Infected dendritic cells release several proinflammatory cytokines and chemokines (S. K. Lau et al., 2005). Lymphopenia and neutrophilia were detected in infected patients, which were likely to be primarily cytokine driven. During the 2002 endemic, SARS-CoV infection showed age-dependent severity. In patients younger than 60 years of age, the estimated case fatality was 6.8%. However,

that of older patients was 43%(Donnelly et al., 2003). Increased disease severity in an age-dependent manner was also observed in the animal experiment (Roberts et al., 2005). The aged mice experimentally infected with the original human isolate showed pathologic signs of ALI, increased levels of proinflammatory chemokines and cytokines, and diminished T-cell responses, suggesting that immune dysregulation contributes to severe disease.

### 1.6.2 MERS-CoV pathogenesis

MERS-CoV infection causes a wide clinical spectrum from asymptomatic infection and upper respiratory tract illness to severe pneumonia and multiorgan failure(Assiri et al., 2013). About one-third of infected patients showed gastrointestinal symptoms such as diarrhea and vomiting. Recent post-mortem histopathological studies reported multi-organ failure including pulmonary diffuse alveolar damage, necrotizing pneumonia, acute kidney injury, portal and lobular hepatitis, and myositis with muscle atrophic changes. Viral particles were localized in not only the pulmonary but also extrapulmonary tissues such as pulmonary macrophage, pneumocytes, renal proximal tubular epithelial cells and macrophages infiltrating the skeletal muscles (Alsaad et al., 2018). MERS-CoV can infect not only human respiratory epithelial cells but also immune cells including macrophages, T-cells, and immature monocyte-derived dendritic cells (J. Zhou, Chu, Chan, & Yuen, 2015). As similar to SARS-CoV, the infection of human macrophages and dendritic cells induced the expression of pro-inflammatory cytokines/chemokines (Cong et al., 2018; J. Zhou et al., 2015). T-cells can be recruited to the site of infection by type-I IFN stimulated secretion of IL-10 and CXCL10. However, the expression of these cytokines is uncontrolled and persistent. The expression of IFN-γ and IL-12, which are required for the T helper cell activation, were inhibited (Ying, Li, & Dimitrov, 2016). Also, MERS-CoV can infect T cells and subsequently

induce both intrinsic and extrinsic apoptosis. These findings could partly explain the lymphopenia observed in MERS-CoV infected patients(H. Chu et al., 2016). Thus, the sequestered T cells in the infected tissue failed to eliminate the virus.

### 1.6.3 Animal coronavirus pathogenesis

Studies of the animal coronaviruses including the Murine Hepatitis Virus(MHV), Transmissible gastroenteritis virus (TGEV), Infectious bronchitis virus (IBV) and Feline infectious peritonitis virus (FIP), have contributed the understanding of coronavirus pathogenesis.

### 1.6.3.1 Murine Hepatitis Virus

MHV is the most extensively studied coronavirus until the emergence of SARS CoV. It causes enteric, hepatic, and neurologic infections to susceptible rodent strains. Each strain of murine coronavirus, all of which use the same host cell receptor(mCEACAM1) for entry (Williams, Jiang, & Holmes, 1991), shows different organ tropisms and levels of virulence. The enteric strains of MHV circulate in animal research facilities(Pritchett-Corning, Cosentino, & Clifford, 2009) and they are generally asymptomatic but may affect experimental results by modulating the host immune response. The neurotropic JHM and A59 strains infect primarily the brain and thus provide animal models for multiple sclerosis (MS). MHV-2 and MHV-3 infect both the liver and the CNS. The MHV-3 strain causes acute hepatitis in susceptible strains of mice. Infection of MHV-3 to macrophages results in the up-regulation of several proinflammatory cytokines, including fibrinogen-like protein 2(FGL2), a transmembrane procoagulant molecule(Marsden et al., 2003), resulting in consequent disseminated intravascular coagulation (DIC), hepatic hypoperfusion, and necrosis. Unlike most other strains of MHV, MHV-3 directly

infects T and B cells and causes lymphocyte apoptosis and lymphopenia(Lamontagne, Descoteaux, & Jolicoeur, 1989).

### 1.6.3.2 Feline Enteric Coronavirus and Feline Infectious Peritonitis virus

Feline enteric coronavirus (FeCoV) generally causes mild or asymptomatic infection in domestic cats. Two serotypes of FeCoV were identified; serotype II strain was emerged by recombination of serotype I FeCoV with canine coronavirus in co-infected animals(Herrewegh, Smeenk, Horzinek, Rottier, & de Groot, 1998). During persistent infection in some cats with FeCoV, mutations in the virus leads to the development of a virulent strain of FeCoV called feline infectious peritonitis virus(FIPV). This FeCoV to FIPV transition appears to involve positive selection for mutants that can replicate in macrophage, which is possibly mediated by mutations in the S protein or the ORF3b(Chang, Egberink, Halpin, Spiro, & Rottier, 2012; Rottier, Nakamura, Schellen, Volders, & Haijema, 2005; Vennema, Poland, Foley, & Pedersen, 1998). Infected macrophages help FIPV spread throughout the body and lead to a pyogranulomatous reaction that causes peritonitis and serositis. The clinical disease of FIPV is characterized by peritonitis, immunosuppression, weight loss, and death. FIP shows the recurrent patterns of fever and lymphopenia accompanied by repeated FIPV replication (de Groot-Mijnes, van Dun, van der Most, & de Groot, 2005). Antibodies against S protein were shown to enhance FIPV infection of macrophages that was mediated by virus entry through Fcγ receptors(Vennema et al., 1990) and contribute type III hypersensitivity vasculitis(Pedersen, 2009). The potential occurrence of the antibody-enhanced disease has made FIP vaccine development difficult.

### 1.6.3.3 Porcine epidemic diarrhea virus

The clinical symptoms of PEDV infection are watery diarrhea and vomiting accompanied by anorexia and depression. PEDV infection can occur in swine of any age but the disease outcome usually varies by age. Piglets under 1 week of age severely affect by PEDV infection with watery diarrhea and vomiting followed by extensive dehydration and electrolyte imbalance leading to death. Mortality rate PEDV in young piglets reaches up to 100%(Shibata et al., 2000). However, older pigs recover the disease by themselves. PEDV infects the villous epithelial cells in the small intestine and destroys target enterocytes leading to villous atrophy and vacuolation. This loss of villi hinders digestion and absorption of nutrients and electrolytes, thereby causing watery diarrhea in piglets(Ducatelle, Coussement, Debouck, & Hoorens, 1982).

## 1.7 Coronavirus replication

### 1.7.1 Coronavirus entry

The interaction of the S protein with specific cellular receptors on the cell surface is the initial step of coronavirus infection. After binding to the receptor, coronavirus entry can take place directly at the cell surface or at the endosome after internalization via endocytosis. During the coronavirus entry, the S protein plays two important roles: a receptor binding and a viral-cellular membrane fusion. The S1 subunit of S protein consists of two major domains, S1-NTD and S1-CTD, which are responsible for sugar and receptor binding, respectively (Du et al., 2013; Godet, Grosclaude, Delmas, & Laude, 1994; H. Hofmann et al., 2005; H. X. Lin et al., 2008; S. K. Wong, Li, Moore, Choe, & Farzan, 2004). Sugar binding by S1-NTD brings the virus in close position to the cell surface membrane. The S1 subunit sits on top of the S2 stalk and fusion peptide is hidden within the trimer interface, all of which protect S protein from undergoing a conformational change in an inappropriate location (Figure 1-4A step1). The conformational change of the S protein

requires additional triggers including receptor binding, proteolytic cleavage, and pH acidification, but the requirement of triggers varies among coronavirus strains(Belouzard, Millet, Licitra, & Whittaker, 2012; Kirchdoerfer et al., 2016a; J. E. Park et al., 2016). After proteolytic activation, the S1 subunit detaches from the S2 subunit (Figure 1-4A step 3) and then the S2 subunit undergoes a rod-like structure (post-fusion structure) with the six-helix bundle, leading to the injection of fusion peptide into target membrane (F. Li et al., 2006) (Figure 1-4 step 4). Then, the dramatic refolding, the inversion of the C-helix packs the grooves of the N-terminal trimeric coiled-coils forming a six-helix bundle (6HB), brings viral and cellular membranes nearby facilitating membrane fusion(Bosch, van der Zee, de Haan, & Rottier, 2003) (Figure 1-4A step 5). This fusion leads to the delivery of the viral genome into the cytoplasm(Figure 1-4A step 6.).
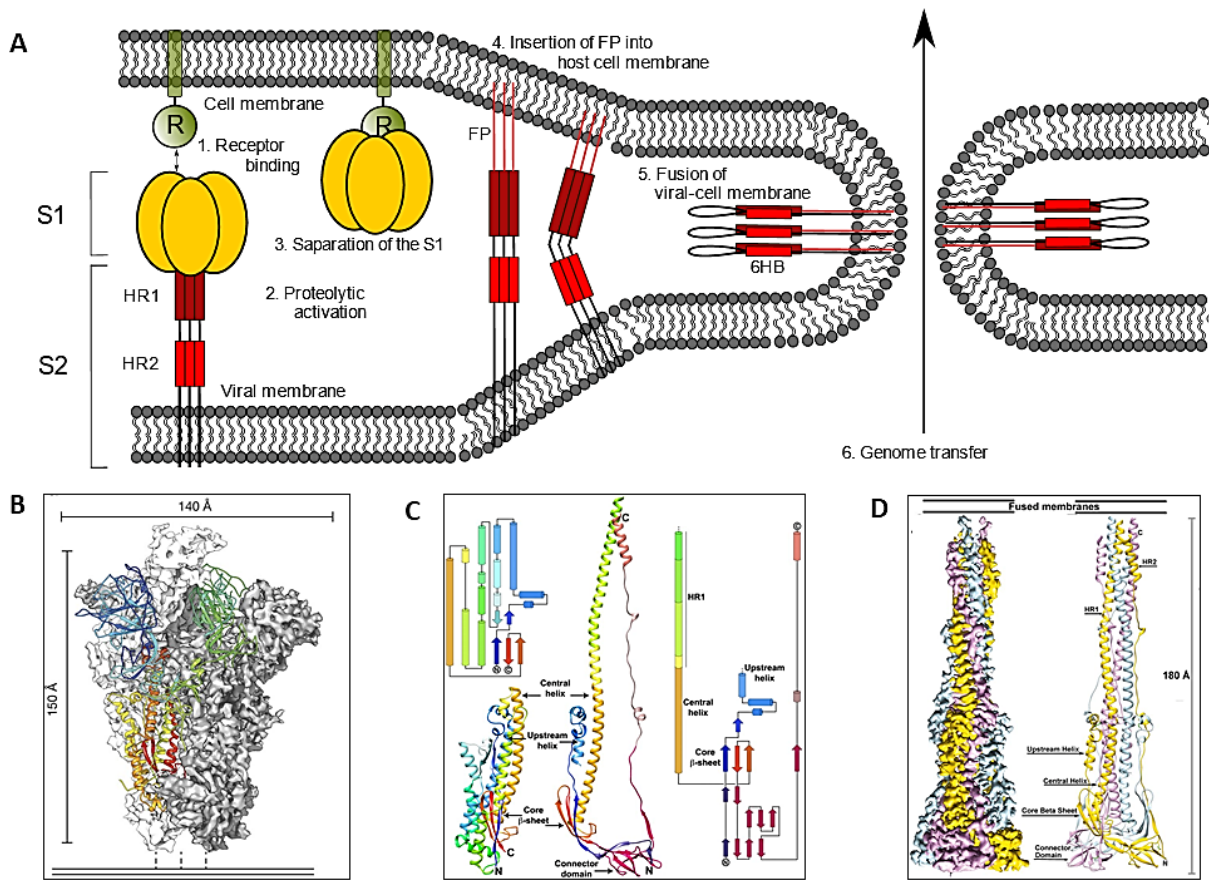
**Figure 1-4. Coronavirus S protein mediated membrane fusion model.**

(A) The Spike protein trimer on the virion surface interacts with the host functional receptor (1). The protease cleaves S protein (2). The S1 subunit separates from S2 (3). The fusion peptide is inserted into the host membrane (4). The S2 subunit folds into post-fusion conformation, the six helix bundle (6HB) (5). Viral-cellular membrane fusion forms a fusion pore to allow entry of viral genome(6)(Tripet et al., 2004). Cryo-EM Structure of HKU1 pre-fusion spike trimer ectodomain(Kirchdoerfer et al., 2016a) (B). Conformational changes of S protein during the fusion. Ribbon and topology diagrams of the S2 subunit in the pre- and postfusion conformation (C). Cryo-EM structure of the MHV S2 postfusion machinery(D) (Walls et al., 2017).

**1.7.1.1 S protein – host receptor interactions**

The binding of coronavirus S protein with its functional receptor is one of the most important determinants of the coronavirus host range. Coronaviruses recognize a wide range of receptors (F. Li, 2015). Many alphacoronaviruses such as Feline Coronavirus (FCoV), Canine Coronavirus (CCoV), Transmissible gastroenteritis virus (TGEV), and HCoV-229E use aminopeptidase N (APN) of their respective host as a receptor(Delmas et al., 1992; Yeager et al., 1992). APN (CD13) is a zinc-binding protease on the cell surface that is expressed on respiratory and enteric epithelial cells. Mutational and inhibitor studies have documented that the enzymatic activity of APN is not necessary for viral attachment and entry. Another alphacoronavirus, PEDV, is also known to use porcine APN as a functional receptor(B. X. Li, Ge, & Li, 2007) but there have been controversial reports. PEDV efficiently replicates in African green monkey kidney cells(Vero cells), which do not express APN(M. Hofmann & Wyler, 1988; Shirato, Matsuyama, Ujike, & Taguchi, 2011). APN knockout Vero cells and porcine ST cells, or APN-deficient pigs were still susceptible to PEDV infection(Ji, Wang, Zhou, & Huang, 2018; W. Li, Luo, et al., 2017; Whitworth et al., 2019).

The receptor for some Betacoronaviruses, SARS-CoV, SARS-CoV-2 and HCo-NL63, is angiotensin-converting enzyme 2 (ACE2). ACE2 is a zinc-binding carboxypeptidase involved in the regulation of cardiac functions and blood pressure existed on the epithelial cell surface of the lung and the small intestine(H. Hofmann et al., 2005; W. Li et al., 2003). Based on structural analysis, both receptor binding domains of SARS-CoV and HCoV-NL63 bind to the same motifs on ACE2(Wu, Li, Peng, & Li, 2009) even if their RBD didn't have sequence and structural homology. This result suggests that they evolved independently to bind to the same motif on the ACE2 surface. The MERS-CoV S protein binds to dipeptidyl-peptidase 4(DPP4) to gain entry into

human cells(Raj et al., 2013). DPP4 is a serine exopeptidase, which expresses in many cell types and organs. S1-CTD of MERS-CoV directly interacts with the 11 critical residues within the β-propeller domain of DPP4. Those residues are conserved in MERS-CoV susceptible species (camelids, primates, and rabbits) but not conserved in non-susceptible species (hamsters, ferrets, or mice)(Bosch, Raj, & Haagmans, 2013; de Wit et al., 2013; Haagmans et al., 2015; van Doremalen et al., 2014) suggesting that DPP4 can determine the host range of MERS-CoV. The functional receptor for MHV is murine carcinoembryonic antigen-related cell adhesion molecule 1 (mCEACAM1) (Williams et al., 1991), and CEACAM1-knockout mice are completely resistant to the infection of the A59 strain of MHV(Hemmila et al., 2004). The functional receptor for a gammacoronaviruses, such as Infectious Bronchitis Virus (IBV) and Beluga Whale coronavirus SW1, and deltacoronaviruses has not been identified yet.

Coronaviruses use sialic acid as a receptor or a coreceptor that mostly interacts with S1-NTD. Human coronavirus OC43 (HCoV-OC43) and bovine coronavirus (BCoV) provide examples of acetylated sialic acid as a coronavirus functional receptor(Schultze, Gross, Brossmer, & Herrler, 1991; Vlasak, Luytjes, Spaan, & Palese, 1988). Interestingly, the similarity of the sugar-binding sites in BCoV S1-NTD with human galectins suggests that ancestral coronaviruses might steel a host galectin gene and insert it into the 5' end of their spike gene, which becomes S1-NTD(F. Li, 2015). The sialic acid is used as a co-receptor providing the primary attachment of viruses on the cell surface. TGEV and PEDV can bind both bovine and porcine mucins, with a preference for N-glycolylneuraminic acid or N-acetylneuraminic acid, respectively(Chang Liu et al., 2015; Schultze et al., 1996). A recent publication demonstrated that MERS-CoV S1-NTD uses sialic acid as a coreceptor and depletion of cell surface sialic acids by neuraminidase treatment inhibited MERS-CoV entry on Calu-3 cells(W. Li, Hulswit, et al., 2017). IBV also binds to sialic

acid with a preference for alpha 2,3-linked sialic acid and neuraminidase treatment made susceptible cells resistant to IBV-Beaudette strain(Winter, Schwegmann-Wessels, Cavanagh, Neumann, & Herrler, 2006). Heavily glycosylated S protein is able to interact with host lectins such as DC/L-SIGN, which has been reported to be an alternative receptor for SARS-CoV and HCoV-229E(Jeffers, Hemmila, & Holmes, 2006; Jeffers et al., 2004). Type 1 and 2 FIPVs exploit DC-SIGN as a coreceptor or an alternative receptor to feline APN, respectively, which may participate in the interaction with immune cells to achieve systemic infection. (Regan, Ousterout, & Whittaker, 2010; Regan & Whittaker, 2008).

### 1.7.1.2 Proteolytic activation of S protein

The cleavage of S protein by proteases is an indispensable process to make S protein fusion competent form (S. Masters Paul & Stanley, 2013). Two major cleavage sites are located at the junction of the S1 and the S2 subunit (S1/S2) and just upstream of the fusion peptide(S2'). The cleavage of those sites by protease(s) results in dissociation of the S1 subunit and exposure of the fusion peptide (Belouzard et al., 2012). Some coronaviruses such as MERS-CoV, IBV, and MHV, their S proteins are cleaved by furin or related proprotein convertases during virus biogenesis (J. E. Park et al., 2016). There have been several reports of the significant role of furin cleavage in virus replication. The presence of furin inhibitors interfered with infection and syncytia formation of the IBV Beaudette strain. Mutation or deletion of the S1/S2 cleavage site in Beaudette S protein delayed virus propagation but does not abolish syncytia formation(Yamada & Liu, 2009). Introduction of a mutation H715D in the spike protein of MHV-A59 strongly impaired the cleavage of the protein and delayed cell-cell fusion(Leparc-Goffart et al., 1997). On the other hand,

the S proteins of many other coronaviruses remain uncleaved in mature virions and require an encounter with protease(s) at the entry step of infection.

Depending on the location of proteases and S protein interaction, coronaviruses entry pathways are divided into be two different ways: fusion at the cell surface (nonendosomal) or fusion at the endosomal membrane (endosomal) (Shutoku Matsuyama, Makoto Ujike, Shigeru Morikawa, Masato Tashiro, & Fumihiro Taguchi, 2005; Simmons et al., 2005; Simmons et al., 2004). In the nonendosomal pathway, uncleaved S protein attachs to cell surface receptor and it is cleaved by an exogenous protease such as trypsin, thermolysin, and elastase(Shutoku Matsuyama et al., 2005; Simmons et al., 2004) or transmembrane protease, all of which allow the virus infection insensitive to lysosomotropic agents. (Glowacka et al., 2011; Matsuyama et al., 2010; Shulla et al., 2011). In the endosomal pathway, the virus particle enters via receptor-mediated endocytosis without interactions of proteases, and then S protein is cleaved by the endosomal proteases, leading to membrane fusion. These two modes of entry, the endosomal or nonendosomal, may be easily shifted by the addition of a protease or mutations on S protein(Gallagher, Escarmis, & Buchmeier, 1991). For example, SARS-CoV enters cells via pH- and receptor-dependent endocytosis without suitable protease (H. Wang et al., 2008) and participation of endosomal cathepsins was required (I. C. Huang et al., 2006). However, in the presence of trypsin in media or infected on TMPRSS2 expressing cells, SARS-CoV enters at the cell surface and is unresponsive to cathepsin inhibitors or lysosomotropic agents. HCoV-229E enters host cells via virus-cell membrane fusion on the cellular surface in the presence of extracellular protease or TMPRSS2, but the virus fuses with endosomal membrane in the absence of them (Bertram et al., 2013; Kawase, Shirato, Matsuyama, & Taguchi, 2009a; Shirato, Kanou, Kawase, & Matsuyama, 2017). Proteolytic activation, cathepsin dependence, and bypass this

dependence by the addition of exogenous protease are also observed with MHV-2, which has an uncleaved S protein (Qiu et al., 2006). PEDV has a unique characteristic that field isolation and efficient replication of most PEDV strains require the presence of exogenous trypsin in culture medium (W. Li, van Kuppeveld, He, Rottier, & Bosch, 2016). The addition of protease or endosomal cathepsins facilitates PEDV escape from the endosome to the cytoplasm(Oh, Kim, & Chang, 2019).
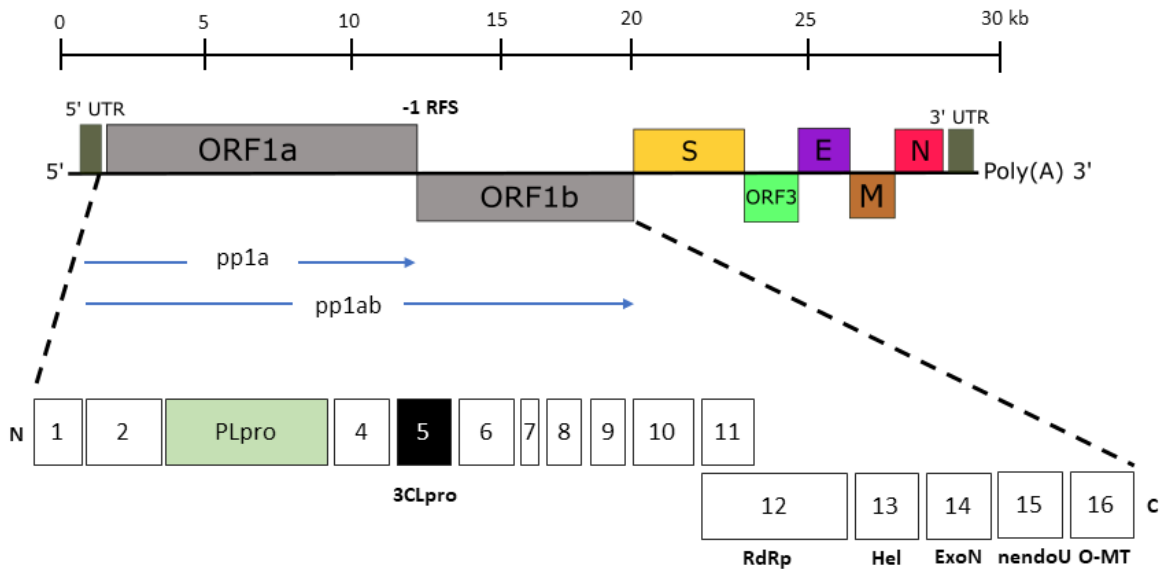


**Figure 1-5. Schematic representation of PEDV genome organization.**
PEDV has approximately 28kb genome with the 5'-cap and 3' polyadenylated tail. The genome contains replicase ORF 1a and 1b followed by the structural protein genes, S, orf3, E, M and N. Two large ORF1a and 1b are translated into polyprotein(pp)1a and then pp1ab following -1 ribosomal frameshift(RFS). The polyproteins are cleaved by the papain-like protease (nsp3) and by 3C-like protease (nsp5) to generate 15 nonstructural proteins(nsps). ORF, open reading frame; RFS, S, spike protein; E , envelope protein; M, membrane protein; N, nucleocapsid protein; PLpro, papain-like protease; RdRp, RNA dependent RNA polymerase; Hel, helicase; ExoN, exonuclease; NendoU, nodovirus uridylate-specific endoribonuclease; O-MT, ribose-2'-O-methyltransferase.

## 1.7.2 Expression of the replicase-transcriptase complex

After the trafficking of the viral genome to the cytoplasm, the next step is the translation of the genomic RNA to the viral replicase. The replicase gene is composed of two large ORFs, rep1a and rep1b, which occupy two-thirds of the genome coding two co-terminal polyproteins, pp1a and pp1ab (Figure 1-5). Mostly, the ribosome unwinds the pseudoknot and continues translation until it reaches the rep1a stop codon. Occasionally the ribosome is blocked by the pseudoknot and paused on the slippery sequence, shifting the reading frame by moving back one nucleotide and extend translation into rep1b (Baranov et al., 2005). Polyproteins pp1a and pp1ab are composed of the nonstructural proteins(nsps), nsp1-11 or nsp1-16, respectively. Proteolytical processing of these polyproteins by virus-encoded two proteases, the papain-like proteases(PLpro) encoded in nsp3 and the main protease or 3C-like protease(Mpro or 3CLpro) encoded in nsp5 generate the individual nsps (Ziebuhr, Snijder, & Gorbalenya, 2000). The PLpro cleaves the cleavage sites at nsp1/2, nsp2/3, and nsp/3/4. The 3CLpro cleaves the remaining 11 cleavage sites.

Next, the nsps assemble into the replicase-transcriptase complex (RTC) to create a suitable environment for RNA replication and transcription of the subgenomic RNAs. The nsps play crucial roles in RNA replication including nsp12 encodes the RNA-dependent RNA polymerase (RdRp) domain, nsp13 encodes the RNA helicase domain and RNA 5'-triphosphatase activity, nsp14 encodes the exoribonuclease(ExoN) and N7-methyltransferase activity, nsp16 encodes 2'-O-methyltransferase activity. Other roles of the nsps, such as blocking innate immune responses (nsp1, nsp16, nsp3) have been identified with other largely unknown functions. Only the *Nidovirales* has ribonucleases nsp15-NendoU and nsp14-ExoN activities, all of which are considered genetic marker(Snijder et al., 2003).

### 1.7.3 Virus replication and transcription

The assembly of the RTC provides an environment for synthesis of both genomic and sub-genomic RNAs(sgRNAs). Each sgRNA consists of a leader RNA joined to a body RNA, which is identical to the 5' and the 3' end of the genome with 5'cap and 3'polyadenylated tail. The fusion of the leader RNA to body RNAs occurs at transcription-regulating sequence(TRS) during the discontinuous synthesis of negative-strand RNA(Sawicki, Sawicki, & Siddell, 2007). The current model proposes that the RdRp pauses at any one of the TRS sequences; following this pause the RdRp either continues elongation to the next TRS or it switches to amplifying the leader sequence at the 5'end of the genome guided by the complementarity of the leader TRS. These processes generate a 3'nested set of sgRNAs, the most unique feature of the order *Nidovirales*.

### 1.7.4 Assembly and Release

Following replication and RNA synthesis, sgRNAs serve as mRNAs for the viral proteins. Genomic RNAs and viral proteins are translocated into the endoplasmic reticulum(ER) and move along the secretory pathway into the endoplasmic reticulum-Golgi intermediate compartment (ERGIC)(Krijnse-Locker, Ericsson, Rottier, & Griffiths, 1994; Tooze, Tooze, & Warren, 1984). N protein and viral genome complex bud into membranes of the ERGIC that contain viral structural proteins and eventually mature virions are formed (de Haan & Rottier, 2005). Most protein-protein interactions required for assembly of coronavirus is mediated by the M protein. The interaction of M and E is sufficient to form VLPs suggesting that two proteins play together to form coronavirus envelop (Bos, Luytjes, van der Meulen, Koerten, & Spaan, 1996). The C-terminal of M protein also binds to the C-terminal domain 3 of N, and this interaction promotes the completion of virion assembly(Kelley R. Hurst et al., 2005). The S protein is not required for

assembly but the S protein trafficking to the ERGIC and S-M interaction is critical for its incorporation into virions(Siu et al., 2008). In several coronaviruses, S proteins that do not participate in virion assembly move to the cell surface where they mediate cell-cell fusion. This leads to the giant cell formation that allows the virus to spread without being detected or neutralized by virus-specific antibodies. After assembly, the newly synthesized virions are transported to the cell surface in vesicles and released by exocytosis.

## 1.8 Vaccine approaches against coronaviruses

### 1.8.1 Animal coronavirus vaccine

Vaccines of animal coronaviruses have been widely used to prevent serious disease development in animals, but their efficiencies are variable. IBV vaccines are shown to be effective to protect IBV infection(Ladman et al., 2002). The efficacy and duration of Canine CoV vaccines vary under field conditions due to the low efficacy of an inactivated vaccine and high rate of serious adverse reactions of a modified-live vaccine(Pratelli et al., 2003; Pratelli et al., 2004). Since the PED outbreaks have been a major economic loss in Asia, several live-attenuated or inactivated PEDV vaccines have been developed and widely used. These vaccines have been reported to be effective with lower virulence and minimum histopathological changes, but they did not provide complete protection from PEDV infection (D. S. Song et al., 2007; Usami, Yamaguchi, Kumanomido, & Matsumura, 1998). The feline infectious peritonitis (FIP) vaccine is known to be deleterious to the health of the cat(Weiss & Scott, 1981) because FIPV infection is greatly enhanced in the presence of antibodies. There have been several efforts to develop efficient FIP vaccines using recombinant viruses(Balint, Farsang, Szeredi, Zadori, & Belak, 2014) or T-helper

1 epitope with CpG-oligodeoxynucleotides as adjuvants(Takano, Tomizawa, Morioka, Doki, & Hohdatsu, 2014) but their protective effects were questionable.

## 1.8.2 Human coronavirus vaccine

Currently, no vaccines are available for any human coronavirus infection. Since SARS-CoV and MERS-CoV outbreaks, various vaccine candidates have been designed and studied. In SARS-CoV, the inactivated virus might be used as the first-generation vaccine because it is easy to generate whole killed virus particles. Mice immunized with several inactivated SARS-CoVs developed humoral and cell-mediated immune responses(Takasuka et al., 2004; Tang et al., 2004; C. H. Zhang et al., 2005). Several attempts of expressing SARS-CoV structural proteins by viral vectors were reported. The live attenuated bovine parainfluenza virus type 3 (BHPIV3), recombinant live attenuated modified vaccinia virus (rMVA-S), or adenovirus could induce neutralizing antibodies in immunized animals(Bisht et al., 2004; Buchholz et al., 2004; Bukreyev et al., 2004; Gao et al., 2003). After injection of a recombinant plasmid vector expressing the N protein, S protein, or S protein of either the S1 or S2 region to mice, high cytotoxic T-lymphocyte (CTL) and antibody responses were observed(Zeng et al., 2004; P. Zhao et al., 2004; M. S. Zhu et al., 2004). Current approaches for the development of MERS-CoV vaccines are mostly similar to the methods used for the development of SARS-CoV vaccines, including subunit vaccines(Tai et al., 2017), recombinant vector vaccines(Gilbert & Warimwe, 2017; E. Kim et al., 2014), and DNA vaccine(Al-Amri et al., 2017; Chi et al., 2017).

HCoV vaccine development remains a major challenge due to highly sophisticated immune evasion mechanisms of viral pathogens (Kaufmann, McElrath, Lewis, & Del Giudice, 2014). Moreover, the development of safe and effective coronavirus vaccines is more challenging.

CoV vaccine may induce harmful immune responses, resulting in liver damage in vaccinated animals or enhancing infection after being challenged (Czub, Weingartl, Czub, He, & Cao, 2005; Enjuanes et al., 2008; Honda-Okubo et al., 2015; Weingartl et al., 2004).

## 1.9 Antiviral approaches against coronaviruses.

Even though many coronavirus antiviral agents have been identified and developed, there is no approved drug to treat highly pathogenic human coronavirus outbreak. Furthermore, several attempts to treat SARS and MERS with approved antivirals (ribavirin and lopinavir-ritonavir) and immunomodulators (corticosteroid, interferons) were made, but their effectivity was questionable (Zumla, Chan, Azhar, Hui, & Yuen, 2016). Different steps of the coronavirus replication including virus entry (S protein-receptor interaction, endosomal proteases and acidification, or membrane fusion) or virus replication (3CLpro, PLpro, RdRp, or 5'-3' helicase) have been considered as viable targets(Adedeji et al., 2012; Barnard & Kumaki, 2011; Liang, 2006).

### 1.9.1 Viral entry inhibitors

Since viral entry is a vital step for virus replication, it has been considered an attractive target for antiviral drug development. The possible targets within coronavirus entry are S protein-host receptor interaction, endosomal maturation and enzymes, and S mediated membrane fusion. First of all, neutralizing antibodies against S protein are possible SARS-CoV and MERS-CoV entry inhibitors. The majority of humanized monoclonal antibodies(HmAbs) against SARS-CoV bind with the receptor binding domain (RBD) of the S protein and likely prevented S protein-receptor interaction (J. D. Berry et al., 2004; M. Coughlin et al., 2007; Greenough et al., 2005; Y. He et al., 2004; H. Hofmann et al., 2004; Sui et al., 2004; Traggiai et al., 2004). There have been

several reports that HmAbs target other regions except RBD including N-terminal and C-terminal of the RBD, proximity of junction of the S1 and S2, and HR2 domain (M. M. Coughlin, Babcook, & Prabhakar, 2009; J. Duan et al., 2005; Keng et al., 2005; H. Zhang et al., 2004). Prophylactic administration of a human monoclonal antibody to ferrets or naïve mice reduced replication of SARS-CoV, prevented the development of lung disease and the shedding of virus in pharyngeal secretions(Subbarao et al., 2004; ter Meulen et al., 2004). In MERS-CoV research, passive transfer of neutralizing antibodies that target functionally distinct domains of S protein also protected mice from the lethal challenge(Widjaja et al., 2019). All of these suggest that neutralizing antibodies provide a new way to gain humoral protection against coronavirus infection. However, the possible antibody-dependent enhancement is the one major concern with this treatment, as shown in FIP. Previous studies with HmAbs showed that infection of pseudotyped viruses was increased in the presence of HmAbs in vitro and this enhancement was not observed vaccination with a cDNA that encoded only the ectodomain of S protein(Z. Y. Yang et al., 2005). Another concern is the potential cross-reactivity of the hmAbs with self-antigens. Two defined epitopes within S2 (amino acids 927-937 and 942-951) were reported to interact with self-antigens causing cytotoxicity *in vitro*(Y. S. Lin et al., 2005). Thus, future studies with therapeutic SARS-CoV and MERS-CoV HmAbs should be tested with these concerns. The host receptor can be targeted by specific monoclonal or polyclonal antibodies, peptides or functional inhibitors. In the SARS-CoV treatment, N-(2-aminoethyl)-1-aziridine-ethanamine(NAAE) showed to inhibit the catalytic activity of ACE2 and S-mediated cell to cell fusion(Huentelman et al., 2004). Synthetic peptides mimicking ACE2 segments also inhibited SARS-CoV replication *in vitro*(Han, Penn-Nicholson, & Cho, 2006). A recombinant humanized IgG1 anti-DPP3 mAbs (YS100) showed to inhibit MERS-CoV entry *in*

*vitro* (Ohnuma et al., 2013). However, the limitation of these approaches is their narrow anti-CoV activity and potential risks of affecting host biological functions.

The cleavage of S protein by a host protease is a crucial trigger for viral-cellular membrane fusion, thus, host proteases are attractive antiviral targets. The type II transmembrane serine protease TMPRSS2 and human airway trypsin-like protease (HAT) have been shown to proteolytically activate the fusion proteins of SARS CoV. Cleaved SARS and HCoV-229E S protein by TMPRSS2 mediate cell surface entry of the viruses(Bertram et al., 2011; Glowacka et al., 2011). They also have shown to be co-localized with each cellular receptor, supporting that these protease families can activate CoVs for respiratory tract infection and participate to spread of CoV in human patients (Bertram et al., 2013). A synthetic low-molecular-weight serine protease inhibitor, camostat mesylate, which inhibits TMPRSS2 and HAT, is shown to inhibit SARS-CoV and MERS-CoV *in vitro* and *in vivo*(Shirato, Kawase, & Matsuyama, 2013; Y. Zhou et al., 2015).

Coronavirus endocytosis is an important target of anti-CoV drugs. Coronaviruses are known to utilize the clathrin-mediated endocytosis for its entry(Inoue et al., 2007; J. E. Park, Cruz, & Shin, 2014). Therefore, chlorpromazine that blocks the assembly of clathrin-coated pits at the plasma membrane (L. H. Wang, Rothberg, & Anderson, 1993) inhibits replication of SARS-CoV and MERS-CoV *in vitro*(de Wilde et al., 2014). Cardiotonic steroids, which bind the ATP1A1 subunit of ATPase, also inhibit clathrin-mediated endocytosis of MERS-CoV(Burkard et al., 2015). The important roles of endosomal acidification and endosomal proteases during virus entry have been documented in numerous coronaviruses. Chloroquine, which is an anti-malarial drug that increases the endosomal pH, has been shown broad-spectrum anti-CoV activity to SARS-CoV, MERS-CoV, HCoV-229E, HCoV-OC43, and PEDV(de Wilde et al., 2014; Keyaerts, Vijgen, Maes, Neyts, & Van Ranst, 2004; Kono et al., 2008; Oh et al., 2019; Vincent et al., 2005)

suggesting it as a potential broad-spectrum antiviral drug candidate. Cathepsins usually exist in the endosomal compartment and are classified into cysteine (cathepsin B, L, H, K, S, and O), aspartyl (cathepsin D and E) and serine (cathepsin G) protease(Vasiljeva et al., 2007a). Cathepsin B and L have been reported to cleave S protein of SARS-CoV, MERS-CoV, HCoV-229E, FCoV and MHV-2(Kawase, Shirato, Matsuyama, & Taguchi, 2009b; Y. Kim, Mandadapu, Groutas, & Chang, 2013; Qiu et al., 2006; Regan & Whittaker, 2008; Simmons et al., 2005; Wicht et al., 2014). Inhibition of cathepsin L by small-molecular compound showed to block entry of SARS-CoV (Simmons et al., 2005; N. Zhou et al., 2016). However, since coronavirus entry can be easily shifted between the cell surface and endosomal pathway, combinations of inhibitors with different mechanism of action should be considered.

## 1.9.2 Coronavirus replication inhibitors

### 1.9.2.1 Viral protease inhibitors

After virus entry and the translation of the viral RNA to the polyproteins, the 3CLpro and the PLpro cleave the polyprotein into individual polypeptides. Thus, 3CLpro and PLpro are functionally critical in the CoV replication (Anand, Ziebuhr, Wadhwani, Mesters, & Hilgenfeld, 2003) and they are regarded as an attractive drug target for anti-CoV drug development(Anand et al., 2003; Thiel, Herold, Schelle, & Siddell, 2001; H. Yang et al., 2005; H. Yang et al., 2003). Numerous 3CLpro inhibitors have been identified not only by screening compound libraries(Kuo et al., 2009; Ramajayam, Tan, & Liang, 2011) but also structure-based drug design(Lu et al., 2006). Activity of SARS-CoV 3CLpro can be inhibited by myriad kinds of protease inhibitors, including zinc or mercury conjugates, C2-symmetric diols, peptidomimetic-α,β-unsaturated esters, anilides, benzotriazole, N-phenyl-2-acetamide, biphenyl sulfone, glutamic acids and glutamine peptides

with a trifluoromethyl ketone group, pyrimidinone, and pyrazole analogs (Adedeji & Sarafianos, 2014). Lopinavir, which is a protease inhibitor against HIV, is the most readily available 3CLpro. It showed anti-CoV activity in vitro, and in vivo (J. F. Chan et al., 2015; K. S. Chan et al., 2003; C. M. Chu et al., 2004). Our lab has developed dipeptidyl compounds targeting coronavirus 3CLpro with broad-spectrum activity against feline CoV, ferret CoV, mink CoV, and feline calicivirus(Y. Kim et al., 2015). Antiviral treatment with one of these compounds, GC376, on experimentally FIP infected cats demonstrated full recovery of disease with a rapid improvement in fever, ascites, lymphopenia(Y. Kim et al., 2016). Since these 3CLpro inhibitors targeting highly conserved key residues for substrate recognition in all coronaviruses and picornaviruses, it has been proposed to be broad-spectrum antiviral drugs (Kumar et al., 2017).

### 1.9.2.2 Helicase inhibitors

Helicase catalyzes the separation of double-stranded oligonucleotides into single. During positive-sense RNA virus replication, the helicase separates nucleic acids and melts highly stable secondary structures within the genomic RNA to increase translational efficiency(Paolini, De Francesco, & Gallinari, 2000). Thus, viral helicase is an important antiviral target. A few potential coronavirus helicase inhibitors have been identified(Adedeji et al., 2012; M. K. Kim et al., 2011; C. Lee et al., 2009; Tanner et al., 2005). SARS-CoV helicase was inhibited via blocking its ATPase activities by the Bananins *in vitro* (M. K. Kim et al., 2011; Tanner et al., 2005). Since these helicase inhibitors have a potential ability to blocks the cellular ATPases, cytotoxicity needs to be evaluated.

### 1.9.2.3 Viral polymerase inhibitors

Coronavirus RNA dependent RNA polymerase (RdRp) is an essential part of the CoV replication-transcription complex due to its participation in genomic and subgenomic RNA synthesis, thus regarded as a validated target for an antiviral drug. Ribavirin, which is a guanosine analog that is known to block viral RNA synthesis and mRNA capping, shows broad-spectrum antiviral. Ribavirin was used to treat SARS patients with high doses, but benefits in SARS patients were uncertain(V. C. Cheng, Lau, Woo, & Yuen, 2007; N. Lee et al., 2003). A report of a combination of ribavirin and interferon therapy to five MERS-CoV patients showed that none of the patients responded to the therapy. However, with the early administration of treatment (8h post challenge), this treatment improved clinical symptoms of MERS-CoV infection in the rhesus macaque model (Falzarano et al., 2013). These results suggest further evaluation of the optimal timing of this therapy(Al-Tawfiq, Momattin, Dib, & Memish, 2014).

**1.9.2.4 Modulation of the host immune system**

The host immune system that was modulated by coronaviruses is appealing antiviral targets due to their potential as a broad-spectrum anti-coronavirus target. Interferons (IFNs) are a group of signaling molecules that enhance cellular antiviral defenses. Because of their beneficial immunomodulatory properties, the antiviral effects of type I IFNs were widely studied for the various viral diseases with no specific antiviral treatment. *In vitro* studies of type I IFNS on SARS- and MERS-CoV were shown to inhibit viral replication (Falzarano et al., 2013; Stroher et al., 2004). IFNs were also used to treat SARS and MERS patients solely or in combination with other drugs including ribavirin and lopinavir-ritonavir but the therapeutic effects were limited, probably due to late administration(Stockman, Bellamy, & Garner, 2006). Poly I:C, an upstream stimulant of INFs signaling cascade, showed to protect SARS- and MERS-CoV infection in a mouse model

with upregulation of INF-β, INF-γ, IL-1β, and tumor necrosis factor(TNF) gene expression (J. Zhao et al., 2012) (J. Zhao et al., 2014).
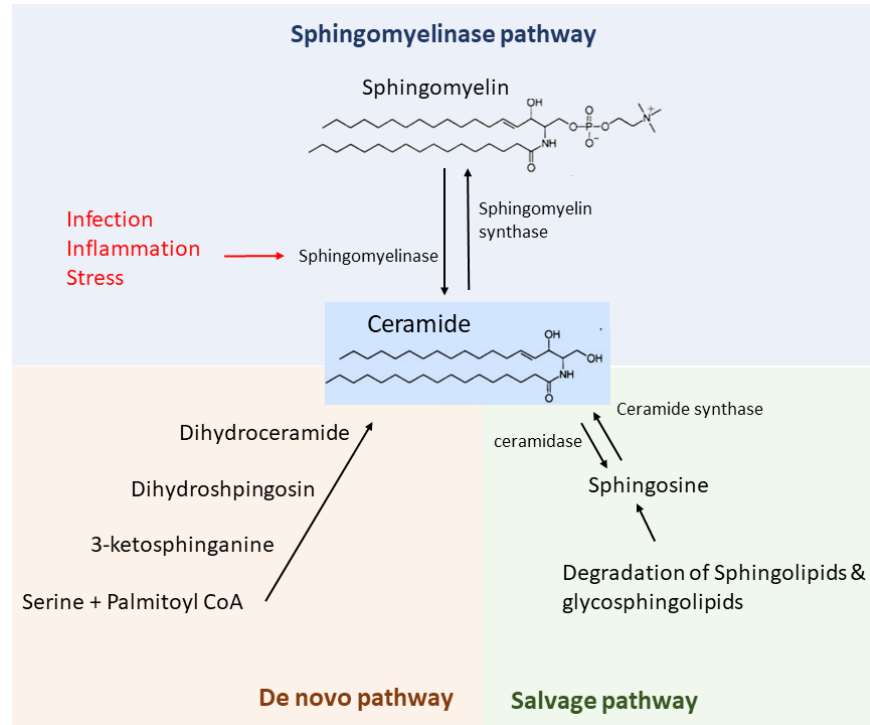


**Figure 1-6. Ceramide synthesis pathways.**

Ceramide synthesis have tree major metabolic pathways: the de novo pathway synthesize ceramide from palmitoyl CoA and serine. The salvage pathway recycles long-chain sphingoid base to generate ceramide using ceramide synthase. The sphingomyelinase pathway breaks down sphingomyelin to ceramide using sphingomyelinase.

## 1.10 Ceramide and Acid sphingomyelinase

Sphingolipids constitute the major class of eukaryotic lipids containing a sphingolipid base as a backbone. Several sphingolipids have been identified including sphingosine, ceramide, ceramide-1-phosphate, and sphingosine-1-phosphate (R. H. Kim, Takabe, Milstien, & Spiegel, 2009; Morales, Lee, Goni, Kolesnick, & Fernandez-Checa, 2007; Ogretmen & Hannun, 2004;

Zheng et al., 2006). Sphingolipids modulate almost all major cell biological processes, including growth regulation, cell migration, adhesion, apoptosis, senescence, and inflammatory responses.

One of the main sphingolipids that have received the most attention is ceramide due to its central role in the sphingolipid metabolic pathway: ceramide was used as a substrate for complex sphingolipids synthesis and various secondary signaling intermediates. Ceramide consists of sphingosine in N-linked to a variety of acyl groups. Followed by various stimulations and stresses, ceramide can be generated via three different pathways, sphingomyelin(SM) hydrolysis pathway, salvage pathway, or *de novo* synthesis(Kitatani, Idkowiak-Baldys, & Hannun, 2008; Kolesnick, Goni, & Alonso, 2000), all of which leads to formation of ceramide-enriched domains or platforms at cellular membrane(Gulbins & Grassme, 2002) (Figure 1-6). In this literature review, we focused on the sphingomyelinase pathway because this rapidly initiating pathway seems to be crucial in relation to the virus entry. Several isoforms of sphingomyelinase have been identified and they are distinguishable by their optimum pH requirement and subcellular localization. Alkaline sphingomyelinases are found in the intestinal tract for digestion of sphingomyelin(R. D. Duan, 2006). Neutral sphingomyelinase activity was first identified in 1967 in the tissues of patients with Niemann-Pick disease(Schneider & Kennedy, 1967) and four mammalian neutral sphingomyelinases have been identified including nSMase1 (gene name: SMPD2), nSMase2 (SMPD3), nSMase3 (SMPD4) and mitochondrial associated-nSMase (SMPD5). The N-SMase2 is well characterized and is an important mediator of cellular stress-induced ceramide production and a special role in bone mineralization. Acid sphingomyelinase (ASM) is found in the lysosome, as a secretory form (Jenkins, Canals, & Hannun, 2009) but also in domains on the outer leaflet of the plasma membrane(M. Xu et al., 2012) suggesting that ASM is not restricted to the lysosome. The localization of these two forms of ASM is determined by the cleavage site on precursor ASM

or the glycosylation pattern on the mature ASM(Ferlinz, Hurwitz, Vielhaber, Suzuki, & Sandhoff, 1994; Newrzella & Stoffel, 1996; Schissel, Keesler, Schuchman, Williams, & Tabas, 1998). Sphingomyelinases catalyze the hydrolysis of the phosphodiester bond in sphingomyelin and separate it to ceramide and phosphorylcholine.

Various stimuli have been reported to activate ASM. The ASM activation is mediated by the engagement of the TNF-receptor superfamily members including FAS(Cremesti et al., 2001; Grassme, Jekle, et al., 2001; Grassme, Jendrossek, & Gulbins, 2001), CD40(Grassme, Bock, Kun, & Gulbins, 2002), DR5(Dumitru & Gulbins, 2006) and TNFα(Schütze et al., 1992). In detail, FAS, as known as CD95, initiates the ASM activation by binding of a small amount of the adaptor protein FADD and initiator caspase 8(Brenner et al., 1998; Grassme, Cremesti, Kolesnick, & Gulbins, 2003). TNF-R55 and its associated proteins TRADD and FADD activate ASM in a caspase-dependent manner(Schwandner, Wiegmann, Bernardo, Kreder, & Kronke, 1998). Various stress stimuli have demonstrated to activate ASM including UV-light(Charruyer et al., 2005; Kashkar, Wiegmann, Yazdanpanah, Haubert, & Kronke, 2005; Rotolo et al., 2005; Y. Zhang et al., 2001), heat(Chung et al., 2003; Verheij et al., 1996), oxidative stress(Sanvicens & Cotter, 2006), ionizing radiation(Paris et al., 2001; Santana et al., 1996), chemotherapeutic agents(Lacour et al., 2004), LPS(Pfeiffer et al., 2001), and engagement of the PAF-receptor(Göggel et al., 2004).

There are numerous reports that infections of pathogens to mammalian cells activate ASM involved in their internalization and host cell interactions. Phagocytosis of *Neisseria gonorrhoeae* mediated by CEACAM receptor led to rapid activation of ASM that is involved in opsonin-independent internalization without affecting bacterial binding(Hauck et al., 2000). Infection of *Pseudomonas aeruginosa* on human nasal epithelial cells activated ASM leading to the formation of ceramide-rich platforms that was required to internalize *P. aeruginosa*(Grassme, Jendrossek, et

al., 2003). Rhinovirus infection triggers rapid activation of ASM with microtubule- and microfilament- mediated translocation of ASM to the plasma membrane(Grassme, Riehle, Wilker, & Gulbins, 2005). Infection of Measles virus to dendritic cells via the pattern recognition receptor activates neutral and acid sphingomyelinases resulting in the formation of the ceramide-enriched platform with the recruitment of CD150, which involves uptake of measles virus (Avota, Gulbins, & Schneider-Schaulies, 2011). The attachment and entry of Ebolavirus required sphingomyelin enriched lipid rafts and its association with lysosomal ASM on the cell surface(Miller, Adhikary, Kolokoltsov, & Davey, 2012). The important roles of ASM activation in pathogen internalization are partly explained by the unique biophysical property of ceramide and ceramide rich platform. They can have self-aggregation, alteration of biophysical properties of the membrane, and membrane fusion. During the generation of ceramide, cleavage of the polar head from cylinder-shaped sphingomyelin forms a cone-shaped ceramide at one leaflet of the lipid bilayer. Accumulation of corn-shape ceramide induces an asymmetric membrane tension(Lopez-Montero, Monroy, Velez, & Devaux, 2010), membrane rearrangements including transbilayer movement of ceramide to the inner monolayer(flip-flop), and membrane curvature, all of which consequently facilitate membrane fusion and help pathogens traverse cellular membranes (Utermohlen, Herz, Schramm, & Kronke, 2008).

Therefore, ASM and ceramide metabolism are potential therapeutic targets for various viral and bacterial infections. Pharmacological and genetic inhibition of ASM and/or ceramide formation were shown to related to a reduction of infection via inhibiting viral and bacterial internalization(Avota et al., 2011; Grassme et al., 2005; Miller et al., 2012)and apoptosis. However, inhibition of ceramide formation significantly impairs host defense. ASM knock-out mice showed high susceptibility to *L.monocytogens* infection with 100-1000 folds higher bacterial

loads of wild-type mice. In ASM knock-out macrophages, *L.monocytogens* could survive extendedly in late phagosomes suggesting defects of phagosomal maturation and perturbation in lysosomal fusion due to the absence of ASM(Utermohlen et al., 2008; Utermohlen, Karow, Lohler, & Kronke, 2003). These results suggest that manipulation of ASM and ceramide formation is a potential, but a delicate therapeutic target for bacterial and viral infection.

## 1.11 Coronavirus infection and cellular apoptosis

### 1.11.1 Apoptosis

Apoptosis is a systemic procedure of cell death. Morphological characteristics of the apoptotic cell are membrane blebbing, pyknosis and cell shrinkage, engulfed by phagocyte before leakage of cellular contents. To date, the two main pathways are known to mediate apoptosis: the intrinsic or mitochondrial pathway in response to a homeostatic mechanism and the extrinsic or death receptor pathway mediated by extracellular stimuli. However, these two pathways are linked with molecules that can influence each other(Igney & Krammer, 2002). Except for the intrinsic and extrinsic pathway, there is an additional pathway that is associated with perforin-granzyme and T-cell mediated cytotoxicity.

The intrinsic pathway is initiated by non-receptor-mediated stimuli that induce intracellular signals to initiate the mitochondrial pathway. The stimuli that trigger the intrinsic pathway are classified into positive and negative signals. Positive signals are radiation, nutrient deprivation, toxins, hypoxia, hypothermia, and viral infections. Negative signals are the lack of certain hormones and cytokines, which cannot suppress death programs. All of these stimuli lead to increasing the mitochondrial outer membrane permeability (MOMP) and opening of the mitochondrial permeability transition (MPT) pore based on the ratio of pro-apoptotic and anti-

apoptotic B-cell lymphoma 2 (Bcl2) family of protein and subsequent release of pro-apoptotic proteins such as cytochrome *c* from the intermembrane space of mitochondria to the cytosol(Saelens et al., 2004). Cytochrome *c* interacts with Apaf-1 and procaspase-9, forming an apoptosome(Chinnaiyan, 1999) and then activating caspase-9.

The extrinsic pathway is initiated by receptor-mediated interactions with tumor necrosis factor (TNF) receptor gene superfamily(Locksley, Killeen, & Lenardo, 2001) and shared by the death domain(Ashkenazi & Dixit, 1998). The known ligands and corresponding death receptors are including FasL/FasR, TNF-α/TNFR1, Apo3L/DR3, Apo2L/DR4 and Apo2L/ DR5(Ashkenazi & Dixit, 1998; Chicheportiche et al., 1997; Peter & Krammer, 1998; Rubio-Moscardo et al., 2005; Suliman, Lam, Datta, & Srivastava, 2001). In the best characterized model, FasL/FasR, the binding of FasL to FasR leads to the association of the FADD, the adapter protein, then FADD interacts with procaspase-8 leading to the formation of the death-induce signaling complex (DISC), resulting in the activation of procaspase-8 with auto-catalysis(Kischkel et al., 1995).

Both extrinsic and intrinsic pathways finally reach the execution phase, considered the final step of apoptosis. In this phase, the activation of a group of cysteine proteases called " caspases" and complex cascade events that link the initiating stimuli occur (J. Li & Yuan, 2008). Caspases can be classified into two classes based on their roles in the apoptotic pathway. Initiator caspases (caspase 2, 8, 9, and 10) respond to proapoptotic signals and facilitate autocatalysis by activating effector caspases (caspase 3, 6, and 7). Once the effector caspases are activated, they create a functional mature protease and demolish key cellular structural proteins, leading to cellular disassembly (McIlwain, Berger, & Mak, 2013). Finally, the apoptotic cell is uptaken without the release of cellular constituents limiting inflammatory response.

**1.11.2 Apoptosis in viral infections**

Viruses, which is an obligate intracellular parasite, produce an extensive number of viral proteins in the infected cells to generate progeny viruses. Most viral infections eventually reach to the host cell death. To limit exploiting cellular machinery by viruses, the host cell undergoes apoptosis to limit viral replication, spread, or persistence. Many viruses prevent host cell death via encoding anti-apoptotic proteins to stop the host cell destruction, which allows them to complete viral replication. Furthermore, some viruses take advantage of apoptosis to facilitate viral replication and spread as well as to induce immune suppression.

**1.11.3 Coronavirus infection and Apoptosis**

Several studies have reported the occurrence of apoptosis during coronavirus infection. Among SARS patients, extensive damages to the alveolar and bronchial epithelial cells and apoptosis of liver and thyroid glands were observed (Chau et al., 2004; Wei et al., 2007). These pathological consequences are likely to be caused by cell death mediated by infection of the SARS-CoV and the inappropriate immune responses. Thus, cellular apoptosis induced by SARS-CoV infection has been extensively studied *in vitro*. SARS-CoV infection and replication induced Vero E6 cells apoptosis with caspases dependent manner (H. Yan et al., 2004) (Ren et al., 2005). The only expression of SARS N, 3a, or 7a protein was shown to induce apoptosis of host cells. N protein expression on COS-1 cells under the starvation of serum led to the release of cytochrome *c* and activation of caspase -3 and -9(L. Zhang et al., 2007). Expression of 3a protein was shown to activate the mitochondrial death pathway in two possible ways, the extrinsic pathway and the intrinsic pathway, all of which resulted in increased Bax and p53(Padhan, Minakshi, Towheed, &

Jameel, 2008). Overexpression of 7a induces apoptosis via a caspase-dependent pathway in cells from the lung, kidney, and liver(Tan et al., 2004).

Replication of IBV in Vero cells caused extensive cytopathic effects that were mediated by both necrosis and apoptosis. The addition of the pan-caspase inhibitor (Z-VAD-fmk) inhibited this CPE progress and increased virus yield suggesting the association of caspase-mediated apoptosis in IBV replication(C. Liu, Xu, & Liu, 2001). Infection of Turkey coronavirus (TCoV) in intestinal organ culture (IOC) induced apoptosis with nuclear fragmentation and DNA ladder formation(Deriane E. Gomes & Alexandre L. Andrade, 2011). MHV infection on 17Cl-1 cells and rat oligodendrocytes induced caspase-dependent apoptosis but infection on DBT cells did not show apoptotic changes, suggesting that MHV infection initiated apoptosis cell-type dependent manner(An, Chen, Yu, Leibowitz, & Makino, 1999; Y. Liu, Pu, & Zhang, 2006). Canine coronavirus II infection triggers apoptosis in A-72 cells by activating initiator and executioner caspases. However, inhibition of the apoptosis by caspase inhibitors did not affect CCoV replication(De Martino et al., 2010).

Interestingly, there have been several reports of coronavirus N protein cleavage by caspases during apoptosis (Diemer et al., 2008; Eleouet et al., 2000; Jaru-Ampornpan, Jengarn, Wanitchang, & Jongkaewwattana, 2017). In SARS-CoV infected cells with a lytic CPE and high virus titer, N protein was proteolytically processed by caspase 3 and 6 and the possible cleavage site located at residues 400 and 403 on C-terminal of N protein(Diemer et al., 2008). Moreover, the mutation on the nuclear localization signal on N protein prevented N from translocating to the nucleus and abolished its cleavage by caspases suggesting that N protein nuclear translocation is closely associated with its caspase cleavage. Infection of TEGV in HRT 18 cells induced apoptosis through a caspase-dependent manner and caspase 6 and 7 cleave N protein at C-terminal (Eleouet,

Chilmonczyk, Besnardeau, & Laude, 1998; Eleouet et al., 2000). The recent PEDV study reported that N protein was cleaved by 3C-like protease (3CLpro) during replication(Jaru-Ampornpan et al., 2017). 3CLpro recognized leucine 381(P2) in PEDV N protein and cleaved glutamine 382(P1). Reverse-genetics-derived PEDV containing uncleavable N protein showed growth detention, suggesting that the 3CLpro cleavage related to cell culture adaptation. This PEDV N protein cleavage is the one topic of my dissertation research.

## 1.12 Study objectives

Although PEDV has been a serious problem in the swine industry and public health, there is still limited information on the PEDV lifecycle, particularly the role of protease in PEDV entry and PEDV-host interaction during viral replication. With these mechanistic understanding of the PEDV life cycle, we may develop rational molecular countermeasures for preventing PEDV or coronavirus infection. Based on this literature review, this dissertation will focus on:

1) To identify the roles of protease during PEDV entry.

Since PEDV is an enteric pig coronavirus with a special requirement of exogenous protease(s) for its efficient replication in cell culture, it represents a unique model for studying roles of protease in coronavirus entry. Using the protease adopted PEDV strains, PEDV KD and AA, we will study the roles of protease(s) on PEDV entry, trafficking and escape from the endosomal compartment for effective replication.

2) To examine PEDV induced apoptosis and N protein cleavage during replication of protease independent PEDV strain and its biological significance.

During protease independent PEDV replication in Vero cells, the cleavage of N protein has been observed in the western blot analysis. We will identify what protease(s) cleave PEDV N

protein and where is the cleavage site on N protein. We will also explore the biological significance of N protein cleavage during protease independent PEDV replication.

3) To study roles of ceramide formation and acid sphingomyelinase during PEDV entry.

Using cell culture adapted PEDV strains, we will study the roles of ceramide formation mediated by ASM activation during PEDV entry.

This dissertation will provide fundamental molecular information for understanding the PEDV entry process and PEDV-host interaction. Such understanding could lead to the development of rational future strategies for preventing or treating PEDV or other coronavirus infections. The new strategies could support to fight against the ongoing new coronavirus outbreak as well as future coronavirus outbreak.

# Chapter 2 - Proteases facilitate the endosomal escape of porcine epidemic diarrhea virus during entry into host cells

## 2.1 Abstract

Exogenous and endogenous proteases play important roles in porcine epidemic diarrhea virus (PEDV) entry and replication. The roles of proteases in the viral endosomal escape and replication using trypsin (KD) or elastase (AA)-adapted US PEDV strains were studied. While PEDV KD and AA require different exogenous protease for efficient replication in cells, PEDV KD was more dependent on the protease than PEDV AA. There was no marked difference in viral trafficking between them during the entry events. Both PEDV strains were observed in the endosomes with or without protease at 1 h after virus inoculation. With protease, viral signals in the endosomes disappeared after 4 h, and newly synthesized viral proteins were detected in the ER after 6 h. However, without protease, viruses remained in the endosomes up to 24 h, which correlated with limited virus replication. Inhibitors of cathepsins, endogenous proteases, significantly reduced the replication of both PEDV by interfering with the viral endosomal escape.

## 2.2 Introduction

Coronavirus entry processes require complex interactions between multiple host and viral factors to enter the cells and initiate viral RNA translation and replication (Belouzard et al., 2012). The coronavirus spike (S) protein, a class I viral fusion protein, is a critical viral factor for coronavirus entry. The S protein contains two subunits: N-terminal S1 subunit which binds to cellular receptors and S2 subunit which is responsible for membrane fusion (S.M. Paul & Perlman,

2013). The S protein undergoes conformation changes exposing two major cleavage sites at the junction of S1 and S2 subunit (S1/S2) and just upstream of the fusion peptide (S2') before and during virus entry into host cells (Belouzard et al., 2012). Cleavage at the S2' site by proteases exposes the fusion peptide, which is mainly composed of hydrophobic amino acids (Belouzard et al., 2012). The fusion peptide is then introduced into the host cell membrane by a conformational change of the S2 subunit mediated by the refolding of heptad repeat 1 (Belouzard et al., 2012). As the fusion protein folds back, viral and cellular membranes are drawn together to initiate the membrane fusion for virus entry (Kirchdoerfer et al., 2016a).

The proteases involved in the proteolytic cleavage of S protein have been studied for several coronaviruses. It was shown that furin processes the S protein of mouse hepatitis virus (MHV) strain A59 and infectious bronchitis virus (IBV) targeting the junction of S1/S2 (Sturman, Ricard, & Holmes, 1985; Yamada & Liu, 2009). Since furin is mainly expressed in the trans-golgi network and the newly produced viruses possess cleaved S protein, the S proteins of those coronaviruses are thought to be processed during the stage of viral assembly (Seidah & Prat, 2012; Sturman et al., 1985; Yamada & Liu, 2009). The S proteins of severe acute respiratory syndrome coronavirus (SARS-CoV), middle east respiratory syndrome coronavirus (MERS-CoV) and HCoV-229E are reported to be activated by a membrane-bound protease, serine 2 (TMPRSS2), which is widely distributed in the respiratory tracts (Bertram et al., 2011; Bugge, Antalis, & Wu, 2009; Shirato et al., 2013). Other cellular proteases such as cathepsins, which exist in the endosomes and lysosomes, have been reported to process coronavirus S protein of SARS-CoV, MERS-CoV, human coronavirus (HCoV)-229E and feline coronavirus (FCoV) and MHV-2 (Kawase et al., 2009a; Y. Kim et al., 2013; Qiu et al., 2006; Regan, Shraybman, Cohen, & Whittaker, 2008; Simmons et al., 2005; Wicht et al., 2014). While the replication of most

coronaviruses does not require exogenous proteases in cell culture media, proteases in the medium have been reported to enhance the replication of some coronaviruses including SARS-CoV (S. Matsuyama, M. Ujike, S. Morikawa, M. Tashiro, & F. Taguchi, 2005). For instance, trypsin, dispase, thermolysin, and elastase have been reported to activate the S protein of SARS-CoV and enhance viral replication in cells (S. Matsuyama et al., 2005). The mutations in S protein are reported to alter protease susceptibility, pathogenicity and host range (Millet & Whittaker, 2015). Therefore, the proteolytic activation of S protein and viral entry are potential targets for antiviral drug development (Du et al., 2017; Simmons, Zmora, Gierer, Heurich, & Pohlmann, 2013).

Porcine epidemic diarrhea virus (PEDV), which belongs to the genus of Alphacoronavirus in the Coronaviridae family, causes porcine epidemic diarrhea (PED), a disease responsible for severe economic losses in the swine industry worldwide (Jung & Saif, 2015). PEDV infects the villous epithelium of the small intestines and causes diarrhea and vomiting in the affected pigs with up to 100% mortality in neonatal piglets (Jung & Saif, 2015). Unlike most coronaviruses, field isolation and efficient replication of most PEDV strains require the presence of exogenous trypsin in culture medium (W. Li et al., 2016). Previous reports have shown that cleavage of PEDV S protein by trypsin occurs after viral receptor binding (W. Li et al., 2016; J. E. Park, Cruz, & Shin, 2011; Wicht et al., 2014). However, the detailed mechanism of proteolytic activation of PEDV S protein by proteases is not well understood. In this study, we aimed to investigate the role of proteases in PEDV entry focusing on the endosomal escape by confocal microscopy. Using two cell-culture-adapted PEDV strains that require trypsin (PEDV KD) or pancreatic elastase (PEDV AA) in cell culture for virus replication (Y. Kim, Oh, Shivanna, Hesse, & Chang, 2017), we examined if exogenous proteases are involved in the endosomal escape of PEDV for efficient viral replication. We also investigated the roles of endogenous proteases (cathepsin B and L) in the

endosomes/lysosomes and endosome maturation in PEDV replication in correlation with the endosomal escape.

## 2.3 Materials and Methods

### 2.3.1 Cells, viruses, and reagents

PEDV KD and AA were described in our previous publication (Y. Kim et al., 2017). PEDV KD and AA were propagated in Vero (ATCC®-CCL-81™) cells in the presence of L-1-tosylamide-2-phenylethyl chloromethyl ketone (TPCK)-treated trypsin (Sigma-Aldrich, St Louis, MO) or elastase (Promega, Madison, WI), respectively, in Eagle's Minimal Essential Medium (MEM) supplemented with 100U/ml penicillin and 100 µg /ml streptomycin and 5% fetal bovine serum (FBS). Concentrated (>100-fold) PEDV KD or AA was prepared by ultracentrifugation of viruses at 100,000×g through a 30% w/v sucrose cushion at 4°C for 2 h. The pellet was resuspended in serum-free MEM and stored at -80°C.

### 2.3.2 Regents and antibodies

Leupeptin (trypsin inhibitor), Elastatinal (elastase inhibitor), CA074-Me (cathepsin B inhibitor) and chloroquine (endosomal acidification inhibitor) were obtained from Sigma-Aldrich (St. Louis, MO). Z-FL-COCHO (Cathepsin L inhibitor) was purchased from Calbiochem (San Diego, CA). The anti-PEDV polyclonal antibody was collected from a pig challenge study previously reported by us (Y. Kim et al., 2017).

### 2.3.3 One-step growth kinetics

Confluent Vero cells were incubated for 1 h at 37°C with PEDV KD or PEDV AA at a MOI of 0.1. After washing 3 times with PBS, fresh MEM containing mock-medium, trypsin (1 µg/ml) or trypsin (1 µg/ml) + leupeptin (5 µM) or elastase (1 µg/ml) was added to the cells infected with PEDV KD, and fresh MEM containing mock-medium, elastase (1 µg/ml), or elastase (1 µg/ml) + elastatinal (5 µM) was added to the cells infected with PEDV AA. Virus infected cells were further incubated at 37°C and virus RNA titers were measured by real-time quantitative RT-PCR at various time points following incubation. For real-time quantitative RT-PCR, total RNA was extracted from the PEDV infected cells using the RNeasy Kit (Qiagen, Valencia, CA) according to the manufacturer's protocol. Real-time quantitative RT-PCR was performed using One-Step Platinum RT-PCR kit (Invitrogen, Carlsbad, CA) with forward primer (5'-GCTATGCTCAGATCGCCAGT-3'), reverse primer (5'-TCTCGTAAGAGTCCGCTAGCTC-3'), and probe (5'-/56-FAM/TGCTCTTTG/ZEN/GTGGTAATGTGGC/3IABkFQ/-3') targeting the PEDV N gene on a Rotor-Gene Q (Qiagen) (Y. Kim et al., 2017). The condition for RT-PCR was 50°C for 30 min (for RT) and 95°C for 5 min, then 40 cycles of denaturation at 95°C for 15s, annealing at 60°C for 60s and elongation at 72°C for 30s. The TCID50 equivalents/ml were calculated from the Ct values based on the equation derived from the standard curve generated with the serial dilution of cell culture-grown PEDV.

### 2.3.4 Leupeptin addition assay

To determine which step of the virus entry is dependent on trypsin, leupeptin (a trypsin inhibitor) addition assay was performed using PEDV KD. Confluent Vero cells were inoculated with PEDV KD at an MOI of 0.1 in the presence of trypsin, and leupeptin (1 µM) was added to

the culture media at a binding (4°C for 1 h), entry (37°C for 1 h) or replication (37°C for 10 h)

stage. Between each stage, cells were washed extensively (3×) with MEM. PEDV KD infection

with trypsin (but without leupeptin) was included a control. PEDV KD infection without trypsin

also served as a control. Virus replication was assessed by real-time quantitative RT-PCR at the

end of a replication stage, and TCID50 equivalents/ml was determined as described above. Virus

RNA titers from each treatment were compared to those with trypsin (without leupeptin).


### 2.3.5 Confocal microscopy

Recently, we demonstrated that PEDV utilizes the endocytic pathway, and successful viral

endosomal escape and subsequent virus replication requires the presence of proteases such as

trypsin or elastase. Therefore, PEDV cellular trafficking with or without protease inhibitors was

investigated by confocal microscopy. Vero cells were seeded onto Lab-Tek™ II CC2™ chamber

slide (Fisher Scientific, Pittsburgh, PA), treated with 5% FBS and grown to 70% confluency. Mock

or PEDV KD or AA at an MOI of 50 were inoculated into the confluent cells on the chamber

slides, and the virus-infected cells were incubated at 4°C for 1 h. After washing with PBS for 3

times, the cells were subject to the following treatment for 1 h, 4 h, 6 h or 8 h prior to confocal

microscopy. The treatments are: 1) Cells infected with PEDV KD were incubated with Mock (no

trypsin), TPCK-treated trypsin (1 µg /ml) or TPCK-treated trypsin (1 µg/ml) + trypsin inhibitor

(PPACK, 2 µM); 2) Cells infected with PEDV AA strain were incubated with Mock (no trypsin),

elastase (1 µg/ml) or elastase (1 µg/ml) + Elastatinal (5 µM); 3) Cells infected with KD were

incubated with TPCK-treated trypsin with or without cathepsin inhibitors [Z-FL-COCHO (10 µM)

or CA074-Me (40 µM)] or chloroquine (75µM). To prepare cells for confocal microscopy, cells

were fixed in 4% formaldehyde (Sigma-Aldrich) in PBS (pH 7.4) at room temperature (RT) for 15

min, permeabilized with 0.1% Triton x-100 (Fisher Scientific) in PBS for 10 min at RT. The cells were then washed three times with PBS and incubated in PBS containing 0.5% bovine serum albumin for 15 min. After washing with PBS three times, cells were further incubated with primary antibody to PEDV (1:200) at 37°C for 2 h. After washing three times with PBS, the slides were incubated with FITC labeled secondary antibodies diluted 1:100 in PBS. The cell nucleus was stained with SYTOX orange (0.5 μM in 0.9% NaCl). To determine the intracellular location of PEDV, the KD-infected cells fixed at 6 and 12 h PI were incubated with the PEDV antibody and mouse monoclonal antibody against VPS26A (endosome marker) or PDIA3 (ER marker), followed by the appropriate secondary antibodies with FITC and AlexFluor®594. Coverslips were mounted with ProLong® Gold antifade reagent (Molecular Probes), and the cells were scanned with a confocal microscope LSM 510 (Zeiss, Oberkochen, Germany) using a 100x oil-immersion objective lens. The images were processed by Image J software 1.51 (http://imagej.nih.gov/ij/). The colocalization analysis was performed using JACoP and colocalization-MBF plugins for ImageJ software.

## 2.3.6 Statistical analysis

The effects of cathepsin or chloroquine in PEDV replication were statistically analyzed using GraphPad Prism (GraphPad Software, La Jolla, CA, USA). Statistical analysis was performed using the student t-test. $P$-value of <0.05 was considered as statistically significant. Data were from at least three independent experiments.

## 2.4 Results

### 2.4.1 Efficient replication of PEDV requires the addition of protease.

To determine the effect of protease in PEDV entry and replication, one-step growth kinetics of PEDV KD and AA were investigated in the presence or absence of trypsin or elastase, respectively. Trypsin inhibitor or elastase inhibitor was also used as additional controls for the study. The RNA levels (or viral titers) at each time point were compared to those at 0 h. During 0-4 h post infection, the titers of PEDV KD in all three groups remained unchanged and statistically not different (Figure 2-1A). The virus RNA titers of the trypsin-treated group increased rapidly after 4 h post-infection (PI) and reached 7.5 log10 TCID50/ml at 24 h PI (Figure 2-1A). However, the virus RNA titers of mock-medium treatment (without trypsin) or trypsin plus inhibitor group did not significantly increase from 4 to 24 h post-infection (PI) (Figure 2-1A). For PEDV AA, virus RNA titers remained unchanged during 0-6 h PI in all three groups (Figure 2-1A). The virus RNA titers of PEDV AA with elastase significantly increased after 6 h PI, reaching 6.9 log10 TCID50/ml at 24 h PI. Interestingly, virus RNA titers of PEDV AA also significantly increased at 24 h with mock-medium (without elastase) or at 12 h and 24 h with elastase plus inhibitor compared to those at 0 h (Figure 2-1B). Although virus RNA titers of PEDV AA also significantly increased without elastase or with elastase plus inhibitor, the increments are only moderate up to 5.0 log10 TCID50/ml (Figure 2-1B).
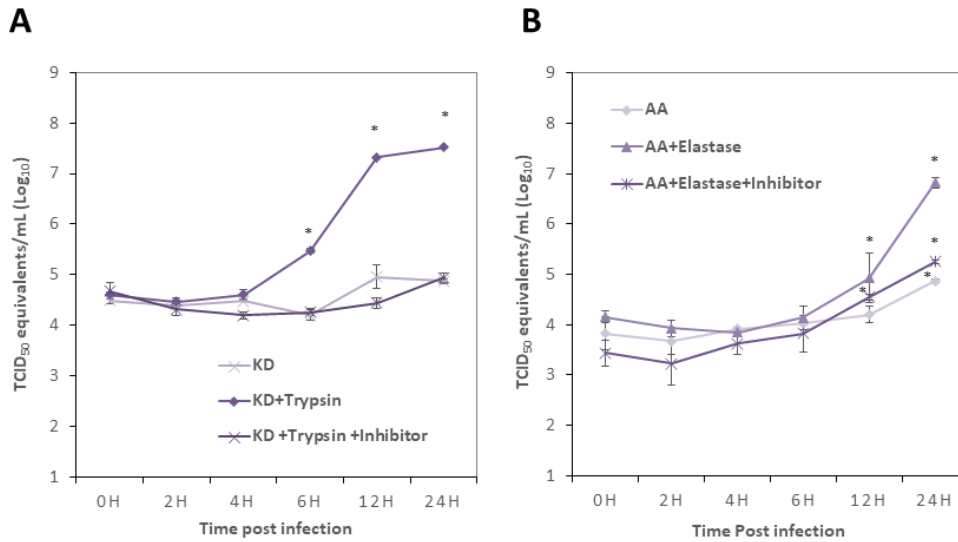
**Figure 2-1. Replication kinetics of PEDV KD & AA.**

Confluent Vero cells were inoculated with PEDV KD (A) or AA (B) at an MOI of 5 and incubated at 37°C for 1 h. After thorough washing with PBS, fresh MEM containing (A) Mock-medium, TPCK-treated trypsin (1 µg/ml) or TPCK-treated trypsin (1 µg/ml)+inhibitor or (B) elastase (1 µg/ml), elastase (1 µg/ml)+inhibitor were added to the virus infected Vero cells. Viral RNA was extracted from the cells at 0, 2, 4, 6, 12 or 24 h post-inoculation (PI) for real-time qRT-PCR, and genome copy numbers were calculated by plotting Ct values against a standard curve gene-rated using a series of dilutions of in-vitro transcribed PEDV RNA genome. Error bars show standard deviations, and asterisks indicate significant difference ($p < 0.05$) in virus RNA titers, compared to those at 0 h.

## 2.4.2 Trypsin is required after viral attachment/entry of PEDV KD.

To determine which stage of PEDV replication is dependent on trypsin, we designed and conducted leupeptin (serine protease inhibitor) inhibition assay as described in Figure 2-2A. The absence of trypsin in the media led to a significant reduction of virus RNA titers, as expected, compared to those with trypsin. Significant changes in virus RNA titers were observed when leupeptin was present in the media during both entry and replication stages (treatments e and f),

indicating trypsin activity is required for both stages (Figure 2-2B). We also tested whether the pre-incubation of cells or viruses with trypsin induces viral replication. Pre-incubation of concentrated PEDV KD with TPCK-treated trypsin (up to 5 µg /ml) or pre-incubation of Vero cells with TPCK-treated trypsin (up to 5 µg /ml) for 1 h at 37°C did not lead to virus replication (data not shown).
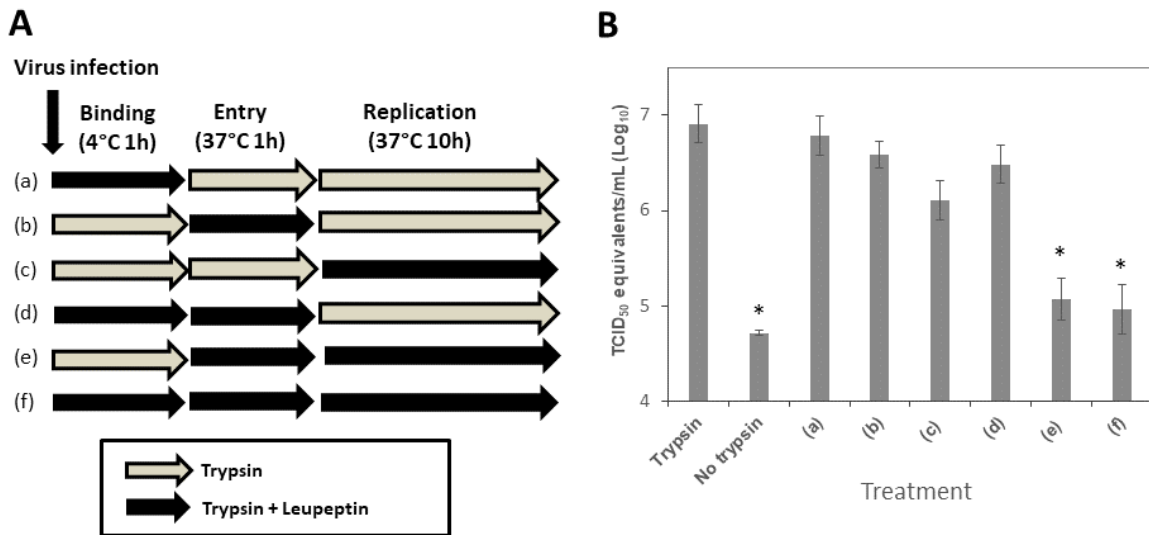


**Figure 2-2. Addition of leupeptin at different virus replication stages (PEDV KD)**
Confluent Vero cells were inoculated with PEDV KD at an MOI of 5 in the presence of trypsin (1 µg/ml) or trypsin + inhibitor (leupeptin, 1 µM) at 4C for 1 h (binding stage). After thorough washing with PBS, virus infected cells were transferred to 37C and incubated for 1 h with trypsin or trypsin+inhibitor (entry stage). After another thorough washing, cells were incubated for additional 10 h with trypsin or trypsin+inhibitor before viral replication was assessed. (A) A schematic drawing shows trypsin or trypsin+leupeptin treatment of cells at various stages of virus replication. (B) Virus replication was quantified by real time qRT-PCR at 12h PI. Error bars show standard deviations. Asterisks indicate significant difference ($p < 0.05$) in virus genome levels, compared to those of PEDV infection with trypsin.

### 2.4.3 The protease was required for the endosomal escape of PEDV.

The effect of protease in the entry events of PEDV KD or PEDV AA in Vero cells was examined by confocal microscopy. While PEDV AA and KD require different protease for replication, there was no difference in the overall viral trafficking between these strains (Figure 2-3A and B). In the cells incubated with protease (trypsin or elastase), aggregated fluorescence signals of PEDV KD or AA were observed within the cell cytoplasm at 1 h PI, but the signals disappeared at 4 h PI. However, fluorescence signals of PEDV KD or AA remained at 4 h or 6 h PI in the cells incubated without protease or with protease + inhibitor (Figure 2-3A, and 2-4). These signals were colocalized with VPS26A (an endosome marker) but not with PDIA3 (an ER marker) (Figure 2-4B). At 6 h PI, diffuse fluorescence signals of PEDV KD or AA were observed around the nucleus in the cells incubated with protease (Figure 2-4, PEDV KD + trypsin and PEDV AA + elastase Panels), and these fluorescence colocalized with PDIA3, which suggests newly synthesized PEDV proteins were detected in ER (Figure 2-4B). However, in the cells incubated without trypsin or elastase (Mock), aggregated fluorescence signals were still visible in the endosomes at 6 h PI (Figure 2-4, PEDV KD + Mock and PEDV AA + Mock Panels) and 24 h PI (data not shown).
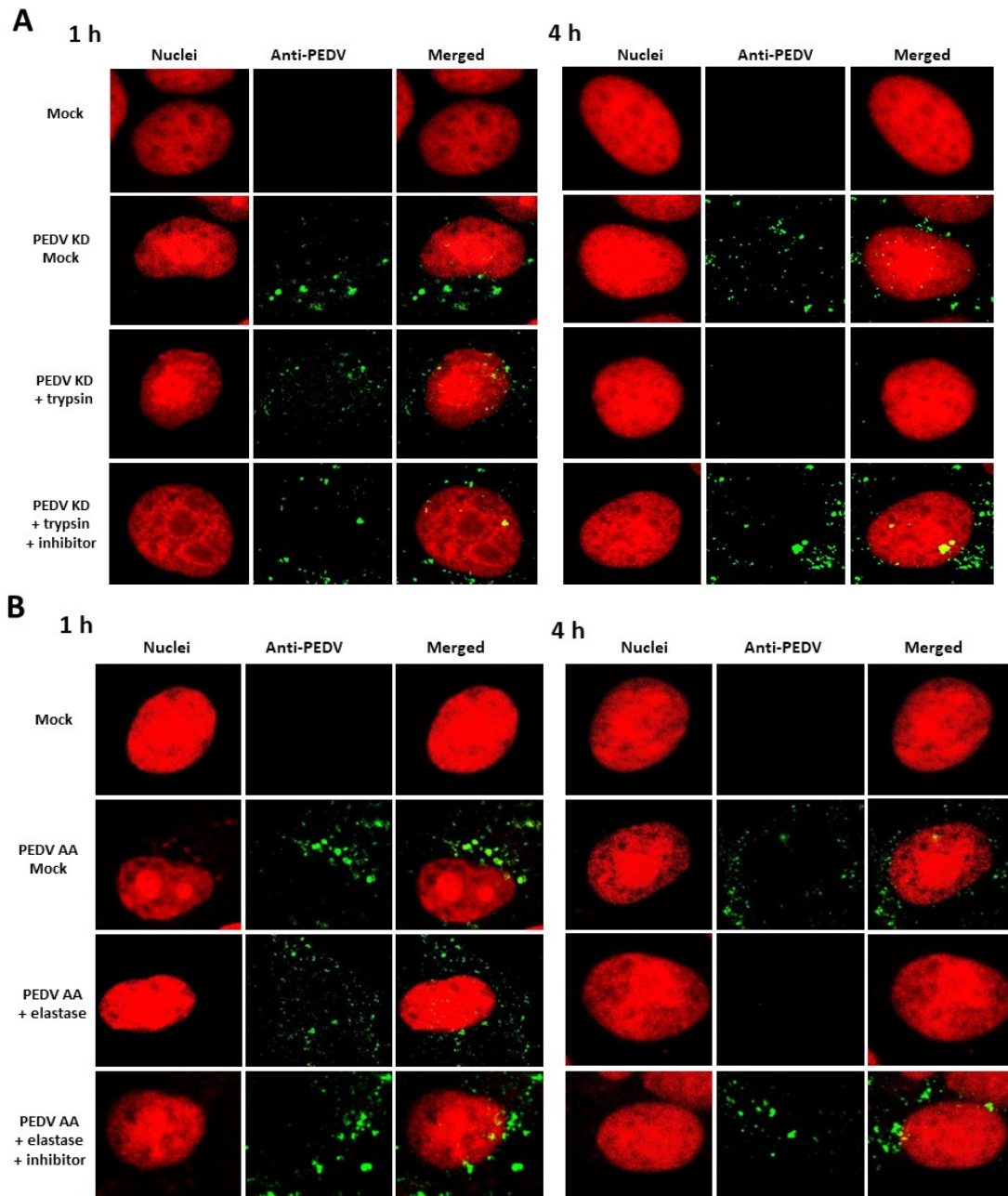
**Figure 2-3. Confocal microscopy of PEDV entry.**

Confluent Vero cells grown on Lab-Tek II CC2 chamber slides were infected either with Mock (medium) or PEDV KD (A) or AA (B) at an MOI of 50, and incubated with Mock-medium, trypsin 1 µg/ml (elastase 1 µg/ml) or trypsin+ inhibitor (elastase +inhibitor) for 1 h or 4 h. Fixed cells were probed with swine polyclonal anti-PEDV primary antibodies, followed by FITC-labelled goat-anti-swine antibody (green). Nuclei were stained with sytox orange (5µM) (red), and merged images for PEDV and nuclei were prepared by using Image J.
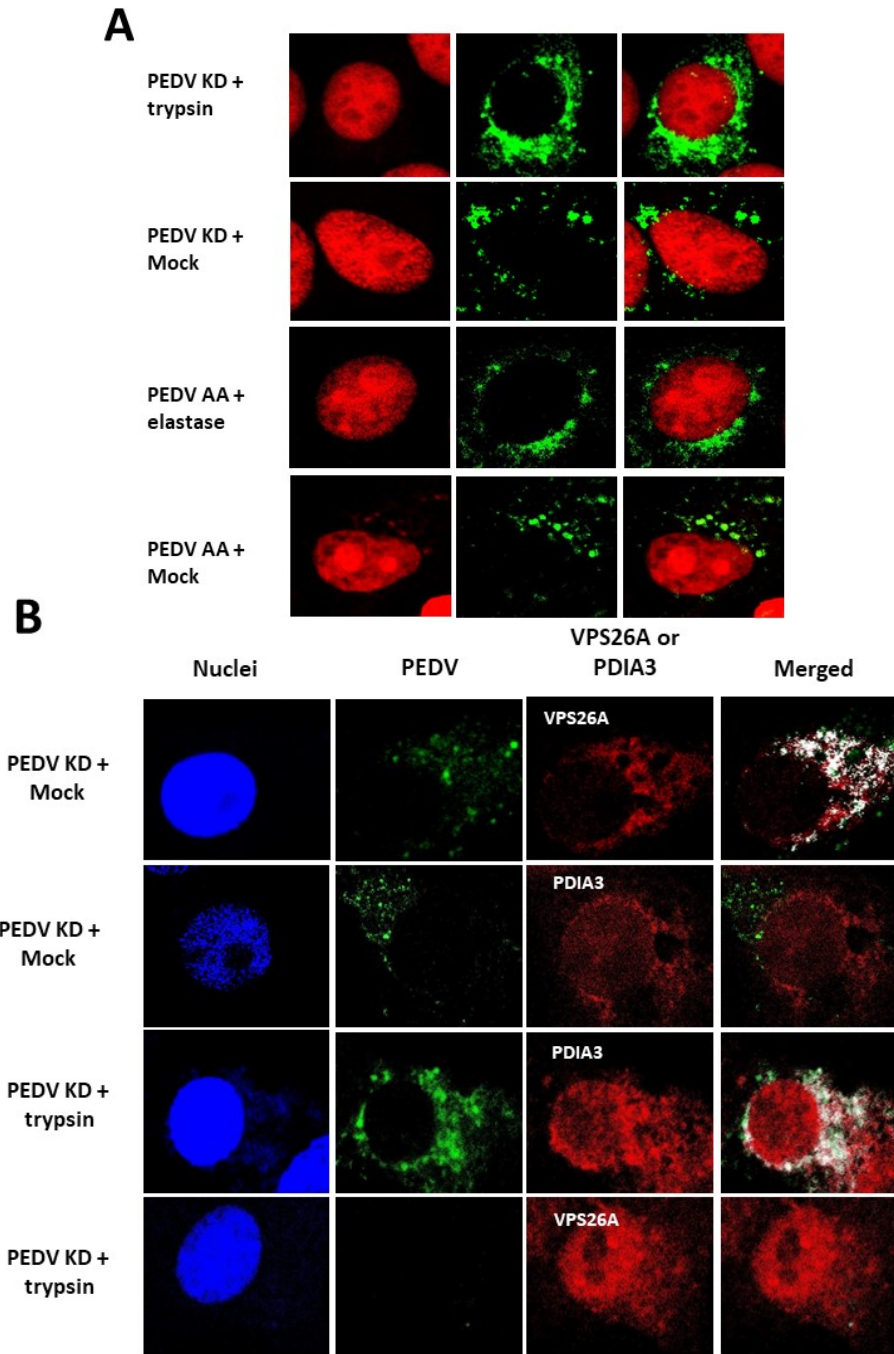
**Figure 2-4. Confocal microscopy of KD or PEDV with or without protease.**

A. Virus infected cells were prepared at 6 h after PEDV KD or PEDV AA with or without (Mock) trypsin or elastase, respectively. Virus infection, treatment and procedures are same as Figure 2-3. B. Co-localization of PEDV KD with the endosomes (VPS26A) or ER (PDIA3) marker. PEDV KD infected cells without (Mock) or with trypsin were fixed at 6 h and PEDV, PEDV (green), VPS26A (red), PDIA3 (red) or merged images were presented.

## 2.4.4 Cathepsin activity is required for efficient replication of PEDV.

As the PEDV KD and PEDV AA travel through the endosomes, the roles of endosomal proteases, cathepsin B and L, in virus replication were examined using inhibitors. The cytotoxicity of each inhibitor was determined in Vero cells, and the concentrations showing minimal toxicity was used (up to 10 µM for Z-FL-COCHO and up to 40 µM for CA074-Me). Treatment of cells with cathepsin L inhibitor (Z-FL-COCHO) significantly reduced PEDV KD or AA replication at 10 and 5 µM (Figure 2-5A). Cathepsin B inhibitor (CA074-Me) also significantly reduced the replication of PEDV KD at 40 and 10 µM (Figure 2-5A) and PEDV AA at 40 µM. Chloroquine which inhibits acidification of endosomes significantly reduced the replication of PEDV KD or AA at 50 µM (Figure 2-5A). In confocal microscopy, there was no difference in the fluorescence signals of PEDV KD between trypsin only and trypsin + cathepsin B or L inhibitor at 1 h PI. At 4 h PI, the fluorescence signals were greatly reduced in cells without inhibitors, while there is still no change in the fluorescence signals in the cells with cathepsin B or L inhibitor (Figure 2-5B).
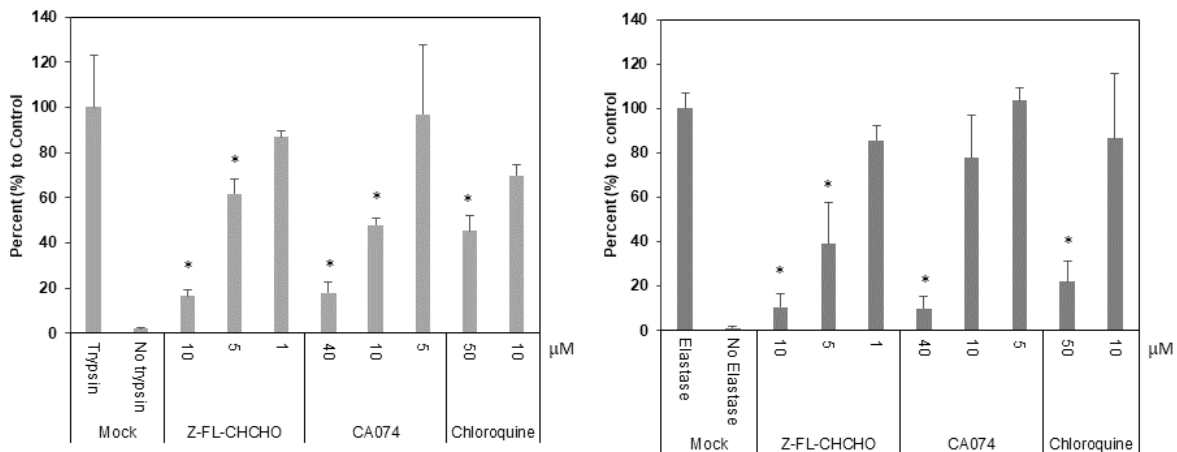
**B**
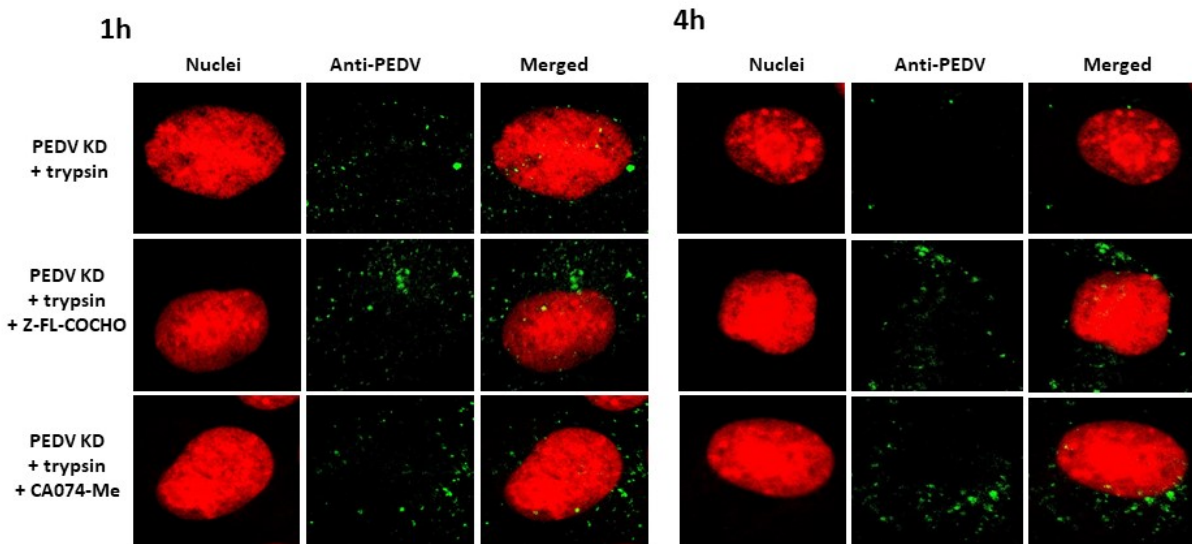


**Figure 2-5. Effect of Cathepsin inhibitors (Z-FL-CHCHO or CA074-Me) or chloroquine in PEDV entry into the cells.**

(A). Confluent Vero cells were pre-treated with mock (medium), Z-FL-CHCHO, CA074-Me or chloroquine for 1h before PEDV inoculation (MOI 10). Following virus infection, cells were incubated with same inhibitor in the presence of TPCK-treated trypsin(1 µg/ml) for PEDV KD (left panel) or elastase (1 µg/ml) for PEDV AA (right panel) at 37°C, and total RNAs were collected at 12 h PI. Viral replication was assessed by real time qRT-PCR. (B) Confluent Vero cells grown on Lab-Tek II CC2 chamber slides were pre-treated with mock(medium), Z-FL-CHCHO, CA074-Me, or chloroquine for 1h prior to PEDV inoculation (MOI 50). Then PEDV KD was inoculated to the cells with TPCK-treated trypsin (1 µg/ml). The cells were incubated at 37°C for 1 or 4 h, then fixed and stained for confocal laser scanning microscopy. Error bars show standard deviations. Asterisks indicate significant difference ($p < 0.05$) compared to the control (trypsin or elastase treatment only).

## 2.5 Discussion

Many viruses, including PEDV, utilize receptor-mediated endocytosis to gain entry into the host cells (J. E. Park et al., 2014). During the endocytic entry processes, viruses or viral genome

translocate to the cytoplasm (endosomal escapes) and initiate virus replication. Because the endosomal escape of the virus is critical for successful virus replication, viruses utilize various mechanisms for the events (Grove & Marsh, 2011; Gruenberg & van der Goot, 2006; Marsh & Helenius, 2006).    Early endosomes become progressively acidic as they mature into late endosomes and eventually into lysosomes. Endosomal proteases have been implicated in the crucial roles by digesting and processing of proteins transported in the endosomal/lysosomal compartments [reviewed in (S. Muller, Dennemarker, & Reinheckel, 2012)]. The S protein of SARS coronavirus and the Glycoprotein (GP) of Ebola virus are cleaved by endosomal proteases, such as cathepsin L and B, to expose a putative fusion domain (Chandran, Sullivan, Felbor, Whelan, & Cunningham, 2005; Cote et al., 2011; Ebert, Deussing, Peters, & Dermody, 2002; Grove & Marsh, 2011). For reovirus, a non-enveloped virus, endosomal proteases remove the outer-capsid protein σ3, which exposes the protein μ1. The μ1protein is involved in viral membrane-penetration, which allows the reovirus core particles to be delivered into the cytoplasm for transcription of the viral genome (Schiff, 1998). Recently we demonstrated that porcine enteric calicivirus (PEC) requires endosomal cathepsins and bile acids that are supplemented in the medium for viral endosomal escape (Shivanna, Kim, & Chang, 2014a, 2014b, 2015).

The addition of exogenous trypsin (or other proteases) is absolutely required for the isolation of PEDV from field samples as well as efficient replication of most PEDV strains (W. Li et al., 2016). It has been shown that proteases activity is required for efficient PEDV replication at the post-viral attachment stage, but where and how they work during virus entry is not clearly understood. Using two different PEDV strains KD or AA that were adapted to grow in the presence of trypsin or elastase, respectively, we investigated the roles of proteases in PEDV replication focusing on the viral entry events. One-step growth kinetic study showed that viral replication (or

RNA synthesis) occurs between 4-12 h PI (Figure 2-1) in the presence of trypsin or elastase. Without trypsin, no significant replication of PEDV KD occurred, indicating that this strain is heavily dependent on the presence of trypsin for replication. PEDV AA replication was significantly hampered by the absence of elastase but, interestingly, limited viral replication occurred even without elastase (or elastase with its inhibitor) (Figure 2-1). It is unclear how this limited viral replication occurs in the absence of elastase, but it is possible that it is associated with the fact that protease independent PEDV such as PEDV 8aa in our previous report (Y. Kim et al., 2017) can be generated by passaging the virus in the absence of any protease. It is possible that a minor population of the protease-independent PEDV may be generated spontaneously during the infection of PEDV KD or AA with trypsin or elastase, respectively, and elastase provides more favorable conditions for producing the protease-independent PEDV.

The leupeptin inhibition assay (Figure 2-2A) showed that trypsin is required for the post-viral attachment stage (Figure 2-2A and B), which is consistent with a previous study by Wicht et al (Wicht et al., 2014) where they reported that PEDV replication is significantly reduced when trypsin is inhibited after viral attachment to cellular receptors. During viral entry through receptors and endosomes, escaping of viral genomes from endosomes is critical for viral replication. Viral proteins in endosomes undergo conformational changes by decreasing pH and/or cleavage of viral proteins by host proteases in the endosomes, which leads to exposure of fusion domains or other mechanisms for membrane fusion and viral genome translocation to the cytoplasm (Grove & Marsh, 2011; Marsh & Helenius, 2006). Recently, our group has demonstrated the crucial events of the endosomal escape of PEDV and caliciviruses using confocal microscopy (Y. Kim et al., 2017; Shivanna et al., 2014b, 2015). In that confocal microscopy study, the fluorescence signals

for PEDV and caliciviruses co-localized with the endosome marker Rab7, and viral escape from the endosomes occurred at 3 h PI (Y. Kim et al., 2017; Shivanna et al., 2014b, 2015).

While PEDV KD and AA require different protease for efficient replication, there was no difference in viral trafficking in the early stages of viral replication (Figure 2-3). Both PEDV KD and AA were detected in the endosomes at 1 h PI regardless of the presence or absence of trypsin or elastase, but viral fluorescence signals disappeared at 4 h PI only in the presence of trypsin or elastase (Figure 2-3A for PEDV KD and 3B for PEDV AA). These suggested both PEDV KD and AA were able to escape from the endosomes at 4 h PI only in the presence of protease. At 6 h PI, viral signals were detected on perinuclear areas for both PEDV KD and AA in the presence of trypsin and elastase, respectively (Figure 2-4A), and the signals were co-localized with ER marker (PDI3A) (only PEDV KD was shown in Figure 2-4B), suggesting active viral protein synthesis (with replication). Without proteases, viral signals remained at endosomes (co-localized with an endosome marker, VPS26A) at 6 h PI (Figure 2-4A and 4B) or later time points up to 24 h PI (data not shown). This is consistent with our previous report with viral trafficking through endosomes, and interference with the proper viral escapes led to a significant reduction of viral replication (Y. Kim et al., 2017; Shivanna et al., 2014b, 2015).

Cathepsins are host proteases that are usually found in the endosomal compartments. The cathepsin family is classified into cysteine (cathepsins B, L, H, K, S, and O), aspartyl (cathepsin D and E) and serine (cathepsin G) proteases (Vasiljeva et al., 2007b). Cathepsin B and L have been reported to be involved in virus fusion and/or uncoating of some coronaviruses including SARS coronavirus, feline coronavirus and murine hepatitis virus (MHV) (Bosch, Bartelink, & Rottier, 2008; Y. Kim et al., 2013; Qiu et al., 2006). A previous study using the pseudovirus of PEDV reported that PEDV S protein is activated by cathepsins, and a lysosomal acidification inhibitor,

or lysosomal cysteine protease inhibitors including cathepsin B (CA074) and L (Z-FY-CHO) inhibitors significantly reduced pseudovirus entry and PEDV replication (C. Liu et al., 2016). The results from this study are consistent with the previous study (C. Liu et al., 2016) demonstrating that cathepsins are required PEDV entry. We further demonstrated that cathepsin L and B inhibitors (Z-FL-CHCHO or CA074, respectively) inhibited the replication of PEDV KD and AA strain via interfering with the endosomal viral escapes (Figure 2-5A and B).

Based on the results, we established a proposed model for protease-mediated PEDV replication in Vero cells. In this model, PEDV binds to its receptor (APN), enters the cells via the endocytic pathway to reach the late endosomes, which is independent of exogenous protease in the medium. In the presence of exogenous protease, the activation of S protein can lead to virus escape from the late endosomes into the cytoplasm to initiate virus replication. In addition to exogenous protease, cathepsins in the endosomes are required for the successful endosomal escape of PEDV. In the absence of protease, PEDV remains in the late endosomes/lysosomes and is destined to be degraded.

## 2.6 Acknowledgement

# Chapter 3 - Endosomal escape of protease independent PEDV is facilitated by acid sphingomyelinase mediated ceramide formation

## 3.1 Abstract

During the receptor-mediated endocytic pathway, viruses need to escape from the endosomes to the cytoplasm to initiate successful replication. The activation of acid sphingomyelinase (ASM) facilitates ceramide formation on the cell membrane and alters membrane permeability. Because it was shown that this ASM/ceramide pathway plays important role in the replication of various viruses, we examined this pathway in the entry events of porcine epidemic diarrhea virus (PEDV) with the trypsin independent strain (PEDV 8aa) with various methods including the confocal microscopy. In this report, we demonstrated the PEDV 8aa induces ASM activation and ceramide formation, which is crucial for viral replication. Inhibition of ASM with small molecule inhibitors or siRNA significantly reduced the replication of PEDV 8aa by inhibition of viral endosomal escape events.

## 3.2 Introduction

The majority of viruses utilize the receptor-mediated endocytosis to deliver their genetic cargo into the cell cytoplasm or nucleus to initiate the RNA/DNA replication (White & Whittaker, 2016; Yamauchi & Helenius, 2013). Viruses traveling the endocytic pathway must escape from the endosome to the cytoplasm to initiate the replication, if not they will be degraded by various endo-lysosomal enzymes (Hogle, 2002; Kielian & Rey, 2006; Moyer & Nemerow, 2011). Therefore, the successful escape from the endosomes is essential for viral infection and replication.

Various constituents of cellular endocytic machinery are reported to participate in the virus entry. One of them is the acid sphingomyelinase (ASM)/ceramide pathway. Activation of ASM (or SMPD1) hydrolyzes sphingomyelin to produce bioactive lipid ceramide (Marchesini & Hannun, 2004) on the cell membranes. The generated ceramides are accumulated, leading to formation of large ceramide-enriched membrane platforms, which modulate the biophysical properties of membranes resulting in shift of the plasma membrane fluidity, and further selectively trap receptors and signaling molecules for amplifying cellular signaling (Grassme, Jekle, et al., 2001; Gulbins & Li, 2006; Utermohlen et al., 2008). ASM can be activated by various stimuli including stress, ionizing, death receptors, irradiation, UV light, or heat (X. He et al., 2003; Stancevic & Kolesnick, 2010). Important roles of ASM mediated ceramide formation have also been documented in studies of various pathogens including Measles virus (Avota et al., 2011), rhinovirus (Grassme et al., 2005), Japanese encephalitis virus (Tani et al., 2010), and Ebolavirus (Miller et al., 2012) as well as *Neisseriae gonorrhea* (Grassme et al., 1997), *Pseudomonas aeruginosa*(Grassme, Jendrossek, et al., 2003) and *Staphylococcus aureus* (Esen et al., 2001). Our previous reports have also demonstrated that ASM/ceramide is important in the entry of caliciviruses including feline calicivirus (FCV), murine norovirus (MNV) and porcine enteric calicivirus (PEC) (Shivanna et al., 2015).

The porcine epidemic diarrhea virus (PEDV) is an alphacoronavirus with a single-stranded, positive-sense RNA genome. The PEDV infection leads to severe liquid diarrhea and vomiting in older pigs or extreme dehydration and death in suckling piglets(Jung & Saif, 2015). Since the 2013 PED outbreak in the US(Stevenson et al., 2013), the highly virulent genotype 2 PEDV strains have spread through Asia, America, and European continents raising significant economic losses in the swine industry. In our previous study, distinct PEDV US strains, 8aa and KD were generated

by serially passaging under different culture conditions including bile acids (glychenodeoxycholic acid, GCDCA) and trypsin to obtain suitable vaccine strains (Y. Kim et al., 2017). While PEDV KD strain requires trypsin for efficient replication in cells like most of PEDV isolates, PEDV 8aa does not need any exogenous protease for efficient replication. Using PEDV 8aa, we studied the role of ASM in PEDV entry, viral endosomal escape, and replication. Here, we demonstrated PEDV can activate ASM and ceramide formation, and inhibition of ASM with small molecule inhibitors or siRNA could reduce PEDV 8aa replication via inhibition of viral endosomal escape events.

## 3.3 Materials and methods

### 3.3.1 Viruses, cells, and reagents.

The cell culture adapted PEDV 8aa was propagated on Vero cells as described previously (Y. Kim et al., 2017). The cultured viruses were concentrated by ultracentrifugation at 25,000 rpm with 30% w/v sucrose cushion at 4°C for 2h in an SW27 rotor. The pellets were resuspended in serum-free MEM and stored in -80°C. Vero cells (ATCC-CCL-81[tm]) were obtained from ATCC (Manassas, VA) and maintained in Dulbecco's minimal essential medium (DMEM) containing 5% fetal bovine serum (FBS) and antibiotics (chlortetracycline [25 μg/ml], penicillin [250 U/ml], and streptomycin [250 μg/ml]). For ASM inhibitors, AY9944 was purchased from Santa Cruz Biotech (Santa Cruz, CA), desipramine and fluoxetine were purchased from Sigma-Aldrich (St Louis, MO). The anti-PEDV polyclonal antibody was collected from a pig challenge study previously reported by our group(Y. Kim et al., 2017). Monoclonal antibody to ceramide, VPS26A

(an endosomal marker), or PDIA3 (an ER marker) was obtained from Santa Cruz Biotech (Santa Cruz, CA).

### 3.3.2 Confocal microscopy.

50% confluent Vero cells on Lab-Tek II CC2 chamber slide (Thermo Fisher Scientific, Waltham, MA) were pretreated with 50 μM of AY9944 at 37°C for 1h. The cells were inoculated with Mock-medium or PEDV 8aa at an MOI of 50 and incubated at 37°C for 1h. Following three times washing with PBS, the cells were replenished with fresh media containing Mock-DMSO or 50 μM of AY9944. Further incubation times differed for the purpose of the study: 4 h for ceramide formation study, 1, 3, 6, 9 and 12 h for endosomal escape study and 12 h for the intracellular location of PEDV. To prepare for the confocal microscopy, cells were fixed in 4% paraformaldehyde (Sigma-Aldrich) in PBS at room temperature (RT) for 15 min, permeabilized with 0.1% Triton x100 in PBS for 10 min at RT. Then, the cells were incubated in blocking buffer (5% bovine serum albumin in PBS) for 15min. After three-time washing with PBS, the cells were incubated with anti-PEDV polyclonal pig serum, mouse anti-ceramide antibody, mouse anti-VPS26A, or mouse anti-PDIA3 at 37°C for 2h. Followed by the appropriate secondary antibodies with FITC and Alexa Flour$^{TM}$ 633, the nucleus was stained with SYTOX orange (0.5 μM in 0.9% NaCl). Coverslips were mounted with ProLong$^{TM}$ Gold antifade reagent (Invitrogen, CA), and the cells were scanned with a confocal microscope LSM 510 (Zeiss, Oberkochen, Germany) using a 100x oil-immersion objective lens. The images were processed by ImageJ software 1.52b (http://imagej.nih.gov/ij/). The amounts of ceramide signal in the cytoplasm of cells were measured with the relative pixel intensity from randomly selected 10 cells of each treatment. Colocalization analysis was conducted using JACoP plugin in ImageJ software. Especially, the

colocalization of PEDV and ceramide was examined carefully with various time points and magnitudes.

### 3.3.3 Inhibition of ASM by ASM inhibitors.

Serial dilutions of ASM inhibitors including AY9944, desipramine or fluoxetine were used to explore an effect of ASM activity on PEDV replication. Confluent Vero cells in 12-well plates were preincubated with serial dilutions of each inhibitor or DMSO (less than 0.1%) at 37°C for 1 h and infected with PEDV 8aa at an MOI of 0.01. After 1h incubation, the cells were washed three times with PBS, replenished with MEM containing the same concentration of the inhibitor or DMSO, and further incubated at 37°C for 24 h. Total RNA was isolated from the cells for real-time qRT-PCR for measuring PEDV RNA levels.

### 3.3.4 Small interfering RNA (siRNA) transfections.

siRNA for ASM was designed based on the green monkey SMPD1 gene (GenBank accession no. NC_023642) and synthesized by Integrated DNA Technology (Coralville, IA). The two sets of ASM siRNAs were designed: ASMsiRNA_1 (5'-rGrGrUrCrUrArUrUrCrArCrCrGrCr CrArUrC and 5'-rCrArArGrGrUrUrGrArUrGrGrCrGrGrUrG) and ASMsiRNA_2 (5'-rCrCrArUr GrArGrArCrUrUrArCrArUrCrCrU and 5'-rCrArGrArUrUrCrArGrGrArUrGrUrArArGrU). One-day old 50~70% confluent Vero cells were transfected with Mock-medium (transfection agent), irrelevant siRNA (negative control from Qiagen) or ASM siRNA sets using Lipofectamine RNAiMAX (Thermo Fisher Scientific) following the manufacturer's protocol and incubated at 37°C. After 48h post-transfection, the cells were inoculated with PEDV 8aa at an MOI of 0.01. After 1h incubation for virus attachment and entry, cells were replenished with fresh media

containing mock-medium, and further incubated for 24h. Total RNA was isolated from the cell lysates using the RNeasy kit (Qiagen, CA) according to the manufacturer's protocol. Viral RNA titers were measured by real-time quantitative RT-PCR.

### 3.3.5 Real-time quantitative RT-PCR.

Real-time quantitative RT-PCR was performed to determine ASM expression levels after siRNA transfection, and PEDV RNA levels after virus infection using the one-step platinum RT-PCR kit (Invitrogen, CA). ASM specific mRNA levels were measured with the primer/probe set with 5'-CCCAGTCTGCAAAGGTCTATT-3', 5'-GCAGATTGCACAGCTTGATG-3', and probe: 5'-56-FAM/TGGGCTGAA/ZEN/GAAGGAA CCCAATGT/3IABkFQ/-3' targeting African green monkey ASM. PEDV RNA levels were determined with the primer/probe set: F-5'-GCTATGCTCAGATCGCCAGT-3', R-5'-TCTCGTAAGAGTCCGCTAGCTC-3', and probe: 5'/56-FAM/TGCTCTTTG/ZEN/ GTGGTAATGTGGC/3IABkFQ/-3' targeting the PEDV N gene (Y. Kim et al., 2017). β-actin expressions were measured using the specific primer sets to normalize variations and calculate $\mathit{\Delta\Delta}$CT values. The condition for both reactions was 50°C for 30 min (for RT) and 95°C for 5 min, then 40 cycles of denaturation at 95°C for 15s, annealing at 60°C for 60s and elongation at 72°C for 30s. The Ct values for PEDV RNA were converted to the $\text{Log}_{10}$ $\text{TCID}_{50}$ equivalents/ml based on the equation derived from the standard curve generated from the serial dilution of cell culture-grown PEDV (Y. Kim et al., 2017).

### 3.3.6 Cathepsin inhibition assay.

Serial dilutions of cathepsin L inhibitor (MDL 28170), cathepsin B inhibitor (CA074-Me) or an endosomal acidification inhibitor (chloroquine) were used to determine an effect of

endosomal proteases or maturation on PEDV replication. Confluent Vero cells in 12-well plates were preincubated with serial dilutions of each inhibitor or DMSO(less than 0.1%) at 37°C for 1 h and infected with PEDV 8aa at an MOI of 0.01. After 1h incubation, the cells were washed three times with PBS, replenished with MEM containing the same concentration of the inhibitor or DMSO, and further incubated at 37°C for 24 h. Total RNA was isolated from the cells for real-time qRT-PCR for measuring PEDV RNA levels.

### 3.3.7 Statistical analysis.

The effect of ASM inhibitors or ASM siRNA and the ceramide pixel intensities were analyzed using Graph Pad Prism 5 (GraphPad Software, La Jolla, CA) with Student's *t*-test. *P*-value < 0.05 (two-tailed) was considered statistically significant. All the results shown were from at least three independent experiments.

## 3.4 Results

### 3.4.1 PEDV infection in Vero cells induces ASM mediated ceramide formation.

We have previously reported that incubation of live or inactivated FCV or MNV to the permissible cells induced the ceramide formation (Shivanna et al., 2015), and the increased ceramide facilitated viral endosomal escape and viral replication. Since PEDV is also known to utilize the endocytic pathway, we investigated if the inoculation of PEDV to Vero cells triggers ceramide formation using confocal microscopy. The confocal images of cells with Mock-medium infection showed minimal levels of ceramide signals (Figure 3-1A). Incubation of PEDV 8aa at an MOI of 50 for 1 h, and further incubation for 4 h, the ceramide signals in cells significantly increased (Figure 3-

1A) up to 4-fold increase from the base-line. The treatment with ASM inhibitor abolished the ceramide induction by PEDV 8aa (Figure 3-1C and 1D). At this time point, PEDV was found in the endosomes in the cells as we reported before(Y. Kim et al., 2017). However, there was no evidence for the co-localization of PEDV and ceramide with various conditions (Figure 3-1B).
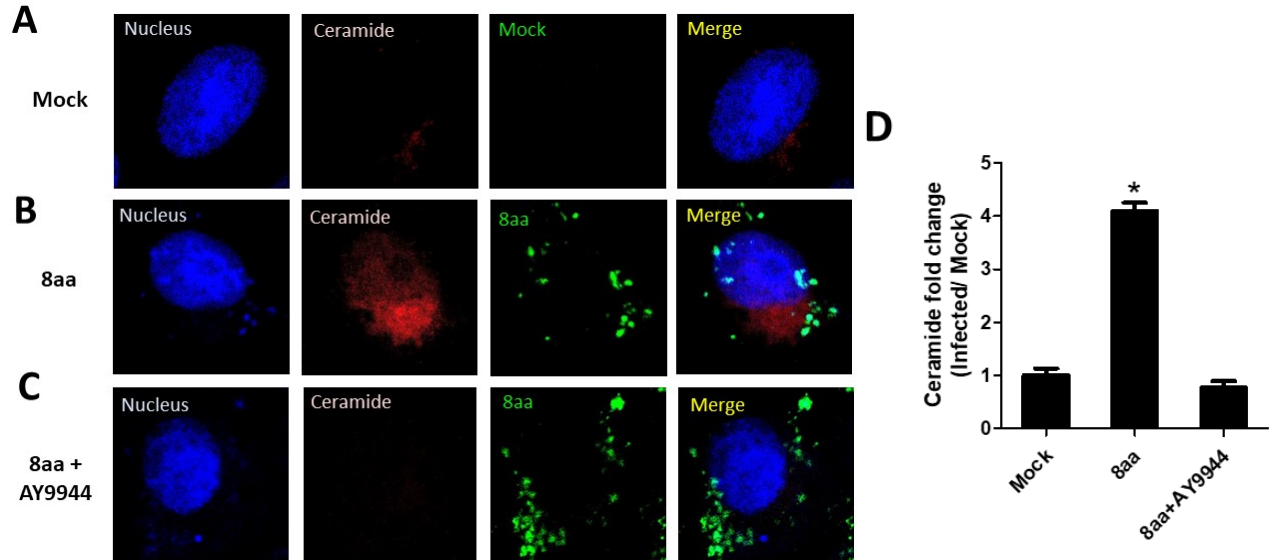


**Figure 3-1. Ceramide formation by PEDV inoculation on Vero cells.**
Vero cells were pretreated with DMSO (0.1%) or 50 μM of AY9944 at 37°C for 1h, followed by inoculation of Mock-medium (A), 50 MOI of PEDV 8aa (B and C). Following 1 h incubation, cells were washed with PBS and then added with fresh media containing same concentration of DMSO or AY9944, further incubated at 37°C for 4h. Cells were then fixed for confocal microscopy. Nuclei (blue), ceramide (red), PEDV(green) or merged images were presented. The relative pixel intensity was measured from randomly selected 10 cells of each treatment. Asterisks indicate a significant difference compared to the Mock (*, $P < 0.05$) (D).
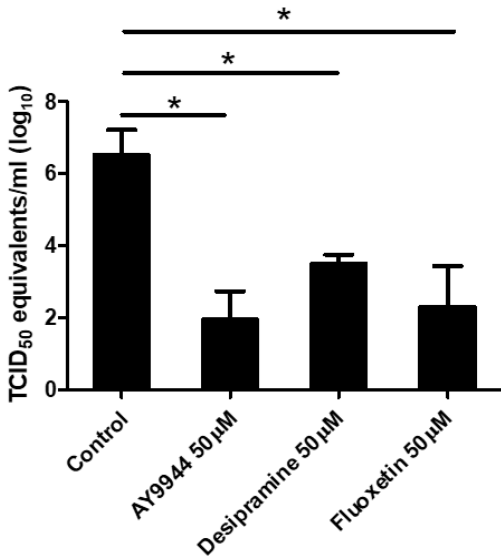
**Figure 3-2. Effect of ASM inhibitors on PEDV replication.**

Confluent Vero cells were preincubated with DMSO or each ASM inhibitor at 37 ° C for 1 h, followed by inoculation with PEDV 8aa. After the incubation, cells were washed 3 times with PBS, replenished with fresh media containing same concentration of inhibitor and further incubated at 37°C for 24 h. Viral replication was determined by real-time qRT-PCR and converted to the $TCID_{50}$ equivalents/ml. Asterisks indicate significant difference compared to the control (*,$P < 0.05$), ns: non-significant difference.

### 3.4.2 The inhibition of ASM significantly reduced the replication of PEDV 8aa.

To determine the roles of ceramide formation by ASM in the PEDV replication, we infected 8aa on Vero cells with ASM inhibitors and measured PEDV replication. Three well-known ASM inhibitors were used in this study including AY9944, desipramine, and fluoxetine. These are known to block and degraded ASM within cells and thereby inhibit ceramide formation (Kornhuber et al., 2010). The cytotoxic concentrations of each inhibitor were tested in Vero cells, and the concentration showing minimal cytotoxicity for each compound was determined. In the presence of each ASM inhibitor at 50 μM, the replication of PEDV 8aa was significantly reduced by 3 - 4.6 $log_{10}$-fold compared to the mock treatment control (Figure 3-2A). To further confirm the effects of ASM on PEDV replication, two ASM specific siRNAs were designed and tested against ASM mRNA levels and PEDV replication. The transfection of each siRNA at 100 nM to Vero cells, significantly decreased ASM RNA levels by at least 85% compared to the transfection with mock-medium or irrelevant siRNA treatment (Figure 3-3A). The transfection of each ASM

siRNA also significantly reduced the replication of PEDV 8aa by 80.7~91.9% compared to the transfection with mock-medium or irreverent siRNA (Figure 3-3B).
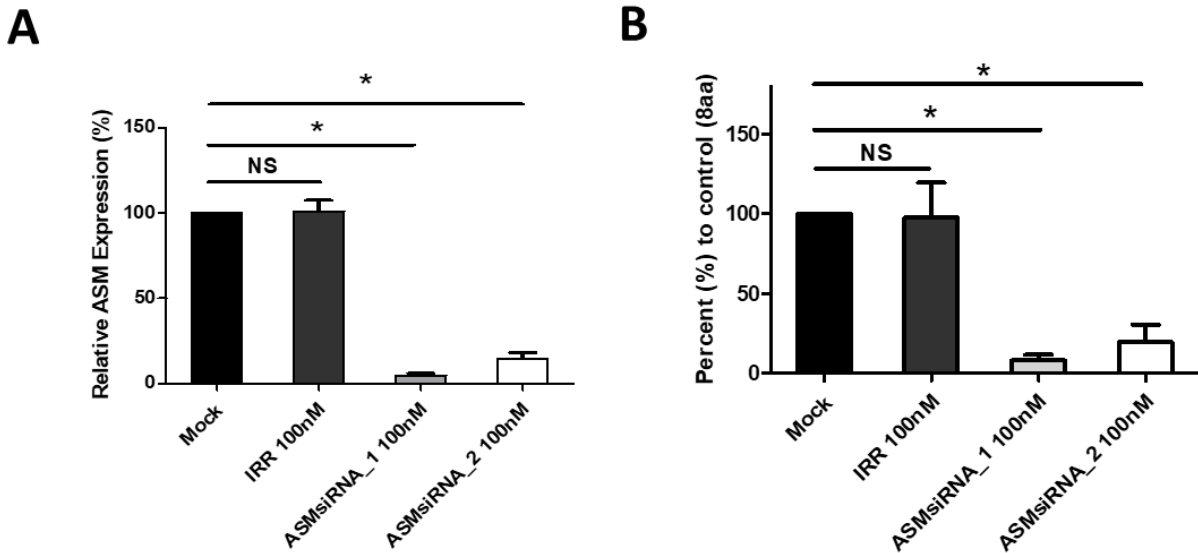


**Figure 3-3. Effect of ASM siRNA on ASM RNA levels (A) and PEDV replication (B).** Vero cells were transfected with Mock-medium, ASM specific siRNA (1 and 2) or irrelevant siRNA (IRR). After 48 h, cells were inoculated with PEDV 8aa at an MOI of 0.01, and viral replication was measured at 24 h PI by real-time qRT-PCR. Asterisks indicate significant difference compared to the control (*,$P < 0.05$), ns: non-significant difference.

### 3.4.3 Ceramide formation facilitated the endosomal escape of PEDV 8aa.

The effects of ASM mediated ceramide formation on PEDV endosomal escape were examined by using the confocal microscopy. Vero cells inoculated with PEDV 8aa, the viral fluorescence signals were detected within the endosomes up to 6 h PI with and without ASM inhibitor (Figure 3-4A top). At 9 h PI, PEDV signals disappeared from the endosomes without the inhibitor (Figure 3-4A middle row), but remained in the endosomes in the presence of the inhibitor (Figure 3-4B middle row), suggesting that virions escaped from the endosome in the absence of the inhibitor, and the inhibitor blocked the escape events. At 12 h PI, strong and diffused fluorescence signals of PEDV were observed around the nucleus without the inhibitor (Figure 3-

4A bottom row), which were colocalized with PDIA3 (an ER marker) (Figure 3-5), which suggests

newly synthesized PEDV proteins and active viral replication (Figure 3-4A bottom, Figure 3-5).

However, in the presence of the inhibitor, PEDV signals remained in the endosomes (Figure 3-4B

bottom row), colocalized with VPS26A (Figure 3-5).
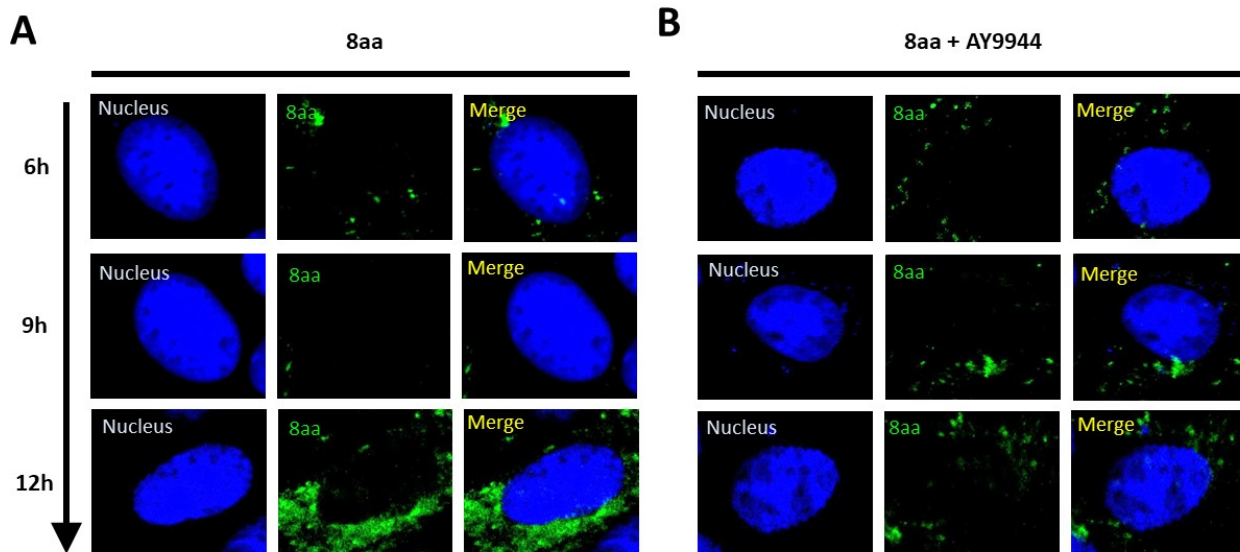


**Figure 3-4. Effects of ASM inhibitor on the endosomal escape of PEDV 8aa.**
Confluent Vero cells were infected with PEDV 8aa at an MOI of 50 and incubated with DMSO or
AY9944 (50 μM) for 1h, 3h, 6h, 9h, or 12h. Cells were fixed and probed with swine polyclonal
anti-PEDV antibody, followed by FITC-labeled goat-anti-swine antibody (green). Nuclei were
stained with SYTOX orange (5 μM)(Blue) as described in the text. Merged images of PEDV with
nuclei were presented.
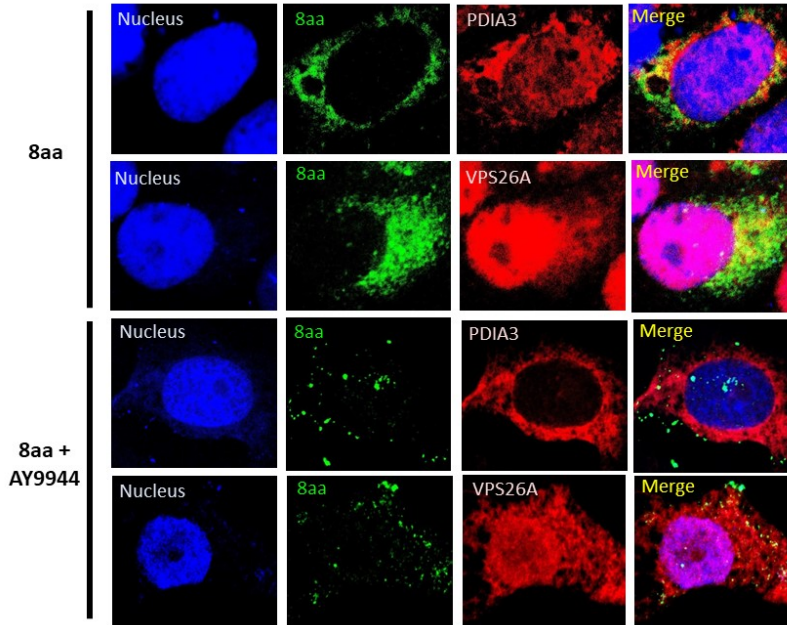
**Figure 3-5. Co-localization of PEDV 8aa with the endosome (VPS25A) or ER(PDIA3) marker.**

Confluent Vero cells were infected with PEDV 8aa at an MOI of 50 and incubated with DMSO or AY9944 (50 μM). Cells were at 12 h PI and probed with the antibody to PEDV, VPS26A and PDIA3, followed by FITC-labelled goat-anti-swine antibody (green), anti-mouse Alexa Flour 633 (red) and nuclei (blue). Merged images were prepared for the colocalization.
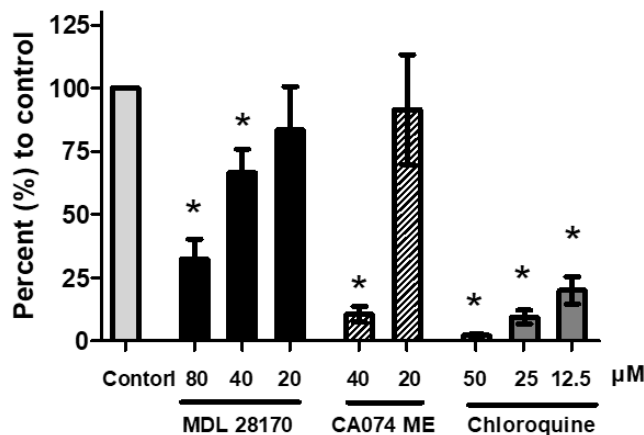


**Figure 3-6. Effect of cathepsin inhibitors (MDL 28170 or CA074 ME) or chloroquine in PEDV 8aa replication.**

Confluent Vero cells were pre-treated with mock (medium), MDL 28170, CA074 ME, or chloroquine for 1h before PEDV inoculation (MOI 0.1). After virus infection, cells were replenished with the same concentration of inhibitor at 37°C and total RNA was isolated at 12h PI. Viral replication was determined by real-time qRT-PCR. Asterisks indicate significant difference compared to the control (*,$P < 0.05$) (D).

### 3.4.4 Cathepsin activity and endosomal maturation are required for efficient replication of PEDV 8aa.

As the PEDV 8aa passes through the endosomal pathway, the roles of endosomal proteases (cathepsin B and L) or the endosomal acidification in PEDV 8aa replication were explored. In advance of the experiment, the cytotoxicity of each inhibitor was established in the Vero cells, and the minimal toxicity concentrations were used. Treatment of the cells with MDL 28170 at 80 and 40 μM or CA0740Me at or 40 μM significantly inhibited PEDV 8aa replication (Figure 3-6). The treatment of chloroquine also significantly reduced the replication of PEDV 8aa (Figure 3-6).

## 3.5 Discussion

It has been shown that ASM-mediated ceramide formation plays an important role in the replication of various viruses including Measles virus (Avota et al., 2011), rhinovirus (Grassme et al., 2005), Japanese encephalitis virus (Tani et al., 2010), and Ebolavirus (Miller et al., 2012). The precise roles of ceramide and ASM in the viral infection remain to be established. There are several possible explanations for the effects of ASM in viral replication including initiating signaling cascade via ceramide, segregation of membrane receptors at large lipid rafts, and alteration of the membrane biophysics which can increase membrane fusogenicity (Grassme et al., 2007; Zhang et al., 2009). Activated ASM cleaves the polar head of compact shaped sphingomyelin, which generates cone-shaped ceramide at one leaflet of the lipid bilayer and induces an asymmetric membrane tension (Lopez-Montero et al., 2010). This increased ceramide on the plasma membrane leads to fluidity change, triggering a sequence of membrane perturbation, all of which consequently propel intracellular membrane fusion (Utermohlen et al., 2008). Thus, ASM and ceramide formation may facilitate viral fusion to cell membranes and viral entry events.

Coronaviruses are not only one of the most important current zoonotic viruses, but also future health threats due to their ability to adapt to new host via rapid mutations. While there are many different coronaviruses infecting humans and animals, they utilize S protein to bind corresponding receptors and the receptor-mediated endocytosis events are well conserved. These conserved features may be the targets for broad-spectrum antiviral drug development. PEDV provides a unique model to study coronavirus entry because most strains require exogenous protease for efficient replication in cultured cells. However, we and others isolated protease independent PEDV strains that can replicate well in cultured cells without any exogenous proteases. Trypsin dependent PEDV KD strain is representing most of the cell-culture adapted PEDV strains which require exogenous protease. This strain enters target cells via the endocytic pathway and subsequently can escape from endosomes only in the presence of exogenous protease (trypsin) (Oh et al., 2019). However, protease-independent PEDV 8aa escapes from the endosomes without any exogenous protease. Because most coronaviruses do not require exogenous protease for efficient replication in cells, this strain may serve a good model for ASM/ceramide studies on the coronavirus entry.

The formation of ceramide by coronavirus infection also has been mentioned by an earlier human coronavirus study (Muller et al., 2018). Lipidome analysis of human coronavirus-229E infected Huh-7 cells demonstrated the upregulation of ceramides and lysophospholipids, but the relationship between the ceramide upregulation and replication of HCoV-229E was not investigated. First, we investigated if PEDV could activate ASM and ceramide formation in Vero cells. Incubation of PEDV 8aa at an MOI of 50 for 1 h (and an additional 4 h), the ceramide signals in cells significantly increased (Figure 3-1) detected by the confocal microscopy. During this time point, virus particles were observed in the endosomes in the cells (Figure 3-1). Previous Ebola

virus study demonstrated that the EBOV pseudotyped virus colocalized with the ASM on the cell surface (non-permeabilized treatment) at an early time of infection (30min – 90min pi) suggesting recruitment of ASM by virus binding (Miller et al., 2012). We tried to explore the same early ASM recruitment by PEDV binding. The number and intensity of ASM signals were gradually increased on the cell surface after PEDV infection. However, there was no evidence for the colocalization of PEDV and ASM (Data not shown), which may be due to the different virus type and entry mechaism.

Recently, our group has demonstrated the importance of ASM activation on viral escapes from endosomes and successful replication with caliciviruses. Among caliciviruses, FCV and MNV can grow well in the cells without any supplement, but PEC can replicate in the cells only in the presence of bile acids. Incubation of live or inactivated FCV or MNV to the permissible cells induced the ceramide formation, viral escapes from endosomes and successful replication (Shivanna et al., 2015). However, when PEC was the inoculation to the cells, while viruses entered into endosomes, they were not able to escape from the compartment, and degraded. Bile acids facilitated viral escapes from endosomes and successful replication (Shivanna et al., 2015). The results with PEDV 8aa were similar to our studies with caliciviruses, showing ASM activation and ceramide formation by PEDV is crucial for viral escapes from endosomes and successful replication. Both small molecule inhibitors and specific siRNA to ASM significantly reduced the replication of PEDV 8aa (Figure 3-2 and 3-3). When we further studied which step of 8aa replication was affected by ASM inhibition, both could block viral escape events from endosomes (Figure 3-4 and 3-5).

There have been numerous reports that cathepsins and endosomal maturation are involved in the various virus lifecycle including influenza A virus, SARS CoV, and  MHV (Edinger, Pohl,

Yángüez, & Stertz, 2015; Qiu et al., 2006; Simmons et al., 2005). That was also previously reported by our group that the treatment of cells with cathepsin inhibitor or chloroquine significantly reduced calicivirus and protease adapted PEDV replication through interfering endosomal escape of the viruses(Shivanna et al., 2014b) (Oh et al., 2019). These previous results are consistent with the results of PEDV 8aa from this study (Figure 3-6) that the treatment of cathepsin inhibitors and chloroquine significantly decreased 8aa titer. The roles of caspases during viral replication can be explained by cleavage of viral structural protein by them. SARS S protein, PEC VP2, or MNV-1 and FCV VP1 are known to be cleaved by cathepsin L (Bosch et al., 2008; Shivanna et al., 2014b) and the cleaved structural protein may contribute to virus-cell membrane fusion or capsid uncoating to allow translocation of viral genomes. These results suggest different viruses (enveloped PEDV or non-enveloped caliciviruses) utilize the same pathways for transferring genetic materials from endosomes to cell cytoplasm where the translation may initiate with positive-sense RNAs. Understanding this shared mechanism may provide therapeutic targets for broad-spectrum antiviral development against diverse viruses from different families.

## 3.6 Acknowledgment

# Chapter 4 - Caspase-Mediated Cleavage of Nucleocapsid protein of a Protease-Independent Porcine Epidemic Diarrhea Virus Strain

## 4.1 Abstract

Porcine epidemic diarrhea virus (PEDV) infection in neonatal piglets can cause up to 100% mortality, resulting in significant economic loss in the swine industry. Like other coronaviruses, PEDV N protein is a nucleocapsid protein and abundantly presents at all stages of infection. Previously, we reported that the N protein of trypsin-independent PEDV 8aa is cleaved during virus replication. In this study, we further investigated the nature of N protein cleavage using various methods including protease cleavage assays with or without various inhibitors and mutagenesis study. We found that PEDV 8aa infection in Vero cells leads to apoptotic cell death, and caspase 6 or 7 can cleave PEDV 8aa N protein at the late stage of the replication. The caspase-mediated cleavage occurs between $D^{424}$ and $G^{425}$ near the C-terminal of N protein. We also report that both cleaved and uncleaved N proteins are exclusively localized in the cytoplasm of PEDV infected cells.

## 4.2 Introduction

Porcine epidemic diarrhea virus (PEDV) is an enveloped virus with a single-stranded positive-sense RNA genome of about 30 kb and a member of the genus Alphacoronavirus in the family *Coronaviridae* (Kocherhans, Bridgen, Ackermann, & Tobler, 2001). PEDV can cause an enteric disease (PED) with high mortality of up to 100% in neonatal piglets. There are at least two genogroups with PEDV with classical genogroup 1 and newly emerging genogroup 2 (Y. W.

Huang et al., 2013; Jung & Saif, 2015). Genogroup 1 PEDV has circulated among countries in Europe and Asia since the early 1980s (Y. W. Huang et al., 2013). In 2013, the first outbreak with genogroup 2a PEDV occurred in the US (Stevenson et al., 2013) and subsequently in Canada and Mexico (Anastasia et al., 2014; Q. Chen et al., 2014; Pasma, Furness, Alves, & Aubry, 2016), resulting in death of 7 million pigs during one year epidemic period (Cima, 2014). Moreover, there are several reports that the US PEDV strains (genogroup 2) caused outbreaks in European (Grasland et al., 2015; Hanke et al., 2015; Theuns et al., 2015) and Asian countries (S. Lee & Lee, 2014; C. N. Lin et al., 2014; Van Diep et al., 2015), which raised significant economic and public health concerns worldwide (Schulz & Tonsor, 2015).

Coronavirus genome encodes four major structural proteins including spike (S), envelope (E), membrane (M) and nucleocapsid (N) (Duarte, Gelfi, Lambert, Rasschaert, & Laude, 1994). Among them, N protein is an abundant structural protein present at all stages of infection. The coronavirus N protein is composed of multiple domains including N1 (or N-terminal domain), N2 (or C-terminal domain) and N3 with spacers between them (K. R. Hurst, Koetzner, & Masters, 2013). Both N1 and N2 are very basic and interact with the viral RNA genome and/or N protein (K. R. Hurst et al., 2013). N3 is the carboxy-terminal part (~45 aa) with an excess of acidic residues and known to interact with M protein (Kelley R. Hurst et al., 2005; Verma, Bednar, Blount, & Hogue, 2006). The primary role of N protein is to act as an essential architecture component in coronavirus assembly through the interactions with N, M and viral RNA (Cavanagh, 1997). In addition to its primary role, N protein appears to perform multiple functions in the viral replication cycle and viral pathogenesis (McBride, van Zyl, & Fielding, 2014). Some previous research suggests that the N protein correlates with optimal coronavirus RNA transcription and/or replication, by acting as RNA chaperones to assist the template-switching steps (Zuniga et al.,

2010; Zuniga et al., 2007), and participating in the replicase components for efficient RNA synthesis (K. R. Hurst et al., 2013; K. R. Hurst, Ye, Goebel, Jayaraman, & Masters, 2010). In several studies, N protein was also shown to be involved in host cell signaling and immune responses to facilitate viral replication (Cao et al., 2015; X. Xu et al., 2013).

It was reported that N protein of acute respiratory syndrome coronavirus (SARS-CoV) or transmissible gastroenteritis virus (TGEV) is processed by caspases during apoptotic cell death (Diemer et al., 2008; Eleouet et al., 2000). The N protein cleavage was implied for playing roles in efficient viral replication and pathogenicity (Diemer et al., 2008; Eleouet et al., 2000). For PEDV N protein, Jaru-Ampornpan et al. demonstrated that virally-encoded 3C-like protease (3CLpro) cleaves PEDV N protein during virus replication and the cleavage is associated with viral adaptation in cell culture (Jaru-Ampornpan et al., 2017). Previously, we reported two forms of N protein from the protease independent PEDV 8aa strain, while only one form from the protease dependent PEDV KD strains (Y. Kim et al., 2017). We hypothesized that the two forms of N protein are generated by a post-translational modification by a host or cellular protease(s) during the replication of the PEDV 8aa strain. Here, we demonstrated that the N protein of PEDV 8aa strain is cleaved by caspases during apoptosis of Vero cells. The PEDV N protein was cleaved by caspase 6 or 7 between $D^{424}$ and $G^{425}$ near the C-terminal of N protein. Furthermore, N protein was localized exclusively in the cytoplasm of PEDV infected cells regardless of N protein cleavage. Our results demonstrated characteristics during the replication of PEDV 8aa, which provides valuable information to understanding PEDV biology.

## 4.3 Materials and methods

### 4.3.1 Viruses, cells, and reagents.

The cell culture adapted PEDV US strains (8aa and KD) were propagated in Vero cells without any protease (8aa strain) or in the presence of TPCK-treated trypsin (1 μg/ml) (KD strain) as described previously (Y. Kim et al., 2017). Vero (ATCC-CCL-81[tm]) cells and HEK 293T cells were obtained from ATCC (Manassas, VA). Vero cells were maintained in Dulbecco's minimal essential medium (DMEM) containing 5% fetal bovine serum (FBS) and antibiotics (chlortetracycline [25 μg/ml], penicillin [250 U/ml], and streptomycin [250 μg/ml]). HEK293T cells were maintained in minimal essential medium (MEM) containing 10% fetal bovine serum (FBS) and the antibiotics. L-1-tosylamide-2-phenylethyl chloromethyl ketone (TPCK)-treated trypsin and Leupeptin was purchased from Sigma-Aldrich (St. Louis, MO). Furin inhibitor I was purchased from Cayman (Ann Arbor, MI). Pan-caspase inhibitor, Z-VAD.fmk was purchased from Enzo (Farmingdale, NY). Recombinant human Caspase 3 and 6 were purchased from Millipore (Temecula, CA) and recombinant caspase 7 were purchased from R&D Systems (Minneapolis, MIN). The synthesis of a coronavirus 3CLpro inhibitor, GC376, was previously described (Tiew et al., 2011). Anti-PEDV polyclonal antibody (Pab) was collected from a pig challenge study previously reported by us (Y. Kim et al., 2017). A monoclonal antibody (Mab) against PEDV N protein was kindly provided by Dr. Ying Fang (Kansas State University).

### 4.3.2 Protein identification by mass spectrometry.

To confirm whether the double bands from PEDV 8aa in SDS-PAGE are both N proteins, they were analyzed by matrix-assisted laser desorption/ionisation-time of flight (MALDI-TOF) mass spectrometry. Briefly, concentrated 8aa strain was loaded on the SDS-PAGE gel and stained

with Coomassie brilliant blue. The two bands that correspond to N protein were cut out separately and sent to Applied Biomics, Inc (Hayward, CA) for MALDI-TOF mass spectrometry study.

### 4.3.3 Western blot analysis of PEDV N protein.

To study the kinetics of PEDV N protein synthesis and cleavage, confluent Vero cells were inoculated with PEDV 8aa or KD at an MOI of 0.01, and incubated with or without trypsin (1 μg/ml). Following 24, 36, or 48 h incubation, cells were lysed with Tris-glycine SDS Sample Buffer (Thermo Fisher Scientific, PA) and subjected for the Western blot analysis. To determine the effect of various protease inhibitors on N protein cleavage, Z-VAD.fmk (pan-caspase inhibitor, 100 μM), furin inhibitor I (20 μM), leupeptin (trypsin inhibitor, 20 μM), or mock-Medium was added to confluent Vero cells in a 12-well plate, and the cells were then immediately inoculated with PEDV 8aa at an MOI of 0.01. Following 24, 36 or 48 h incubation at 37°C, cells were then lysed with Tris-glycine SDS sample buffer. Cell lysates were resolved by SDS-PAGE (4-12% Tris-glycine gel) and transferred onto nitrocellulose membranes. The membranes were blocked with 5% non-fat milk in phosphate-buffered saline with Tween-20 for 1 h and probed with PEDV Pab antibody followed by horseradish peroxidase(HRP)-conjugated goat anti-swine IgG. Virus proteins were visualized by chemiluminescence reagents (Thermo Fisher Scientific, PA).

### 4.3.4 Effects of Z-VAD-fmk on PEDV 8aa replication.

Confluent Vero cells in 12 well plates were inoculated with PEDV 8aa (MOI of 0.01) for 1 h at 37°C in the presence of Z-VAD-fmk (100 μM, 10 μM, or mock (Medium). Following incubation, the plates were washed three times with PBS and replenished with fresh media containing the same concentration of Z-VAD-fmk or mock-medium. After 24 h or 48 h incubation, cells were subjected

to three times of freezing and thawing and PEDV titers were determined by the 50% tissue culture infective dose ($TCID_{50}$) method (Reed & Muench, 1938).

## 4.3.5 DNA fragmentation assay.

To determine if Vero cells infected with PEDV 8aa undergo apoptosis, DNA fragmentation assay was performed. Vero cells inoculated with PEDV 8aa or mock-medium were incubated for 48 h before DNA isolation as described previously (Hinshaw, Olsen, Dybdahl-Sissoko, & Evans, 1994). Briefly, infected or uninfected cells were detached with 0.5 ml of detergent buffer (10mM Tris [pH7.4], 5mM EDTA, 0.2%Triton) and incubated on ice for 30 minutes. The cell lysates were centrifuged at 10,000 x g at 4°C for 30 min, and supernatants were used for extraction of DNA with buffered phenol, once with buffered phenol-chloroform, and once with chloroform-isoamyl alcohol (24:1). DNA was ethanol precipitated with 500 mM NaCl and resuspended in 15 μl of sterile water. The samples were run on a 2% agarose gel with ethidium bromide.

## 4.3.6 Cell-free cleavage of PEDV N protein by recombinant caspases.

To examine if caspases can cleave N protein, the N gene of PEDV US 8aa strain was cloned into pIRES (Clontech, CA) plasmid. The sequences encoding HA tag was added to the N- or C-terminus of N protein using the primers, 5'-AATTCTCGAGATGTACCCATACGATGTTCCAG ATTACGCTGGTGGAGCTTCTGTCAGTTTTCAG-3 and 5'-AATTCTCGAGATGGCTTCT GTCAGTTTTCA-3' for N-terminal tag; and 5'-AATTCTCGAGATGGCTTCTGTCAGTTTTC AG-3' and 5'-AATTCTCGAGTTAATTTCCTGTGTCGAAGATAGCGTAATCTGGAACAT CGTATGGGTATCCACC-3' for C-terminal tag. The amplified DNA was cloned into the plasmid in the downstream of the CMV promoter and the resulting plasmid was designated as pCI-N-nHA

or pCI-N-cHA. The 60-80% confluent 293T cells were transfected with pCI-N-nHA or pCI-N-cHA using Lipofectamine 3000 reagent (Thermo Fisher Scientific, PA) according to the instructions of the manufacturer and incubated for 48h for N protein expression. Following incubation, cell lysates (5 μl) were prepared and incubated with the equal volume of recombinant human caspase 3, 6 or 7, which contains containing 20 or 2 unit, 1:2 or 1:10, respectively) respectively, in the reaction buffer (20 μl) for 2 h at 37°C (Stennicke & Salvesen, 1997). The samples were then subjected to SDS-PGE using 4-12% Tricine gel (Thermo Fisher Scientific, PA) and the proteins were transferred onto nitrocellulose membranes. The membranes were probed with anti-HA mouse monoclonal antibodies followed by horseradish peroxidase-conjugated anti-mouse secondary antibody for Western blot analysis.

### 4.3.7 Plasmid constructions and mutagenesis assay.

First, using the N protein with HA tag at N- and or C-terminal tag and caspase 6, the cleavage site was determined at the C-terminus. To determine the exact cleavage site in N protein, aspartic acid at four different locations (345, 372, 424, and 427) at the C-terminus was mutated to glycine using pIRES-N-nHA and the QuikChange site-directed mutagenesis kit (Agilent, CA). These four putative cleave sites were selected using the online tool (Cascleave: http://sunflower.kuicr.kyoto-u.ac.jp/~sjn/Cascleave/index.html) (Song et al., 2010). The plasmids carrying each mutation were generated with following primers: for pIRES-N-nHA[D345G], 5' GTT CGT GAG CTA GCG GGC TCT TAC GAG ATT ACA 3' and 5' TGT AAT CTC GTA AGA GCC CGC TAG CTC ACG AAC 3', for pIRES-N-nHA[D372G], 5' CTT GTT TCA CAG GTG G*G*T GCA TTT AAA ACT GGG 3' and 5' CCC AGT TTT AAA TGC A*C*C CAC CTG TGA AAC AAG 3',  for pIRES-N-nHA[D424G],  5' TGG GAC ACA GCT GTT G*G*T GGT GGT GAC ACG

88

GCC 3' and 5' GGC CGT GTC ACC ACC A*C*C AAC AGC TGT GTC CCA 3'), and for pIRES-N-nHA[D427G], 5' GCT GTT GAT GGT GGT G*G*C ACG GCC GTT GAA ATT 3' and 5' AAT TTC AAC GGC CGT G*C*C ACC ACC ATC AAC AGC 3'. The underlined bold italic nucleotide in each primer is for the change in the mutagenesis analysis. The mutated sequence in each plasmid was confirmed by sequencing analysis. Each mutated N protein was expressed in 293T cells by transfecting the cells with each mutated plasmid and cell-free cleavage assay with the recombinant caspases 6 was done using the mutated N protein as described above.

## 4.3.8 Antiviral effects of GC376 on PEDV in cell culture.

Because the previous report suggested that PEDV 3CLpro can cleave N protein (Jaru-Ampornpan et al., 2017), we used a 3CLpro inhibitor GC376 to determine its effect on N protein cleavage. First, we examined the effectiveness of GC376 against PEDV replication and determined the effective concentrations inhibiting 50% and 90% of viral replication ($EC_{50}$ and $EC_{90}$, respectively). Serial concentrations of GC376 were added to confluent Vero cells in 24-well plates and the cells were promptly infected with PEDV 8aa at an MOI of 0.01. The cells were then further incubated at 37°C in the presence of GC376 until an extensive cytopathic effect was observed in the mock-treated well (up to 48 h). After three times freezing and thawing of the plates, viral titers were determined by real-time quantitative RT-PCR as described previously (Y. Kim et al., 2017). The $TCID_{50}$ equivalents/ml was calculated by a standard curve generated from the CT values plotted against the corresponding $TCID_{50}$ titers/ml. The $EC_{50}$ and $EC_{90}$ values were calculated by non-linear regression analysis (four-parameter variable slope) using GraphPad Prism software version 6.07 (GraphPad Software, La Jolla, CA). To determine whether 3CLpro or caspases cleave N protein, GC376 (20 μM), Z-VAD-fmk (100 μM) or DMSO (Mock) was added to PEDV 8aa-

infected Vere cells at 24 h after virus inoculation. Cells lysates were prepared at 0, 12 and 24 h (24, 36 and 48 post virus inoculation (hpi), respectively) after the addition of the inhibitors for Western blot analysis as described above.

### 4.3.9 Confocal laser scanning microscopy for N protein localization.

A confocal microscopy study was performed to determine whether N protein cleavage affects the localization of the N protein. Semi-confluent Vero cells on Lab-Tek II CC2 chamber slide (Thermo Fisher Scientific, PA) were inoculated with PEDV 8aa strain at an MOI of 1 in the presence of Z-VAD-fmk (100 μM) or DMSO. Following 1h incubation at 37°C, the cells were washed three times with PBS, replenished with fresh media containing the same concentration of Z-VAD-fmk and further incubated for 36 h at 37°C. In another experiment, PEDV KD strain was used to infect the cells on Lab-Tek II CC2 chamber slide, and the cells were incubated for 12 h in the presence of trypsin (1 μM) at 37°C. In addition, Vero cells were transfected with pIRES-N-nHA and incubated for 24 h. The cells in these experiments were fixed in 4% paraformaldehyde (Sigma-Aldrich, MO) in PBS (pH 7.4) for 15 min at room temperature (RT), permeabilized with 0.1% Triton X-100 in PBS for 10min at RT, washed three times with PBS and further incubated with 0.5% bovine serum albumin in PBS for 15 min. The cells were then incubated with Mab against PEDV N protein for 1 h at 37°C.  Then, the cells were washed three times with PBS and further incubated with FITC-labeled secondary antibody against mouse IgA, IgG or IgM (KPL, Gaithersburg, MD) for 1h at 37°C. The cells were also stained with SYTOX orange (Invitrogen, CA) for 15 minutes. Coverslips were mounted with ProLong® Gold antifade reagent (Invitrogen, CA), and the cells were observed with a confocal microscope LSM 510 (Zeiss, Oberkochen,

Germany) using a 100x oil-immersion objective lens. The images were processed by Image J

software 1.52n (http://imagej.nih.gov/ij/).

### 4.3.10 Statistical analysis.

The effects of Z-VAD-fmk in PEDV 8aa replication were compared to the Mock treatment

using GraphPad Prism (GraphPad Software, La Jolla, CA, USA). Statistical analysis was

performed using student t-test. *P*-value of <0.05 was considered as statistically significant. Data

were from at least three independent experiments.

## 4.4 Results
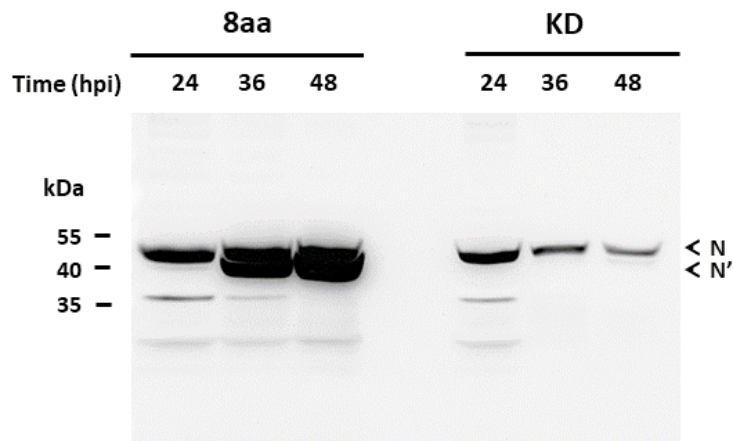


**Figure 4-1. The kinetics of PEDV N protein synthesis and cleavage.**

Confluent Vero cells were inoculated with PEDV 8aa (left lanes) or KD (right lanes) at an MOI of
0.1. Cell lysates were prepared at 24, 36 or 48 h post inoculation (hpi), and Western blot analysis
was performed with an anti-PEDV positive serum. Uncleaved (N) and cleaved (N') N protein are
indicated by arrowheads.

### 4.4.1 The N protein of PEDV 8aa is cleaved during virus replication.

We have previously generated two distinct PEDV strains, 8aa and PEDV KD by serially passaging a field-isolated PEDV in different culture conditions (Y. Kim et al., 2017). Some distinct characteristics of PEDV 8aa strain include protease independence, no cell fusion formation, efficient virus replication (viral titers reach over $10^8$ TCID$_{50}$/ml) and putative N protein cleavage (Y. Kim et al., 2017). In this current study, we confirmed that these bands are both N proteins by analyzing the two protein bands at approximately 49 and 47 kDa on an SDS-PAGE gel using MALDI-TOF mass spectrometry (data not shown). Next, we examined the kinetics of N protein cleavage in the cells (cell lysates). The cleaved N protein appeared at 36 and 48 hpi, but not at 24 hpi (Figure 4-1, left lanes). The ratios of the intact and cleaved N protein were approximately 1:1 for both 36 and 48 hpi (Figure 4-1). In contrast, no cleaved N protein from PEDV KD strain grown in the presence of trypsin (1 μg/ml) was detected for up to 48 hpi (Figure 4-1, right lanes). Of note, PEDV KD infection produced extensive cell-fusion and cell lysis after 24 hpi, which resulted in reduced levels of N protein in 36 and 48 hpi (Figure 4-1, right lanes).

### 4.4.2 N protein cleavage is dependent on the induction of apoptosis.

We explored potential protease(s) that can cleave N protein during PEDV 8aa replication using protease inhibitors. As shown in Figure 4-2A, the N protein cleavage was abolished by the addition of Z-VAD-fmk (36 and 48 hpi). However, furin or trypsin inhibitors did not block N protein cleavage (Figure 4-2A). Because activation of the caspase family plays central roles in cellular apoptosis, we conducted DNA fragmentation assay in PEDV 8aa infected cells. As expected, the low molecular weight DNA from the 8aa infected Vero cells showed a typical feature of apoptosis, fragmentation of DNA (Figure 4-2B). The DNA fragmentation was not observed in

the mock-infected cells. Inhibition of caspase by Z-VAD-fmk led to significantly increased viral

replication compared to DMSO (mock) (Figure 4-3).
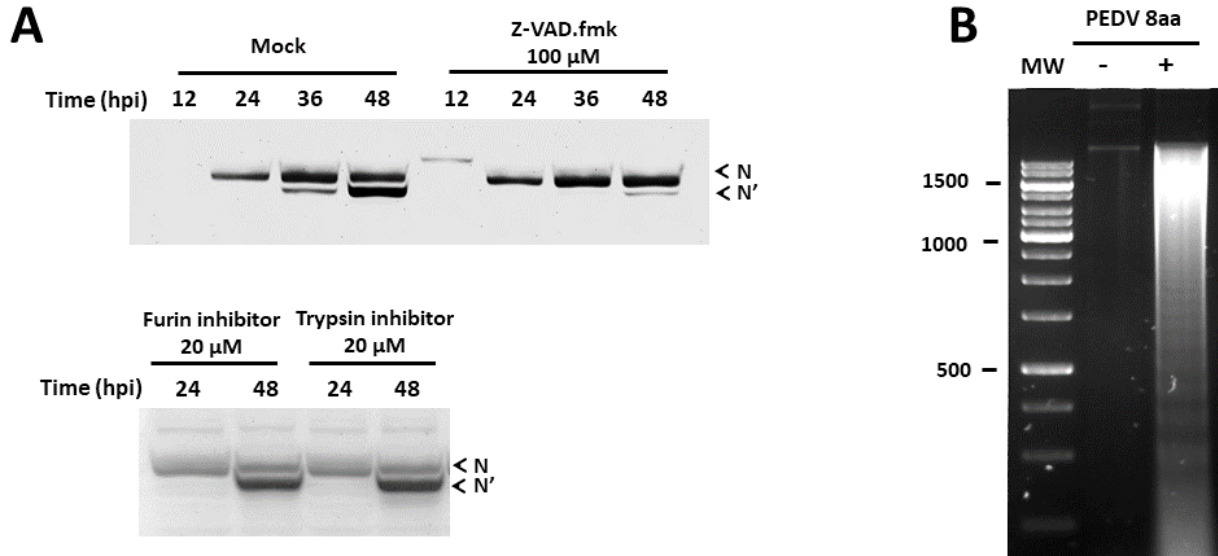


**Figure 4-2. Effects of protease inhibitors on the cleavage of PEDV N protein.**

A. Confluent Vero cells were inoculated with PEDV 8aa at an MOI of 0.1. Cell lysates were prepared at 24, 36 or 48 hpi. Pan-caspase inhibitor (Z-VAD.fmk, 100 uM), furin inhibitor (20 uM) or trypsin inhibitor (leupeptin, 20 uM) was added at 0 hpi. Uncleaved (N) and cleaved (N') N protein are indicated by arrowheads. (B) DNA fragmentation assay was performed using Vero cells infected with PEDV 8aa or mock-Medium. Low-molecular-weight DNA was extracted at 48 hpi and loaded on 2% agarose gel. MW is a DNA marker.

**A**
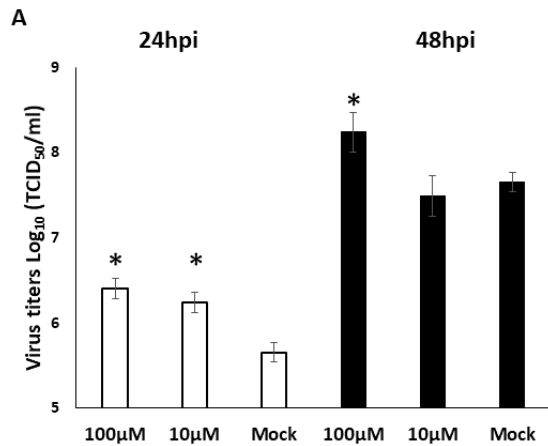
**Figure 4-3. Effects of caspase inhibition on PEDV 8aa replication.**

Confluent Vero cells were inoculated with PEDV 8aa at an MOI of 0.01 for 1 h with Z-VAD-fmk or Mock (medium), washed three times, replenished with fresh media containing the same concentration of Z-VAD-fmk or Mock (medium), and further incubated at 37°C. At 24 (open bars) or 48 hpi (closed bars), cells were subjected for virus titration using the $TCID_{50}$ assay. The mean and the standard deviations of the mean was acquired from three independent experiments. Asterisks indicate the statistical significance compared to the Mock treatment.
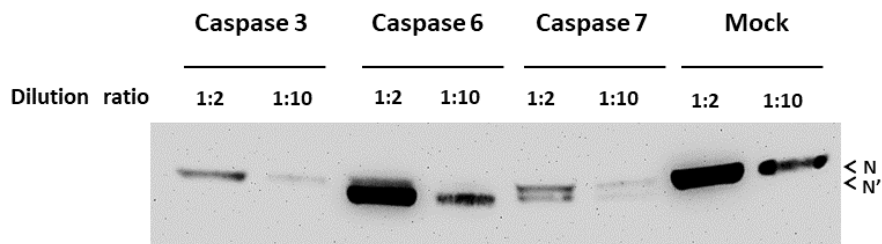


**Figure 4-4. Cleavage of the PEDV N protein with recombinant caspase 3,6 or 7.**

Expressed N protein was incubated with recombinant caspase 3, 6, or 7 with different dilution ratios (1:2 or 1:10) at 37°C for 2 h. The mixtures were subjected to SDS-PAGE, and Western blot analysis was performed with the anti-HA monoclonal antibody. Uncleaved (N) and cleaved (N') N protein are indicated by arrowheads.

### 4.4.3 Caspase 6 or 7 cleave N protein at $D^{424}G^{425}$.

To determine which caspase cleaves N protein, a cell-free cleavage assay was performed with the recombinant caspase 3, 6 or 7. The Western blot analysis demonstrated that caspase 6 or 7 cleaved PEDV N protein, whereas caspase 3 did not cleave the N protein (Figure 4). Mock treatment (PBS) was used as a control (Figure 4-4). The mutation study on the four mutated N proteins carrying a single mutation of $D^{345}G$, $D^{372}G$, $D^{424}G$ or $D^{427}G$ at the putative caspase cleavage site showed that D424G mutation abolished the N protein cleavage by caspase 6 (Figure 4-5), which revealed N protein cleavage occurs between $D^{424}G^{425}$ (Figure 4-5).
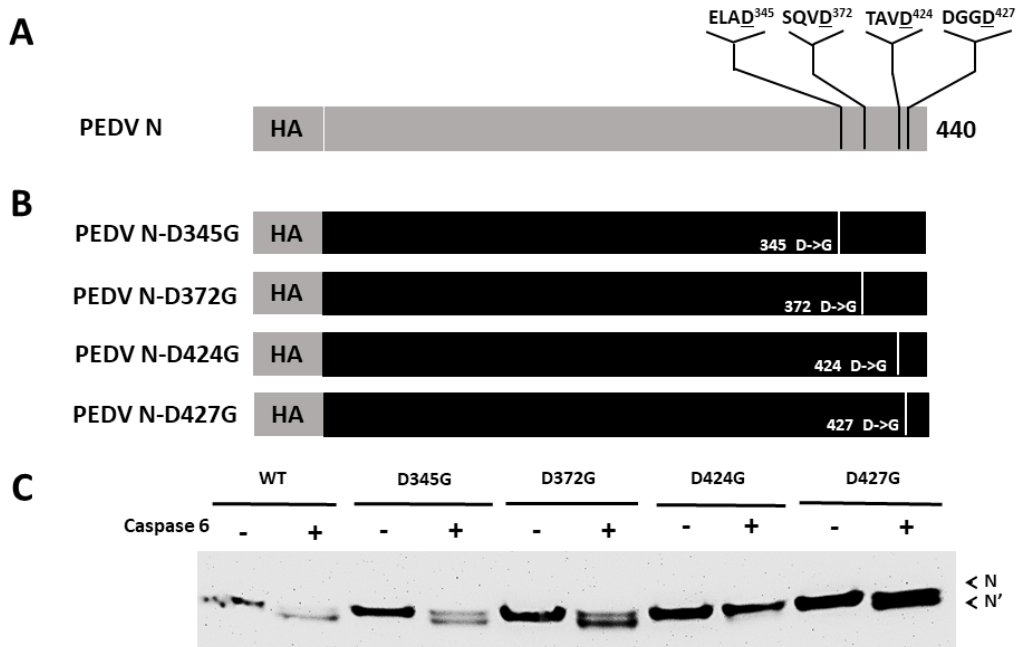
**Figure 4-5. Identification of the N protein cleavage site by caspase 6 with mutagenesis assay and the Western blot analysis.**

(A) A schematic representation of PEDV N protein with putative C-terminal caspase cleavage sites predicted by the Cascleave. (B) Four mutant recombinant N proteins carrying a single mutation of D345G, D372G, D424G or D427G were generated by site-directed mutagenesis. (C) Wild-type N protein (WT) or mutant N proteins ($D^{345}G$, $D^{372}G$, $D^{424}G$, or $D^{427}G$) were incubated for 2 h at 37°C with a recombinant caspase 6. The mixtures were analyzed by the Western blot with anti-HA antibody. Uncleaved (N) and cleaved (N') N protein are indicated by arrowheads.
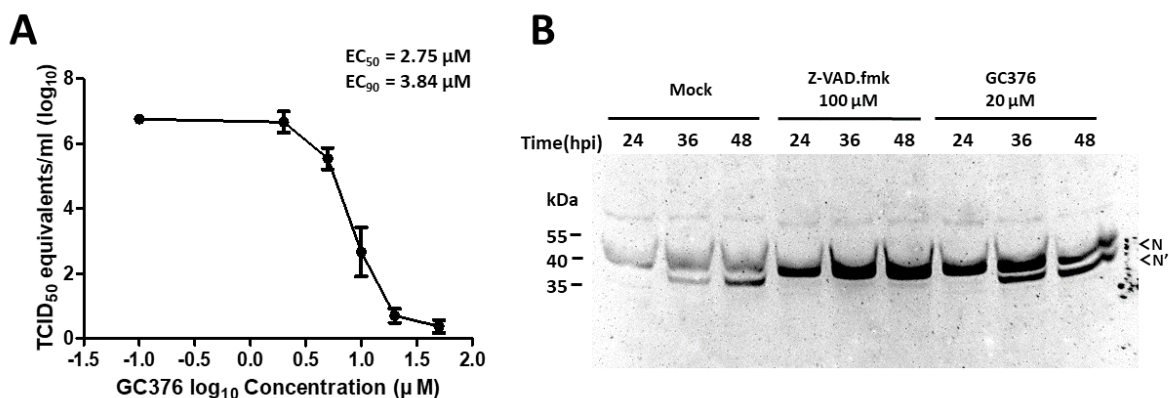
**Figure 4-6. Effects of a 3CLpro inhibitor (GC376) on PEDV replication and N protein cleavage.**

(A)  Inhibition of PEDV replication by GC376. Confluent cells were inoculated with PEDV 8aa at an MOI of  0.01 and incubated with serial dilutions of GC376 for 48 h. Viral titers were measured by real-time qRT-PCR and converted to $TCID_{50}$ equivalents/ml, and $EC_{50}$ and $EC_{90}$ were calculated.  (B) The effects of GC376 on the cleavage of PEDV N protein. Cells were inoculated with PEDV 8aa at an MOI of 0.1, and Z-VAD-fmk (100 μM), GC376 (20 μM ) or Mock(DMSO) was added at 24 hpi. Cells were further incubated for additional 12 or 24 h. Cell lysates were then prepared, and Western blot analysis was performed with an anti-PEDV positive serum. Uncleaved (N) and cleaved (N') N protein are indicated by arrowheads.


### 4.4.4 PEDV 3CLpro did not affect N protein cleavage.

First, the inhibitory effects of GC376 against PEDV 8aa were determined with the $EC_{50}$ and $EC_{90}$ at 2.75 and 3.84 μM, respectively (Figure 4-6A). To examine the effect of 3CLpro on N protein cleavage, GC376 at 20 μM was added at 24 hpi, and the N cleavage was monitored at 36 or 48 hpi.  The addition of GC376 or Mock (DMSO) did not block N protein cleavage at 36 or 48 hpi (Figure 4-6B). As a positive control, Z-VAD-fmk at 100 μM prevented the N protein cleavage at 36 or 48 hpi (Figure 4-6B).
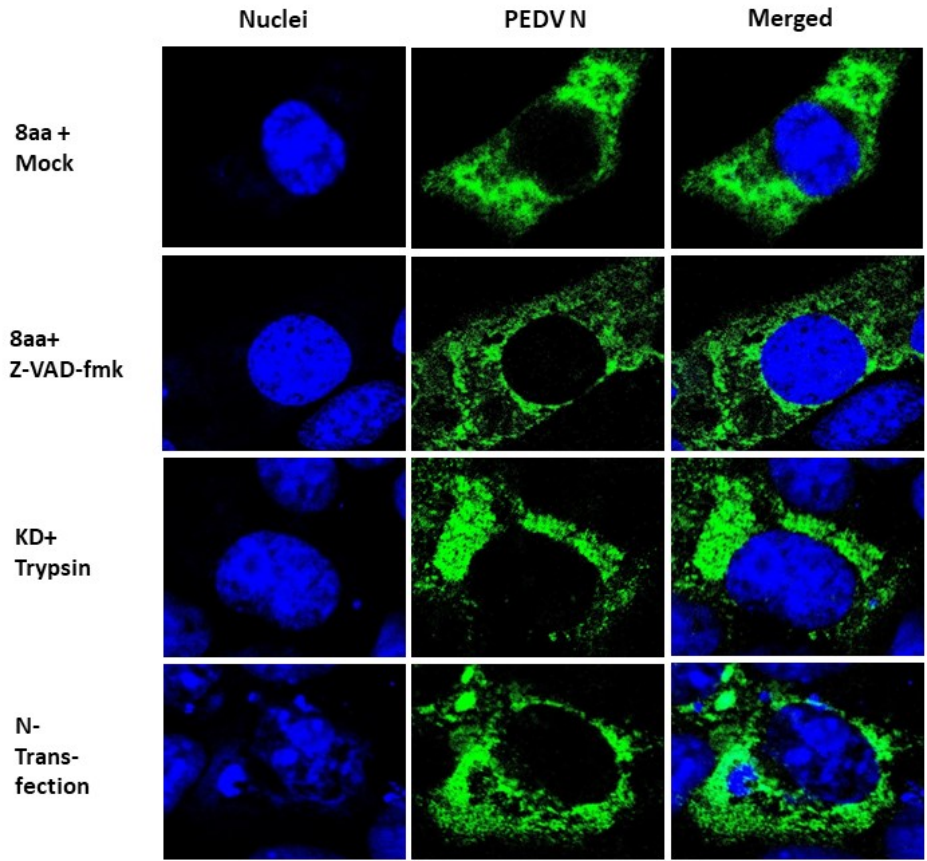
**Figure 4-7. Subcellular localizations of N protein in Vero cells by the confocal microscopy.**

Vero cells were inoculated with PEDV 8aa or KD at an MOI of 1. For PEDV 8aa, Z-VAD-fmk (100 μM), or Mock (DMSO) was added to the virus infected cells. For PEDV KD, trypsin (1 μg/ml) was added. Virus infected cells were further incubated for 36 (8aa) or 12 (KD) h. For the expression of N protein, 24 h-old semi-confluent cells were transfected with pIRES-N-nHA, and cells were incubated for 24 h. Cell were fixed, and N proteins were probed with anti PEDV N monoclonal antibody (green). Nuclei were stained with SYTOX orange (Blue), and single or merged images were prepared with the ImageJ software.

## 4.4.5 PEDV N protein localizes in the cytoplasm.

Because previous studies suggested PEDV N protein was localized in both nucleus and cytoplasm (Shi et al., 2014), and the localization of SARS-CoV N protein was affected by N

protein cleavage by caspases (Diemer et al., 2008), we analyzed the localization of N protein of PEDV 8aa (and KD) with or without Z-VAD-fmk (100 μM) using the confocal microscopy. With or without Z-VAD-fmk, N protein was exclusively localized in the cytoplasm at 36 hpi of PEDV 8aa (Figure 4-7). In addition, the N protein of PEDV KD (with trypsin) was also localized in the cytoplasm at 12 hpi (Figure 4-7). The N protein expressed from the transfection of pIRES-N-nHA also localized in the cytoplasm at 24 hpi (Figure 4-7).

## 4.5 Discussion

It has been shown that coronavirus infection can induce apoptosis and N protein cleavage by caspases (Diemer et al., 2008; Eleouet et al., 2000). TGEV N protein is cleaved by caspase 6 and 7 during replication in HRT18 cells, which resulted in 22 amino acid fragment from the C-terminal of N protein (Eleouet et al., 2000). SARS-CoV N protein is also cleaved by caspase 6 and potentially by caspase 3, and the possible cleavage site is located at residues 400 and 403 on the C-terminal of N protein (Diemer et al., 2008). The biological significance of the virus-induced apoptosis and N protein cleavages is still unclear, but it is suggested to be involved in the pathogenicity (Diemer et al., 2008; Eleouet et al., 2000). Previously, we reported that the N protein of trypsin-independent PEDV 8aa was cleaved during virus replication. In this study, we demonstrated the cleaved N band (N') appeared at the late stage (after 36 hpi) of PEDV 8aa infection (Figure 4-1) and required caspase activities because the N' product was abolished by the addition of pan-caspase inhibitor (Z-VAD-fmk) (Figure 4-2A). In addition, this cleavage was associated with the virus induced apoptosis evident with the DNA fragmentation at 48 hpi (Figure 4-2B). However, N protein of PEDV KD did not show any evidence of the N cleavage during virus replication (Figure 4-1). Because PEDV KD, a trypsin-dependent strain, causes the extensive

cell fusion formation with lysis, there were significant differences in the virus induced cell death by these two different PEDV strains. It is possible that protease-independent PEDV strains can target tissues (cells) which are not exposed to high concentrations of proteases, and induce significantly different pathogenicity in the hosts.

There have been numerous reports on the induction of apoptosis of virus-infected cells, which raised a discussion of whether apoptosis is favorable to host or virus. In a host defense point of view, apoptosis curtails the use of cellular machinery necessary for viral protein synthesis and facilitates the elimination of viral proteins through caspase-mediated proteolysis, resulting in the reduction of viral replication and spread (Danthi, 2011; F. Yan, Xia, Lv, Qi, & Xu, 2010). Thus, viruses in diverse families encode anti-apoptotic proteins (Clem, Fechheimer, & Miller, 1991) to limit apoptosis. On the other hand, viruses can take advantage of the apoptosis of host cells to facilitate virus replication. Various viruses have utilized caspases to cleave their viral proteins for successful replication, which is aborted when the caspase cleavage sites on the viral proteins are eliminated (Best, Shelton, Pompey, Wolfinbarger, & Bloom, 2003; Moody & Laimins, 2009). It was shown that PEDV infection induces apoptotic cell death in a caspase-independent manner (Kim and Lee, 2014). In this study, we observed that PEDV 8aa induces apoptosis in the infected cells caspase-dependent manner because pan-caspase inhibitor (Z-VAD-fmk) blocked apoptotic cell death (data not shown). Furthermore, the replication of PEDV 8aa was slightly but significantly increased in the presence of Z-VAD-fmk (Figure 4-3), suggesting the apoptosis is not favorable for viruses. Of note, the replication of PEDV KD in the presence of trypsin induced extensive fusions with cell lysis starting 12 hpi, and the addition of Z-VAD-fmk in the medium did not affect virus replication (data not shown).

Then we investigated which caspases are involved in the N protein cleavage using 3 individual recombinant caspases. We demonstrated that caspase 6 or 7, but not caspase 3, is responsible for the N protein cleavage (Figure 4-4). Furthermore, we identified that caspase 6 cleaves the C-terminal of the PEDV N protein between $D^{424}/G^{425}$ (Figure 4-5). This cleavage location is similar to that of TGEV N protein (Eleouet et al., 2000). This site is located at the domain 3 on the PEDV N protein. Because domain 3 is not involved in N-N interaction and RNA binding, the cleavage may not affect these functions of N protein. Because domain 3 is to interact with M protein and this interaction is known to plays an important role in coronavirus replication (Narayanan et al., 2000), the cleavage may result in the reduction of replication. In this study, we found that the N protein cleavage occurred at the late stage of virus replication (Figure 4-1), which may be the reason for slightly increased viral replication in the presence of Z-VAD-fmk. Interestingly, we observed that both forms of N proteins were present in the concentrated (purified) PEDV 8aa virus at the ratio of 1:1 (Kim et al., 2017). The results suggest that the cleaved form of N protein could still integrate into virions at similar rates as the uncleaved form.

It was previously reported in a study that PEDV N protein is processed by viral 3CLpro glutamine at the position 382 (P1) and leucine at the position 381 (P2), and this cleavage was speculated to be associated with cell culture adaptation of PEDV (Jaru-Ampornpan et al., 2017). In this study, we used a specific inhibitor (GC376) of PEDV 3CLpro to investigate whether the N protein of PEDV 8aa is cleaved by 3CLpro. However, inhibition of 3CLpro did not abolish N protein cleavage for PEDV 8aa (Figure 4-6). It is possible that 3CLpro-mediated N protein cleavage may dependent on the different PEDV strains.

A nucleus localization of N protein has been reported for several coronaviruses including PEDV, TGEV, MHV, SARS-CoV, and infectious bronchitis virus (IBV) (Diemer et al., 2008;

Hiscox et al., 2001; Shi et al., 2014; Wurm et al., 2001). The nuclear localization signals (NLS) in N proteins are composed of "pat 7" NLS sequences, including 261-PKKNKSR-267 and 381-PQRKKEK-387 and well conserved among PEDV (441 amino acids), including PEDV 8aa or KD strains. Shi et al. (Shi et al., 2014) reported nuclear localization of PEDV N protein in Vero E6 cells after transfection with N genes. For SARS-CoV, Rowland et al. reported that there is no evidence of N protein nuclear localization during SARS-CoV infection and after the transfection of plasmids encoding the N protein in Vero cells (Rowland et al., 2005). However, it was shown that SARS-CoV could induce apoptosis, N protein cleavage, and nuclear localization, and these were dependent on cell types and levels of viral replication (Diemer et al., 2008). Diemer et al. (Diemer et al., 2008) further demonstrated that the cleavage of N protein (by caspase) could change its subcellular localizations from the cytoplasm (uncleaved) to both cytoplasm and nucleus (cleaved N protein). To study the localization of PEDV 8aa N protein, we examined two aspects: 1) whether N protein of PEDV 8aa or KD is found in both cytoplasm and nucleus; 2) whether N protein cleavage can change its subcellular localizations. First, we discovered that the N protein of PEDV 8aa or KD, or the recombinant of N protein expressed from PEDV 8aa N gene exclusively localized in the cytoplasm (Figure 4-7). Second, N protein localization was not changed by Z-VAD-fmk (and N protein cleavage) (Figure 4-7). The localization of N protein was consistently shown in the cytoplasm when it was examined at different time points for both PEDV 8aa and KD (data not shown). It is possible a minor population of N protein (with or without N protein cleavage) may be localized to nucleus, and there could be variations among strains. To further elucidate the functional role of N protein and its cleavage, we are currently investigating the cleaved (and uncleaved) N protein in viral assembly and replication.

## 4.6 Acknowledgement

# Chapter 5 - Summary and Future Directions

The family Coronaviridae contains viruses infecting humans and animals with broad ranges of symptoms from common colds in humans or acute gastroenteritis in animals to lethal lower respiratory infection or lethal systemic infections in cats. Especially, COVID 19 currently spreads throughout the whole world due to their high infectivity and high mortality in elderly people, causing severe public health and economic problem. Developments in coronavirus countermeasures need to be considered a high mutant rate and immune evasion strategies of the coronavirus. Studies have shown that blocking coronavirus infection at the entry step can be a good target for antiviral drug development. However, the entry events of coronavirus are not well understood till date due to its complexity mediated by the spike protein. Thus, understanding the viral and host factors during coronavirus entry events will help in the development of coronavirus countermeasures to current coronavirus outbreaks and maybe future outbreaks.

Entry events of coronavirus replication start from the binding of its host receptor with the S1 receptor-binding domain(RBD) of S protein. Following receptor binding, S protein exposes cleavage sites and undergoes priming by protease(s). This proteolytic activation exposes fusion peptide in the S2 subunit, which leads to viral-cellular membrane fusion mediated by its dramatic conformational change, finally translocating viral genome. Various host factors, which constitute the cargo delivery pathway, are also used by coronaviruses. The study demonstrated in this dissertation examines the entry events during PEDV replication and identifies the roles of exogenous protease and the host factors required by PEDV endosomal escape.

In our first study, we examined the role of exogenous protease during the entry of PEDV using two different protease-adapted PEDV US strains, PEDV KD and AA. We demonstrated that the activity of protease was required at an early stage of PEDV KD replication, particularly after

virus binding to cells. Further, we showed that PEDV was able to enter the endosome without the presence of protease. The addition of protease facilitated the escape of viruses from the endosome. The host endosomal protease, cathepsin B and L were also shown to be important in the endosomal escape of PEDV.

The second study identified the roles of the acid sphingomyelinase (ASM) /ceramide pathway in the entry of PEDV. We reported that PEDV infection in Vero cells triggered ceramide formation by activation of ASM. The Inhibition of ASM significantly reduced protease independent PEDV replication by inhibiting viral endosomal escape. These results demonstrated the importance of interactions among viruses, host cells, and proteases during coronavirus entry for successful replication.

The third study examined that protease independent PEDV 8aa strain infection in Vero cells led to caspases mediated apoptotic cell death. PEDV nucleocapsid (N) protein was cleaved by caspase 6 and 7 at the late stage of the replication while the cells were undergoing the apoptotic process. The caspase-mediated cleavage occurred between $D^{424}$ and $G^{425}$ near the C-terminal of N protein. Addition of a pan-caspase inhibitor to prevent the N protein cleavage significantly increased 8aa replication. We further demonstrated that N protein exclusively localized in the cytoplasm regardless of N cleavage and time post-infection.

Our studies have demonstrated important factors affecting PEDV entry (exogenous or endosomal protease and ASM /ceramide pathway) and virus-host interaction (caspase-mediated apoptosis/N protein cleavage), all of which provide fundamental information for understanding the PEDV replication. We will further identify (1) genetic mutation(s) in the PEDV structural proteins, especially spike protein, that switch protease dependency, (2) the detailed mechanism of action of ASM/ceramide formation during protease independent PEDV entry, and (3) effects of

ASM inhibition to other coronaviruses in the presence of relevant proteases. Such understanding

could lead to the development of rational future strategies for preventing coronavirus infections.

## 5.1 References

Adedeji, A. O., & Sarafianos, S. G. (2014). Antiviral drugs specific for coronaviruses in preclinical development. *Curr Opin Virol, 8*, 45-53. doi: 10.1016/j.coviro.2014.06.002

Adedeji, A. O., Singh, K., Calcaterra, N. E., DeDiego, M. L., Enjuanes, L., Weiss, S., & Sarafianos, S. G. (2012). Severe acute respiratory syndrome coronavirus replication inhibitor that interferes with the nucleic acid unwinding of the viral helicase. *Antimicrob Agents Chemother, 56*(9), 4718-4728. doi: 10.1128/AAC.00957-12

Al-Amri, S. S., Abbas, A. T., Siddiq, L. A., Alghamdi, A., Sanki, M. A., Al-Muhanna, M. K., . . . Hashem, A. M. (2017). Immunogenicity of Candidate MERS-CoV DNA Vaccines Based on the Spike Protein. *Sci Rep, 7*, 44875. doi: 10.1038/srep44875

Al-Tawfiq, J. A., Momattin, H., Dib, J., & Memish, Z. A. (2014). Ribavirin and interferon therapy in patients infected with the Middle East respiratory syndrome coronavirus: an observational study. *Int J Infect Dis, 20*, 42-46. doi: 10.1016/j.ijid.2013.12.003

Alsaad, K. O., Hajeer, A. H., Al Balwi, M., Al Moaiqel, M., Al Oudah, N., Al Ajlan, A., . . . Arabi, Y. M. (2018). Histopathology of Middle East respiratory syndrome coronavirus (MERS-CoV) infection - clinicopathological and ultrastructural study. *Histopathology, 72*(3), 516-524. doi: 10.1111/his.13379

An, S., Chen, C. J., Yu, X., Leibowitz, J. L., & Makino, S. (1999). Induction of apoptosis in murine coronavirus-infected cultured cells and demonstration of E protein as an apoptosis inducer. *J Virol, 73*(9), 7853-7859.

Anand, K., Ziebuhr, J., Wadhwani, P., Mesters, J. R., & Hilgenfeld, R. (2003). Coronavirus main proteinase (3CLpro) structure: basis for design of anti-SARS drugs. *Science, 300*(5626), 1763-1767. doi: 10.1126/science.1085658

Anastasia, N. V., Douglas, M., Qiuhong, W., Marie, R. C., Kurt, R., Albert, R., . . . Kwonil, J. (2014). Distinct Characteristics and Complex Evolution of PEDV Strains, North America, May 2013–February 2014. *Emerging Infectious Disease journal, 20*(10), 1620. doi: 10.3201/eid2010.140491

Ashkenazi, A., & Dixit, V. M. (1998). Death receptors: signaling and modulation. *Science, 281*(5381), 1305-1308. doi: 10.1126/science.281.5381.1305

Assiri, A., Al-Tawfiq, J. A., Al-Rabeeah, A. A., Al-Rabiah, F. A., Al-Hajjar, S., Al-Barrak, A., . . . Memish, Z. A. (2013). Epidemiological, demographic, and clinical characteristics of 47 cases of Middle East respiratory syndrome coronavirus disease from Saudi Arabia: a descriptive study. *Lancet Infect Dis, 13*(9), 752-761. doi: 10.1016/S1473-3099(13)70204-4

Avota, E., Gulbins, E., & Schneider-Schaulies, S. (2011). DC-SIGN mediated sphingomyelinase-activation and ceramide generation is essential for enhancement of viral uptake in dendritic cells. *PLoS Pathog, 7*(2), e1001290. doi: 10.1371/journal.ppat.1001290

Bailey, O. T., Pappenheimer, A. M., Cheever, F. S., & Daniels, J. B. (1949). A Murine Virus (Jhm) Causing Disseminated Encephalomyelitis with Extensive Destruction of Myelin : Ii.

Pathology. *J Exp Med, 90*(3), 195-212. doi: 10.1084/jem.90.3.195

Balint, A., Farsang, A., Szeredi, L., Zadori, Z., & Belak, S. (2014). Recombinant feline coronaviruses as vaccine candidates confer protection in SPF but not in conventional cats. *Vet Microbiol, 169*(3-4), 154-162. doi: 10.1016/j.vetmic.2013.10.015

Baranov, P. V., Henderson, C. M., Anderson, C. B., Gesteland, R. F., Atkins, J. F., & Howard, M. T. (2005). Programmed ribosomal frameshifting in decoding the SARS-CoV genome. *Virology, 332*(2), 498-510. doi: 10.1016/j.virol.2004.11.038

Barcena, M., Oostergetel, G. T., Bartelink, W., Faas, F. G., Verkleij, A., Rottier, P. J., . . . Bosch, B. J. (2009). Cryo-electron tomography of mouse hepatitis virus: Insights into the structure of the coronavirion. *Proc Natl Acad Sci U S A, 106*(2), 582-587. doi: 10.1073/pnas.0805270106

Barnard, D. L., & Kumaki, Y. (2011). Recent developments in anti-severe acute respiratory syndrome coronavirus chemotherapy. *Future Virol, 6*(5), 615-631. doi: 10.2217/fvl.11.33

Belouzard, S., Millet, J. K., Licitra, B. N., & Whittaker, G. R. (2012). Mechanisms of coronavirus cell entry mediated by the viral spike protein. *Viruses, 4*(6), 1011-1033. doi: 10.3390/v4061011

Berry, J. D., Jones, S., Drebot, M. A., Andonov, A., Sabara, M., Yuan, X. Y., . . . Plummer, F. (2004). Development and characterisation of neutralising monoclonal antibody to the SARS-coronavirus. *Journal of Virological Methods, 120*(1), 87-96. doi: 10.1016/j.jviromet.2004.04.009

Berry, M., Gamieldien, J., & Fielding, B. C. (2015). Identification of new respiratory viruses in the new millennium. *Viruses, 7*(3), 996-1019. doi: 10.3390/v7030996

Bertram, S., Dijkman, R., Habjan, M., Heurich, A., Gierer, S., Glowacka, I., . . . Pohlmann, S. (2013). TMPRSS2 activates the human coronavirus 229E for cathepsin-independent host cell entry and is expressed in viral target cells in the respiratory epithelium. *J Virol, 87*(11), 6150-6160. doi: 10.1128/JVI.03372-12

Bertram, S., Glowacka, I., Muller, M. A., Lavender, H., Gnirss, K., Nehlmeier, I., . . . Pohlmann, S. (2011). Cleavage and activation of the severe acute respiratory syndrome coronavirus spike protein by human airway trypsin-like protease. *J Virol, 85*(24), 13363-13372. doi: 10.1128/JVI.05300-11

Best, S. M., Shelton, J. F., Pompey, J. M., Wolfinbarger, J. B., & Bloom, M. E. (2003). Caspase cleavage of the nonstructural protein NS1 mediates replication of Aleutian mink disease parvovirus. *J Virol, 77*(9), 5305-5312. doi: 10.1128/jvi.77.9.5305-5312.2003

Bisht, H., Roberts, A., Vogel, L., Bukreyev, A., Collins, P. L., Murphy, B. R., . . . Moss, B. (2004). Severe acute respiratory syndrome coronavirus spike protein expressed by attenuated vaccinia virus protectively immunizes mice. *Proc Natl Acad Sci U S A, 101*(17), 6641-6646. doi: 10.1073/pnas.0401939101

Bos, E. C., Luytjes, W., van der Meulen, H. V., Koerten, H. K., & Spaan, W. J. (1996). The production of recombinant infectious DI-particles of a murine coronavirus in the absence of helper virus. *Virology, 218*(1), 52-60. doi: 10.1006/viro.1996.0165

Bosch, B. J., Bartelink, W., & Rottier, P. J. (2008). Cathepsin L functionally cleaves the severe acute respiratory syndrome coronavirus class I fusion protein upstream of rather than adjacent to the fusion peptide. *J Virol, 82*(17), 8887-8890. doi: 10.1128/JVI.00415-08

Bosch, B. J., Raj, V. S., & Haagmans, B. L. (2013). Spiking the MERS-coronavirus receptor. *Cell Res, 23*(9), 1069-1070. doi: 10.1038/cr.2013.108

Bosch, B. J., van der Zee, R., de Haan, C. A., & Rottier, P. J. (2003). The coronavirus spike protein

is a class I virus fusion protein: structural and functional characterization of the fusion core complex. *J Virol, 77*(16), 8801-8811. doi: 10.1128/jvi.77.16.8801-8811.2003

Brenner, B., Ferlinz, K., Grassme, H., Weller, M., Koppenhoefer, U., Dichgans, J., . . . Gulbins, E. (1998). Fas/CD95/Apo-I activates the acidic sphingomyelinase via caspases. *Cell Death Differ, 5*(1), 29-37. doi: 10.1038/sj.cdd.4400307

Brian, D. A., & Baric, R. S. (2005). Coronavirus genome structure and replication. *Curr Top Microbiol Immunol, 287*, 1-30. doi: 10.1007/3-540-26765-4_1

Buchholz, U. J., Bukreyev, A., Yang, L., Lamirande, E. W., Murphy, B. R., Subbarao, K., & Collins, P. L. (2004). Contributions of the structural proteins of severe acute respiratory syndrome coronavirus to protective immunity. *Proc Natl Acad Sci U S A, 101*(26), 9804-9809. doi: 10.1073/pnas.0403492101

Bugge, T. H., Antalis, T. M., & Wu, Q. (2009). Type II transmembrane serine proteases. *J Biol Chem, 284*(35), 23177-23181. doi: 10.1074/jbc.R109.021006

Bukreyev, A., Lamirande, E. W., Buchholz, U. J., Vogel, L. N., Elkins, W. R., St Claire, M., . . . Collins, P. L. (2004). Mucosal immunisation of African green monkeys (Cercopithecus aethiops) with an attenuated parainfluenza virus expressing the SARS coronavirus spike protein for the prevention of SARS. *Lancet, 363*(9427), 2122-2127. doi: 10.1016/S0140-6736(04)16501-X

Burkard, C., Verheije, M. H., Haagmans, B. L., van Kuppeveld, F. J., Rottier, P. J., Bosch, B. J., & de Haan, C. A. (2015). ATP1A1-mediated Src signaling inhibits coronavirus entry into host cells. *J Virol, 89*(8), 4434-4448. doi: 10.1128/JVI.03274-14

Cao, L., Ge, X., Gao, Y., Ren, Y., Ren, X., & Li, G. (2015). Porcine epidemic diarrhea virus infection induces NF-kappaB activation through the TLR2, TLR3 and TLR9 pathways in porcine intestinal epithelial cells. *J Gen Virol, 96*(Pt 7), 1757-1767. doi: 10.1099/vir.0.000133

Cavanagh, D. (1997). Nidovirales: a new order comprising Coronaviridae and Arteriviridae. *Arch Virol, 142*(3), 629-633.

Cavanagh, D. (2007). Coronavirus avian infectious bronchitis virus. *Vet Res, 38*(2), 281-297. doi: 10.1051/vetres:2006055

Chan, J. F.-W., Yuan, S., Kok, K.-H., To, K. K.-W., Chu, H., Yang, J., . . . Yuen, K.-Y. (2020). A familial cluster of pneumonia associated with the 2019 novel coronavirus indicating person-to-person transmission: a study of a family cluster. *The Lancet, 395*(10223), 514-523. doi: 10.1016/S0140-6736(20)30154-9

Chan, J. F., Yao, Y., Yeung, M. L., Deng, W., Bao, L., Jia, L., . . . Yuen, K. Y. (2015). Treatment With Lopinavir/Ritonavir or Interferon-beta1b Improves Outcome of MERS-CoV Infection in a Nonhuman Primate Model of Common Marmoset. *J Infect Dis, 212*(12), 1904-1913. doi: 10.1093/infdis/jiv392

Chan, K. S., Lai, S. T., Chu, C. M., Tsui, E., Tam, C. Y., Wong, M. M., . . . Yuen, K. Y. (2003). Treatment of severe acute respiratory syndrome with lopinavir/ritonavir: a multicentre retrospective matched cohort study. *Hong Kong Med J, 9*(6), 399-406.

Chandran, K., Sullivan, N. J., Felbor, U., Whelan, S. P., & Cunningham, J. M. (2005). Endosomal Proteolysis of the Ebola Virus Glycoprotein Is Necessary for Infection. *Science, 308*(5728), 1643-1645. doi: 10.1126/science.1110656

Chang, H. W., Egberink, H. F., Halpin, R., Spiro, D. J., & Rottier, P. J. (2012). Spike protein fusion peptide and feline coronavirus virulence. *Emerg Infect Dis, 18*(7), 1089-1095. doi: 10.3201/eid1807.120143

Charruyer, A., Grazide, S., Bezombes, C., Muller, S., Laurent, G., & Jaffrezou, J. P. (2005). UV-C light induces raft-associated acid sphingomyelinase and JNK activation and translocation independently on a nuclear signal. *J Biol Chem, 280*(19), 19196-19204. doi: 10.1074/jbc.M412867200

Chau, T. N., Lee, K. C., Yao, H., Tsang, T. Y., Chow, T. C., Yeung, Y. C., . . . Lai, C. L. (2004). SARS-associated viral hepatitis caused by a novel coronavirus: report of three cases. *Hepatology, 39*(2), 302-310. doi: 10.1002/hep.20111

Chen, J., Lee, K. H., Steinhauer, D. A., Stevens, D. J., Skehel, J. J., & Wiley, D. C. (1998). Structure of the Hemagglutinin Precursor Cleavage Site, a Determinant of Influenza Pathogenicity and the Origin of the Labile Conformation. *Cell, 95*(3), 409-417. doi: 10.1016/S0092-8674(00)81771-7

Chen, N., Zhou, M., Dong, X., Qu, J., Gong, F., Han, Y., . . . Zhang, L. (2020). Epidemiological and clinical characteristics of 99 cases of 2019 novel coronavirus pneumonia in Wuhan, China: a descriptive study. *The Lancet, 395*(10223), 507-513. doi: 10.1016/S0140-6736(20)30211-7

Chen, Q., Li, G., Stasko, J., Thomas, J. T., Stensland, W. R., Pillatzki, A. E., . . . Zhang, J. (2014). Isolation and characterization of porcine epidemic diarrhea viruses associated with the 2013 disease outbreak among swine in the United States. *J Clin Microbiol, 52*(1), 234-243. doi: 10.1128/JCM.02820-13

Cheng, J., Zhao, Y., Xu, G., Zhang, K., Jia, W., Sun, Y., . . . Zhang, G. (2019). The S2 Subunit of QX-type Infectious Bronchitis Coronavirus Spike Protein Is an Essential Determinant of Neurotropism. *Viruses, 11*(10), 972. doi: 10.3390/v11100972

Cheng, V. C., Lau, S. K., Woo, P. C., & Yuen, K. Y. (2007). Severe acute respiratory syndrome coronavirus as an agent of emerging and reemerging infection. *Clin Microbiol Rev, 20*(4), 660-694. doi: 10.1128/CMR.00023-07

Chi, H., Zheng, X., Wang, X., Wang, C., Wang, H., Gai, W., . . . Xia, X. (2017). DNA vaccine encoding Middle East respiratory syndrome coronavirus S1 protein induces protective immune responses in mice. *Vaccine, 35*(16), 2069-2075. doi: 10.1016/j.vaccine.2017.02.063

Chicheportiche, Y., Bourdon, P. R., Xu, H., Hsu, Y. M., Scott, H., Hession, C., . . . Browning, J. L. (1997). TWEAK, a new secreted ligand in the tumor necrosis factor family that weakly induces apoptosis. *J Biol Chem, 272*(51), 32401-32410. doi: 10.1074/jbc.272.51.32401

Chinnaiyan, A. M. (1999). The apoptosome: heart and soul of the cell death machine. *Neoplasia (New York, N.Y.), 1*(1), 5-15. doi: 10.1038/sj.neo.7900003

Chu, C. M., Cheng, V. C., Hung, I. F., Wong, M. M., Chan, K. H., Chan, K. S., . . . Yuen, K. Y. (2004). Role of lopinavir/ritonavir in the treatment of SARS: initial virological and clinical findings. *Thorax, 59*(3), 252-256. doi: 10.1136/thorax.2003.012658

Chu, H., Zhou, J., Wong, B. H., Li, C., Chan, J. F., Cheng, Z. S., . . . Yuen, K. Y. (2016). Middle East Respiratory Syndrome Coronavirus Efficiently Infects Human Primary T Lymphocytes and Activates the Extrinsic and Intrinsic Apoptosis Pathways. *J Infect Dis, 213*(6), 904-914. doi: 10.1093/infdis/jiv380

Chung, H. S., Park, S. R., Choi, E. K., Park, H. J., Griffin, R. J., Song, C. W., & Park, H. (2003). Role of sphingomyelin-MAPKs pathway in heat-induced apoptosis. *Experimental & molecular medicine, 35*(3), 181-188. doi: 10.1038/emm.2003.25

Cima, G. (2014). [PED virus reinfecting U.S. herds].

Clem, R. J., Fechheimer, M., & Miller, L. K. (1991). Prevention of apoptosis by a baculovirus gene

during infection of insect cells. *Science, 254*(5036), 1388-1390. doi: 10.1126/science.1962198

Cong, Y., Hart, B. J., Gross, R., Zhou, H., Frieman, M., Bollinger, L., . . . Holbrook, M. R. (2018). MERS-CoV pathogenesis and antiviral efficacy of licensed drugs in human monocyte-derived antigen-presenting cells. *PLOS ONE, 13*(3), e0194868. doi: 10.1371/journal.pone.0194868

Cornelissen, L. A., Wierda, C. M., van der Meer, F. J., Herrewegh, A. A., Horzinek, M. C., Egberink, H. F., & de Groot, R. J. (1997). Hemagglutinin-esterase, a novel structural protein of torovirus. *J Virol, 71*(7), 5277-5286.

Cote, M., Misasi, J., Ren, T., Bruchez, A., Lee, K., Filone, C. M., . . . Cunningham, J. (2011). Small molecule inhibitors reveal Niemann-Pick C1 is essential for Ebola virus infection. *Nature, 477*(7364), 344-U122. doi: Doi 10.1038/Nature10380

Coughlin, M., Lou, G., Martinez, O., Masterman, S. K., Olsen, O. A., Moksa, A. A., . . . Prabhakar, B. S. (2007). Generation and characterization of human monoclonal neutralizing antibodies with distinct binding and sequence features against SARS coronavirus using XenoMouse. *Virology, 361*(1), 93-102. doi: 10.1016/j.virol.2006.09.029

Coughlin, M. M., Babcook, J., & Prabhakar, B. S. (2009). Human monoclonal antibodies to SARS-coronavirus inhibit infection by different mechanisms. *Virology, 394*(1), 39-46. doi: 10.1016/j.virol.2009.07.028

Cremesti, A., Paris, F., Grassme, H., Holler, N., Tschopp, J., Fuks, Z., . . . Kolesnick, R. (2001). Ceramide enables fas to cap and kill. *J Biol Chem, 276*(26), 23954-23961. doi: 10.1074/jbc.M101866200

Cucinotta, D., & Vanelli, M. (2020). WHO Declares COVID-19 a Pandemic. *Acta Biomed, 91*(1), 157-160. doi: 10.23750/abm.v91i1.9397

Czub, M., Weingartl, H., Czub, S., He, R., & Cao, J. (2005). Evaluation of modified vaccinia virus Ankara based recombinant SARS vaccine in ferrets. *Vaccine, 23*(17-18), 2273-2279. doi: 10.1016/j.vaccine.2005.01.033

Danthi, P. (2011). Enter the kill zone: initiation of death signaling during virus entry. *Virology, 411*(2), 316-324. doi: 10.1016/j.virol.2010.12.043

Davies, H. A., & Macnaughton, M. R. (1979). Comparison of the morphology of three coronaviruses. *Arch Virol, 59*(1-2), 25-33. doi: 10.1007/bf01317891

De Benedictis, P., Marciano, S., Scaravelli, D., Priori, P., Zecchin, B., Capua, I., . . . Cattoli, G. (2014). Alpha and lineage C betaCoV infections in Italian bats. *Virus genes, 48*(2), 366-371. doi: 10.1007/s11262-013-1008-x

de Groot-Mijnes, J. D., van Dun, J. M., van der Most, R. G., & de Groot, R. J. (2005). Natural history of a recurrent feline coronavirus infection and the role of cellular immunity in survival and disease. *J Virol, 79*(2), 1036-1044. doi: 10.1128/JVI.79.2.1036-1044.2005

de Groot, R. J., Baker, S., Baric, R., Enjuanes, L., Gorbalenya, A., Holmes, K., . . . Talbot, P. (2012). Family coronaviridae. *Virus taxonomy*, 806-828.

De Groot, R. J., Baker, S. C., Baric, R., Enjuanes, L., Gorbalenya, A., Holmes, K. V., . . . Talbot, P. J. (2011). Virus taxonomy: classification and nomenclature of viruses. *Ninth Report of the International Committee on Taxonomy of Viruses*, 806-828.

de Haan, C. A., & Rottier, P. J. (2005). Molecular interactions in the assembly of coronaviruses. *Adv Virus Res, 64*, 165-230. doi: 10.1016/S0065-3527(05)64006-7

De Martino, L., Marfe, G., Longo, M., Fiorito, F., Montagnaro, S., Iovane, V., . . . Pagnini, U. (2010). Bid cleavage, cytochrome c release and caspase activation in canine coronavirus-

induced apoptosis. *Vet Microbiol, 141*(1-2), 36-45. doi: 10.1016/j.vetmic.2009.09.001

de Vries, A. A. F., Horzinek, M. C., Rottier, P. J. M., & de Groot, R. J. (1997). The Genome Organization of the Nidovirales: Similarities and Differences between Arteri-, Toro-, and Coronaviruses. *Seminars in Virology, 8*(1), 33-47. doi: 10.1006/smvy.1997.0104

de Wilde, A. H., Jochmans, D., Posthuma, C. C., Zevenhoven-Dobbe, J. C., van Nieuwkoop, S., Bestebroer, T. M., . . . Snijder, E. J. (2014). Screening of an FDA-approved compound library identifies four small-molecule inhibitors of Middle East respiratory syndrome coronavirus replication in cell culture. *Antimicrob Agents Chemother, 58*(8), 4875-4884. doi: 10.1128/AAC.03011-14

de Wit, E., Rasmussen, A. L., Falzarano, D., Bushmaker, T., Feldmann, F., Brining, D. L., . . . Munster, V. J. (2013). Middle East respiratory syndrome coronavirus (MERS-CoV) causes transient lower respiratory tract infection in rhesus macaques. *Proceedings of the National Academy of Sciences, 110*(41), 16598-16603. doi: 10.1073/pnas.1310744110

de Wit, E., van Doremalen, N., Falzarano, D., & Munster, V. J. (2016). SARS and MERS: recent insights into emerging coronaviruses. *Nat Rev Microbiol, 14*(8), 523-534. doi: 10.1038/nrmicro.2016.81

Delmas, B., Gelfi, J., L'Haridon, R., Vogel, L. K., Sjostrom, H., Noren, O., & Laude, H. (1992). Aminopeptidase N is a major receptor for the entero-pathogenic coronavirus TGEV. *Nature, 357*(6377), 417-420. doi: 10.1038/357417a0

Deriane E. Gomes, H. F. F., Ana C. G. Rosa, Andrea F. Garcia, Lívia C. Bregano,, & Alexandre L. Andrade, T. C. C. (2011). Poult Intestinal Organ Culture for Propagation of Turkey

Coronavirus and Assessment of Host-virus Interactions *Brazilian Journal of Veterinary Pathology, 4*(05), 30-35.

Desforges, M., Desjardins, J., Zhang, C., & Talbot, P. J. (2013). The acetyl-esterase activity of the hemagglutinin-esterase protein of human coronavirus OC43 strongly enhances the production of infectious virus. *J Virol, 87*(6), 3097-3107. doi: 10.1128/JVI.02699-12

Diemer, C., Schneider, M., Seebach, J., Quaas, J., Frosner, G., Schatzl, H. M., & Gilch, S. (2008). Cell type-specific cleavage of nucleocapsid protein by effector caspases during SARS coronavirus infection. *J Mol Biol, 376*(1), 23-34. doi: 10.1016/j.jmb.2007.11.081

Donnelly, C. A., Ghani, A. C., Leung, G. M., Hedley, A. J., Fraser, C., Riley, S., . . . Anderson, R. M. (2003). Epidemiological determinants of spread of causal agent of severe acute respiratory syndrome in Hong Kong. *Lancet, 361*(9371), 1761-1766. doi: 10.1016/S0140-6736(03)13410-1

Doyle, L. P., & Hutchings, L. M. (1946). A transmissible gastroenteritis in pigs. *J Am Vet Med Assoc, 108*, 257-259.

Du, L., Yang, Y., Zhou, Y., Lu, L., Li, F., & Jiang, S. (2017). MERS-CoV spike protein: a key target for antivirals. *Expert Opin Ther Targets, 21*(2), 131-143. doi: 10.1080/14728222.2017.1271415

Du, L., Zhao, G., Kou, Z., Ma, C., Sun, S., Poon, V. K., . . . Jiang, S. (2013). Identification of a receptor-binding domain in the S protein of the novel human coronavirus Middle East respiratory syndrome coronavirus as an essential target for vaccine development. *J Virol, 87*(17), 9939-9942. doi: 10.1128/JVI.01048-13

Duan, J., Yan, X., Guo, X., Cao, W., Han, W., Qi, C., . . . Jin, G. (2005). A human SARS-CoV neutralizing antibody against epitope on S2 protein. *Biochem Biophys Res Commun, 333*(1), 186-193. doi: 10.1016/j.bbrc.2005.05.089

Duan, R. D. (2006). Alkaline sphingomyelinase: an old enzyme with novel implications. *Biochim*

*Biophys Acta, 1761*(3), 281-291. doi: 10.1016/j.bbalip.2006.03.007

Duarte, M., Gelfi, J., Lambert, P., Rasschaert, D., & Laude, H. (1994). Genome Organization of Porcine Epidemic Diarrhoea Virus (pp. 55-60): Springer, Boston, MA.

Ducatelle, R., Coussement, W., Debouck, P., & Hoorens, J. (1982). Pathology of experimental CV777 coronavirus enteritis in piglets. II. Electron microscopic study. *Vet Pathol, 19*(1), 57-66. doi: 10.1177/030098588201900109

Dumitru, C. A., & Gulbins, E. (2006). TRAIL activates acid sphingomyelinase via a redox mechanism and releases ceramide to trigger apoptosis. *Oncogene, 25*(41), 5612-5625. doi: 10.1038/sj.onc.1209568

Ebert, D. H., Deussing, J., Peters, C., & Dermody, T. S. (2002). Cathepsin L and cathepsin B mediate reovirus disassembly in murine fibroblast cells. *The Journal of biological chemistry, 277*(27), 24609-24617. doi: 10.1074/jbc.M201107200

Edinger, T. O., Pohl, M. O., Yángüez, E., & Stertz, S. (2015). Cathepsin W Is Required for Escape of Influenza A Virus from Late Endosomes. *mBio, 6*(3), e00297-e00297. doi: 10.1128/mBio.00297-15

Eleouet, J. F., Chilmonczyk, S., Besnardeau, L., & Laude, H. (1998). Transmissible gastroenteritis coronavirus induces programmed cell death in infected cells through a caspase-dependent pathway. *J Virol, 72*(6), 4918-4924.

Eleouet, J. F., Slee, E. A., Saurini, F., Castagne, N., Poncet, D., Garrido, C., . . . Martin, S. J. (2000). The viral nucleocapsid protein of transmissible gastroenteritis coronavirus (TGEV) is cleaved by caspase-6 and-7 during TGEV-induced apoptosis. *Journal of Virology, 74*(9), 3975-3983. doi: Doi 10.1128/Jvi.74.9.3975-3983.2000

Enjuanes, L., Dediego, M. L., Alvarez, E., Deming, D., Sheahan, T., & Baric, R. (2008). Vaccines to prevent severe acute respiratory syndrome coronavirus-induced disease. *Virus Res, 133*(1), 45-62. doi: 10.1016/j.virusres.2007.01.021

Erles, K., Toomey, C., Brooks, H. W., & Brownlie, J. (2003). Detection of a group 2 coronavirus in dogs with canine infectious respiratory disease. *Virology, 310*(2), 216-223. doi: 10.1016/s0042-6822(03)00160-0

Esen, M., Schreiner, B., Jendrossek, V., Lang, F., Fassbender, K., Grassme, H., & Gulbins, E. (2001). Mechanisms of Staphylococcus aureus induced apoptosis of human endothelial cells. *Apoptosis, 6*(6), 431-439. doi: 10.1023/a:1012445925628

Falzarano, D., de Wit, E., Rasmussen, A. L., Feldmann, F., Okumura, A., Scott, D. P., . . . Feldmann, H. (2013). Treatment with interferon-alpha2b and ribavirin improves outcome in MERS-CoV-infected rhesus macaques. *Nat Med, 19*(10), 1313-1317. doi: 10.1038/nm.3362

Fehr, A. R., & Perlman, S. (2015). Coronaviruses: an overview of their replication and pathogenesis. *Methods Mol Biol, 1282*, 1-23. doi: 10.1007/978-1-4939-2438-7_1

Ferlinz, K., Hurwitz, R., Vielhaber, G., Suzuki, K., & Sandhoff, K. (1994). Occurrence of two molecular forms of human acid sphingomyelinase. *Biochem J, 301 ( Pt 3)*, 855-862. doi: 10.1042/bj3010855

Göggel, R., Winoto-Morbach, S., Vielhaber, G., Imai, Y., Lindner, K., Brade, L., . . . Uhlig, S. (2004). PAF-mediated pulmonary edema: a new role for acid sphingomyelinase and ceramide. *Nature Medicine, 10*(2), 155-160. doi: 10.1038/nm977

Gallagher, T. M., Escarmis, C., & Buchmeier, M. J. (1991). Alteration of the pH dependence of coronavirus-induced cell fusion: effect of mutations in the spike glycoprotein. *J Virol, 65*(4), 1916-1928.

Gao, W., Tamin, A., Soloff, A., D'Aiuto, L., Nwanegbo, E., Robbins, P. D., . . . Gambotto, A. (2003).

Effects of a SARS-associated coronavirus vaccine in monkeys. *Lancet, 362*(9399), 1895-1896. doi: 10.1016/S0140-6736(03)14962-8

Gilbert, S. C., & Warimwe, G. M. (2017). Rapid development of vaccines against emerging pathogens: The replication-deficient simian adenovirus platform technology. *Vaccine, 35*(35 Pt A), 4461-4464. doi: 10.1016/j.vaccine.2017.04.085

Glowacka, I., Bertram, S., Muller, M. A., Allen, P., Soilleux, E., Pfefferle, S., . . . Pohlmann, S. (2011). Evidence that TMPRSS2 activates the severe acute respiratory syndrome coronavirus spike protein for membrane fusion and reduces viral control by the humoral immune response. *J Virol, 85*(9), 4122-4134. doi: 10.1128/JVI.02232-10

Godet, M., Grosclaude, J., Delmas, B., & Laude, H. (1994). Major receptor-binding and neutralization determinants are located within the same domain of the transmissible gastroenteritis virus (coronavirus) spike protein. *J Virol, 68*(12), 8008-8016.

Gorbalenya, A. E., Enjuanes, L., Ziebuhr, J., & Snijder, E. J. (2006). Nidovirales: evolving the largest RNA virus genome. *Virus Res, 117*(1), 17-37. doi: 10.1016/j.virusres.2006.01.017

Grasland, B., Bigault, L., Bernard, C., Quenault, H., Toulouse, O., Fablet, C., . . . Blanchard, Y. (2015). Complete genome sequence of a porcine epidemic diarrhea s gene indel strain isolated in france in december 2014. *Genome Announc, 3*(3), e00535-00515. doi: 10.1128/genomeA.00535-15

Grassme, H., Bock, J., Kun, J., & Gulbins, E. (2002). Clustering of CD40 ligand is required to form a functional contact with CD40. *J Biol Chem, 277*(33), 30289-30299. doi: 10.1074/jbc.M200494200

Grassme, H., Cremesti, A., Kolesnick, R., & Gulbins, E. (2003). Ceramide-mediated clustering is required for CD95-DISC formation. *Oncogene, 22*(35), 5457-5470. doi: 10.1038/sj.onc.1206540

Grassme, H., Gulbins, E., Brenner, B., Ferlinz, K., Sandhoff, K., Harzer, K., . . . Meyer, T. F. (1997). Acidic sphingomyelinase mediates entry of N. gonorrhoeae into nonphagocytic cells. *Cell, 91*(5), 605-615. doi: 10.1016/s0092-8674(00)80448-1

Grassme, H., Jekle, A., Riehle, A., Schwarz, H., Berger, J., Sandhoff, K., . . . Gulbins, E. (2001). CD95 signaling via ceramide-rich membrane rafts. *J Biol Chem, 276*(23), 20589-20596. doi: 10.1074/jbc.M101207200

Grassme, H., Jendrossek, V., & Gulbins, E. (2001). Molecular mechanisms of bacteria induced apoptosis. *Apoptosis, 6*(6), 441-445. doi: 10.1023/a:1012485506972

Grassme, H., Jendrossek, V., Riehle, A., von Kurthy, G., Berger, J., Schwarz, H., . . . Gulbins, E. (2003). Host defense against Pseudomonas aeruginosa requires ceramide-rich membrane rafts. *Nat Med, 9*(3), 322-330. doi: 10.1038/nm823

Grassme, H., Riehle, A., Wilker, B., & Gulbins, E. (2005). Rhinoviruses infect human epithelial cells via ceramide-enriched membrane platforms. *J Biol Chem, 280*(28), 26256-26262. doi: 10.1074/jbc.M500835200

Greenough, T. C., Babcock, G. J., Roberts, A., Hernandez, H. J., Thomas, W. D., Jr., Coccia, J. A., . . . Ambrosino, D. M. (2005). Development and characterization of a severe acute respiratory syndrome-associated coronavirus-neutralizing human monoclonal antibody that provides effective immunoprophylaxis in mice. *J Infect Dis, 191*(4), 507-514. doi: 10.1086/427242

Grove, J., & Marsh, M. (2011). The cell biology of receptor-mediated virus entry. *J Cell Biol, 195*(7), 1071-1082. doi: 10.1083/jcb.201108131

Gruenberg, J., & van der Goot, F. G. (2006). Mechanisms of pathogen entry through the endosomal

compartments. *Nat Rev Mol Cell Biol, 7*(7), 495-504. doi: 10.1038/nrm1959

Guan, Y., Zheng, B. J., He, Y. Q., Liu, X. L., Zhuang, Z. X., Cheung, C. L., . . . Poon, L. L. (2003). Isolation and characterization of viruses related to the SARS coronavirus from animals in southern China. *Science, 302*(5643), 276-278. doi: 10.1126/science.1087139

Gulbins, E., & Grassme, H. (2002). Ceramide and cell death receptor clustering. *Biochim Biophys Acta, 1585*(2-3), 139-145. doi: 10.1016/s1388-1981(02)00334-7

Gulbins, E., & Li, P. L. (2006). Physiological and pathophysiological aspects of ceramide. *Am J Physiol Regul Integr Comp Physiol, 290*(1), R11-26. doi: 10.1152/ajpregu.00416.2005

Haagmans, B. L., Al Dhahiry, S. H., Reusken, C. B., Raj, V. S., Galiano, M., Myers, R., . . . Koopmans, M. P. (2014). Middle East respiratory syndrome coronavirus in dromedary camels: an outbreak investigation. *Lancet Infect Dis, 14*(2), 140-145. doi: 10.1016/S1473-3099(13)70690-X

Haagmans, B. L., van den Brand, J. M., Provacia, L. B., Raj, V. S., Stittelaar, K. J., Getu, S., . . . Osterhaus, A. D. (2015). Asymptomatic Middle East respiratory syndrome coronavirus infection in rabbits. *J Virol, 89*(11), 6131-6135. doi: 10.1128/JVI.00661-15

Han, D. P., Penn-Nicholson, A., & Cho, M. W. (2006). Identification of critical determinants on ACE2 for SARS-CoV entry and development of a potent entry inhibitor. *Virology, 350*(1), 15-25. doi: 10.1016/j.virol.2006.01.029

Hanke, D., Jenckel, M., Petrov, A., Ritzmann, M., Stadler, J., Akimkin, V., . . . Hoper, D. (2015). Comparison of porcine epidemic diarrhea viruses from Germany and the United States, 2014. *Emerg Infect Dis, 21*(3), 493-496. doi: 10.3201/eid2103.141165

Hauck, C. R., Grassme, H., Bock, J., Jendrossek, V., Ferlinz, K., Meyer, T. F., & Gulbins, E. (2000). Acid sphingomyelinase is involved in CEACAM receptor-mediated phagocytosis of Neisseria gonorrhoeae. *FEBS Lett, 478*(3), 260-266. doi: 10.1016/s0014-5793(00)01851-2

He, X., Okino, N., Dhami, R., Dagan, A., Gatt, S., Schulze, H., . . . Schuchman, E. H. (2003). Purification and characterization of recombinant, human acid ceramidase. Catalytic reactions and interactions with acid sphingomyelinase. *J Biol Chem, 278*(35), 32978-32986. doi: 10.1074/jbc.M301936200

He, Y., Zhou, Y., Liu, S., Kou, Z., Li, W., Farzan, M., & Jiang, S. (2004). Receptor-binding domain of SARS-CoV spike protein induces highly potent neutralizing antibodies: implication for developing subunit vaccine. *Biochem Biophys Res Commun, 324*(2), 773-781. doi: 10.1016/j.bbrc.2004.09.106

Hemida, M. G., Chu, D. K., Poon, L. L., Perera, R. A., Alhammadi, M. A., Ng, H. Y., . . . Peiris, M. (2014). MERS coronavirus in dromedary camel herd, Saudi Arabia. *Emerg Infect Dis, 20*(7), 1231-1234. doi: 10.3201/eid2007.140571

Hemmila, E., Turbide, C., Olson, M., Jothy, S., Holmes, K. V., & Beauchemin, N. (2004). Ceacam1a-/- mice are completely resistant to infection by murine coronavirus mouse hepatitis virus A59. *J Virol, 78*(18), 10156-10165. doi: 10.1128/JVI.78.18.10156-10165.2004

Herrewegh, A. A., Smeenk, I., Horzinek, M. C., Rottier, P. J., & de Groot, R. J. (1998). Feline coronavirus type II strains 79-1683 and 79-1146 originate from a double recombination between feline coronavirus type I and canine coronavirus. *J Virol, 72*(5), 4508-4514.

Hinshaw, V. S., Olsen, C. W., Dybdahl-Sissoko, N., & Evans, D. (1994). Apoptosis: a mechanism of cell killing by influenza A and B viruses. *J Virol, 68*(6), 3667-3673.

Hiscox, J. A., Wurm, T., Wilson, L., Britton, P., Cavanagh, D., & Brooks, G. (2001). The coronavirus infectious bronchitis virus nucleoprotein localizes to the nucleolus. *J Virol,*

114

*75*(1), 506-512. doi: 10.1128/JVI.75.1.506-512.2001

Hoffmann, M., Kleine-Weber, H., Krüger, N., Müller, M., Drosten, C., & Pöhlmann, S. (2020). The novel coronavirus 2019 (2019-nCoV) uses the SARS-coronavirus receptor ACE2 and the cellular protease TMPRSS2 for entry into target cells. *bioRxiv*, 2020.2001.2031.929042. doi: 10.1101/2020.01.31.929042

Hofmann, H., Hattermann, K., Marzi, A., Gramberg, T., Geier, M., Krumbiegel, M., . . . Pohlmann, S. (2004). S protein of severe acute respiratory syndrome-associated coronavirus mediates entry into hepatoma cell lines and is targeted by neutralizing antibodies in infected patients. *J Virol, 78*(12), 6134-6142. doi: 10.1128/JVI.78.12.6134-6142.2004

Hofmann, H., Pyrc, K., van der Hoek, L., Geier, M., Berkhout, B., & Pohlmann, S. (2005). Human coronavirus NL63 employs the severe acute respiratory syndrome coronavirus receptor for cellular entry. *Proc Natl Acad Sci U S A, 102*(22), 7988-7993. doi: 10.1073/pnas.0409465102

Hofmann, M., & Wyler, R. (1988). Propagation of the virus of porcine epidemic diarrhea in cell culture. *Journal of clinical microbiology, 26*(11), 2235-2239.

Hogle, J. M. (2002). Poliovirus cell entry: common structural themes in viral cell entry pathways. *Annu Rev Microbiol, 56*, 677-702. doi: 10.1146/annurev.micro.56.012302.160757

Honda-Okubo, Y., Barnard, D., Ong, C. H., Peng, B. H., Tseng, C. T., & Petrovsky, N. (2015). Severe acute respiratory syndrome-associated coronavirus vaccines formulated with delta inulin adjuvants provide enhanced protection while ameliorating lung eosinophilic immunopathology. *J Virol, 89*(6), 2995-3007. doi: 10.1128/JVI.02980-14

Huang, I. C., Bosch, B. J., Li, F., Li, W., Lee, K. H., Ghiran, S., . . . Choe, H. (2006). SARS coronavirus, but not human coronavirus NL63, utilizes cathepsin L to infect ACE2-expressing cells. *J Biol Chem, 281*(6), 3198-3203. doi: 10.1074/jbc.M508381200

Huang, Y. W., Dickerman, A. W., Pineyro, P., Li, L., Fang, L., Kiehne, R., . . . Meng, X. J. (2013). Origin, evolution, and genotyping of emergent porcine epidemic diarrhea virus strains in the United States. *mBio, 4*(5), e00737-00713. doi: 10.1128/mBio.00737-13

Huentelman, M. J., Zubcevic, J., Hernandez Prada, J. A., Xiao, X., Dimitrov, D. S., Raizada, M. K., & Ostrov, D. A. (2004). Structure-based discovery of a novel angiotensin-converting enzyme 2 inhibitor. *Hypertension, 44*(6), 903-906. doi: 10.1161/01.HYP.0000146120.29648.36

Hurst, K. R., Koetzner, C. A., & Masters, P. S. (2009). Identification of in vivo-interacting domains of the murine coronavirus nucleocapsid protein. *J Virol, 83*(14), 7221-7234. doi: 10.1128/JVI.00440-09

Hurst, K. R., Koetzner, C. A., & Masters, P. S. (2013). Characterization of a critical interaction between the coronavirus nucleocapsid protein and nonstructural protein 3 of the viral replicase-transcriptase complex. *J Virol, 87*(16), 9159-9172. doi: 10.1128/JVI.01275-13

Hurst, K. R., Kuo, L., Koetzner, C. A., Ye, R., Hsue, B., & Masters, P. S. (2005). A major determinant for membrane protein interaction localizes to the carboxy-terminal domain of the mouse coronavirus nucleocapsid protein. *Journal of Virology, 79*(21), 13285-13297. doi: 10.1128/JVI.79.21.13285-13297.2005

Hurst, K. R., Ye, R., Goebel, S. J., Jayaraman, P., & Masters, P. S. (2010). An interaction between the nucleocapsid protein and a component of the replicase-transcriptase complex is crucial for the infectivity of coronavirus genomic RNA. *J Virol, 84*(19), 10276-10288. doi: 10.1128/JVI.01287-10

Igney, F. H., & Krammer, P. H. (2002). Death and anti-death: tumour resistance to apoptosis. *Nat*

*Rev Cancer, 2*(4), 277-288. doi: 10.1038/nrc776

Inoue, Y., Tanaka, N., Tanaka, Y., Inoue, S., Morita, K., Zhuang, M., . . . Sugamura, K. (2007). Clathrin-dependent entry of severe acute respiratory syndrome coronavirus into target cells expressing ACE2 with the cytoplasmic tail deleted. *J Virol, 81*(16), 8722-8729. doi: 10.1128/JVI.00253-07

Jaru-Ampornpan, P., Jengarn, J., Wanitchang, A., & Jongkaewwattana, A. (2017). Porcine Epidemic Diarrhea Virus 3C-Like Protease-Mediated Nucleocapsid Processing: Possible Link to Viral Cell Culture Adaptability. *J Virol, 91*(2). doi: 10.1128/JVI.01660-16

Jeffers, S. A., Hemmila, E. M., & Holmes, K. V. (2006). Human coronavirus 229E can use CD209L (L-SIGN) to enter cells. *Adv Exp Med Biol, 581*, 265-269. doi: 10.1007/978-0-387-33012-9_44

Jeffers, S. A., Tusell, S. M., Gillim-Ross, L., Hemmila, E. M., Achenbach, J. E., Babcock, G. J., . . . Holmes, K. V. (2004). CD209L (L-SIGN) is a receptor for severe acute respiratory syndrome coronavirus. *Proc Natl Acad Sci U S A, 101*(44), 15748-15753. doi: 10.1073/pnas.0403812101

Jenkins, R. W., Canals, D., & Hannun, Y. A. (2009). Roles and regulation of secretory and lysosomal acid sphingomyelinase. *Cell Signal, 21*(6), 836-846. doi: 10.1016/j.cellsig.2009.01.026

Ji, C. M., Wang, B., Zhou, J., & Huang, Y. W. (2018). Aminopeptidase-N-independent entry of porcine epidemic diarrhea virus into Vero or porcine small intestine epithelial cells. *Virology, 517*, 16-23. doi: 10.1016/j.virol.2018.02.019

Jung, K., & Saif, L. J. (2015). Porcine epidemic diarrhea virus infection: Etiology, epidemiology, pathogenesis and immunoprophylaxis. *Vet J, 204*(2), 134-143. doi: 10.1016/j.tvjl.2015.02.017

Kashkar, H., Wiegmann, K., Yazdanpanah, B., Haubert, D., & Kronke, M. (2005). Acid sphingomyelinase is indispensable for UV light-induced bax conformational change at the mitochondrial membrane. *Journal of Biological Chemistry, 280*(21), 20804-20813. doi: 10.1074/jbc.M410869200

Kaufmann, S. H., McElrath, M. J., Lewis, D. J., & Del Giudice, G. (2014). Challenges and responses in human vaccine development. *Curr Opin Immunol, 28*, 18-26. doi: 10.1016/j.coi.2014.01.009

Kawase, M., Shirato, K., Matsuyama, S., & Taguchi, F. (2009a). Protease-mediated entry via the endosome of human coronavirus 229E. *J Virol, 83*(2), 712-721. doi: 10.1128/JVI.01933-08

Kawase, M., Shirato, K., Matsuyama, S., & Taguchi, F. (2009b). Protease-Mediated Entry via the Endosome of Human Coronavirus 229E. *Journal of Virology, 83*(2), 712-721. doi: 10.1128/JVI.01933-08

Keng, C. T., Zhang, A., Shen, S., Lip, K. M., Fielding, B. C., Tan, T. H., . . . Tan, Y. J. (2005). Amino acids 1055 to 1192 in the S2 region of severe acute respiratory syndrome coronavirus S protein induce neutralizing antibodies: implications for the development of vaccines and antiviral agents. *J Virol, 79*(6), 3289-3296. doi: 10.1128/JVI.79.6.3289-3296.2005

Keyaerts, E., Vijgen, L., Maes, P., Neyts, J., & Van Ranst, M. (2004). In vitro inhibition of severe acute respiratory syndrome coronavirus by chloroquine. *Biochem Biophys Res Commun, 323*(1), 264-268. doi: 10.1016/j.bbrc.2004.08.085

Kielian, M., & Rey, F. A. (2006). Virus membrane-fusion proteins: more than one way to make a

hairpin. *Nat Rev Microbiol, 4*(1), 67-76. doi: 10.1038/nrmicro1326

Kim, E., Okada, K., Kenniston, T., Raj, V. S., AlHajri, M. M., Farag, E. A., . . . Gambotto, A. (2014). Immunogenicity of an adenoviral-based Middle East Respiratory Syndrome coronavirus vaccine in BALB/c mice. *Vaccine, 32*(45), 5975-5982. doi: 10.1016/j.vaccine.2014.08.058

Kim, K. H., Tandi, T. E., Choi, J. W., Moon, J. M., & Kim, M. S. (2017). Middle East respiratory syndrome coronavirus (MERS-CoV) outbreak in South Korea, 2015: epidemiology, characteristics and public health implications. *J Hosp Infect, 95*(2), 207-213. doi: 10.1016/j.jhin.2016.10.008

Kim, M. K., Yu, M. S., Park, H. R., Kim, K. B., Lee, C., Cho, S. Y., . . . Chong, Y. (2011). 2,6-Bis-arylmethyloxy-5-hydroxychromones with antiviral activity against both hepatitis C virus (HCV) and SARS-associated coronavirus (SCV). *Eur J Med Chem, 46*(11), 5698-5704. doi: 10.1016/j.ejmech.2011.09.005

Kim, R. H., Takabe, K., Milstien, S., & Spiegel, S. (2009). Export and functions of sphingosine-1-phosphate. *Biochim Biophys Acta, 1791*(7), 692-696. doi: 10.1016/j.bbalip.2009.02.011

Kim, Y., Liu, H., Galasiti Kankanamalage, A. C., Weerasekara, S., Hua, D. H., Groutas, W. C., . . . Pedersen, N. C. (2016). Reversal of the Progression of Fatal Coronavirus Infection in Cats by a Broad-Spectrum Coronavirus Protease Inhibitor. *PLoS Pathog, 12*(3), e1005531. doi: 10.1371/journal.ppat.1005531

Kim, Y., Mandadapu, S. R., Groutas, W. C., & Chang, K. O. (2013). Potent inhibition of feline coronaviruses with peptidyl compounds targeting coronavirus 3C-like protease. *Antiviral Res, 97*(2), 161-168. doi: 10.1016/j.antiviral.2012.11.005

Kim, Y., Oh, C., Shivanna, V., Hesse, R. A., & Chang, K. O. (2017). Trypsin-independent porcine epidemic diarrhea virus US strain with altered virus entry mechanism. *BMC Vet Res, 13*(1), 356. doi: 10.1186/s12917-017-1283-1

Kim, Y., Shivanna, V., Narayanan, S., Prior, A. M., Weerasekara, S., Hua, D. H., . . . Chang, K. O. (2015). Broad-spectrum inhibitors against 3C-like proteases of feline coronaviruses and feline caliciviruses. *J Virol, 89*(9), 4942-4950. doi: 10.1128/JVI.03688-14

Kirchdoerfer, R. N., Cottrell, C. A., Wang, N., Pallesen, J., Yassine, H. M., Turner, H. L., . . . Ward, A. B. (2016a). Pre-fusion structure of a human coronavirus spike protein. *Nature, 531*(7592), 118-121. doi: 10.1038/nature17200

Kirchdoerfer, R. N., Cottrell, C. A., Wang, N., Pallesen, J., Yassine, H. M., Turner, H. L., . . . Ward, A. B. (2016b). Prefusion structure of a human coronavirus spike protein. *Nature, 531*(7592), 118-121. doi: 10.1038/nature17200

Kischkel, F. C., Hellbardt, S., Behrmann, I., Germer, M., Pawlita, M., Krammer, P. H., & Peter, M. E. (1995). Cytotoxicity-dependent APO-1 (Fas/CD95)-associated proteins form a death-inducing signaling complex (DISC) with the receptor. *Embo j, 14*(22), 5579-5588.

Kitatani, K., Idkowiak-Baldys, J., & Hannun, Y. A. (2008). The sphingolipid salvage pathway in ceramide metabolism and signaling. *Cell Signal, 20*(6), 1010-1018. doi: 10.1016/j.cellsig.2007.12.006

Kocherhans, R., Bridgen, A., Ackermann, M., & Tobler, K. (2001). Completion of the porcine epidemic diarrhoea coronavirus (PEDV) genome sequence. *Virus genes, 23*(2), 137-144. doi: 10.1023/a:1011831902219

Kolesnick, R. N., Goni, F. M., & Alonso, A. (2000). Compartmentalization of ceramide signaling: physical foundations and biological effects. *J Cell Physiol, 184*(3), 285-300. doi: 10.1002/1097-4652(200009)184:3<285::AID-JCP2>3.0.CO;2-3

Kono, M., Tatsumi, K., Imai, A. M., Saito, K., Kuriyama, T., & Shirasawa, H. (2008). Inhibition of human coronavirus 229E infection in human epithelial lung cells (L132) by chloroquine: involvement of p38 MAPK and ERK. *Antiviral Res, 77*(2), 150-152. doi: 10.1016/j.antiviral.2007.10.011

Kornhuber, J., Tripal, P., Reichel, M., Muhle, C., Rhein, C., Muehlbacher, M., . . . Gulbins, E. (2010). Functional Inhibitors of Acid Sphingomyelinase (FIASMAs): a novel pharmacological group of drugs with broad clinical applications. *Cell Physiol Biochem, 26*(1), 9-20. doi: 10.1159/000315101

Krijnse-Locker, J., Ericsson, M., Rottier, P. J., & Griffiths, G. (1994). Characterization of the budding compartment of mouse hepatitis virus: evidence that transport from the RER to the Golgi complex requires only one vesicular transport step. *J Cell Biol, 124*(1-2), 55-70. doi: 10.1083/jcb.124.1.55

Kumar, V., Shin, J. S., Shie, J. J., Ku, K. B., Kim, C., Go, Y. Y., . . . Liang, P. H. (2017). Identification and evaluation of potent Middle East respiratory syndrome coronavirus (MERS-CoV) 3CL(Pro) inhibitors. *Antiviral Res, 141*, 101-106. doi: 10.1016/j.antiviral.2017.02.007

Kuo, C. J., Liu, H. G., Lo, Y. K., Seong, C. M., Lee, K. I., Jung, Y. S., & Liang, P. H. (2009). Individual and common inhibitors of coronavirus and picornavirus main proteases. *FEBS Lett, 583*(3), 549-555. doi: 10.1016/j.febslet.2008.12.059

Kweon, C.-h., Kwon, B.-j., Jung, T.-s., Kee, Y.-j., Hur, D.-h., Hwang, E.-k., . . . An, S.-h. (1993). Isolation of porcine epidemic diarrhea virus (PEDV) in Korea. *Korean Journal of Veterinary Research, 33*(2), 249-254.

Kweon, C. H., Kwon, B. J., Lee, J. G., Kwon, G. O., & Kang, Y. B. (1999). Derivation of attenuated porcine epidemic diarrhea virus (PEDV) as vaccine candidate. *Vaccine, 17*(20-21), 2546-2553. doi: 10.1016/s0264-410x(99)00059-6

Lacour, S., Hammann, A., Grazide, S., Lagadic-Gossmann, D., Athias, A., Sergent, O., . . . Dimanche-Boitrel, M. T. (2004). Cisplatin-induced CD95 redistribution into membrane lipid rafts of HT29 human colon cancer cells. *Cancer research, 64*(10), 3593-3598. doi: 10.1158/0008-5472.CAN-03-2787

Ladman, B. S., Pope, C. R., Ziegler, A. F., Swieczkowski, T., Callahan, C. J., Davison, S., & Gelb, J., Jr. (2002). Protection of chickens after live and inactivated virus vaccination against challenge with nephropathogenic infectious bronchitis virus PA/Wolgemuth/98. *Avian Dis, 46*(4), 938-944. doi: 10.1637/0005-2086(2002)046[0938:POCALA]2.0.CO;2

Lamontagne, L., Descoteaux, J. P., & Jolicoeur, P. (1989). Mouse hepatitis virus 3 replication in T and B lymphocytes correlate with viral pathogenicity. *J Immunol, 142*(12), 4458-4465.

Lau, S. K., Woo, P. C., Li, K. S., Huang, Y., Tsoi, H. W., Wong, B. H., . . . Yuen, K. Y. (2005). Severe acute respiratory syndrome coronavirus-like virus in Chinese horseshoe bats. *Proc Natl Acad Sci U S A, 102*(39), 14040-14045. doi: 10.1073/pnas.0506735102

Lau, S. K. P., Wong, A. C. P., Lau, T. C. K., & Woo, P. C. Y. (2017). Molecular Evolution of MERS Coronavirus: Dromedaries as a Recent Intermediate Host or Long-Time Animal Reservoir? *Int J Mol Sci, 18*(10). doi: 10.3390/ijms18102138

Lau, Y. L., & Peiris, J. S. (2005). Pathogenesis of severe acute respiratory syndrome. *Curr Opin Immunol, 17*(4), 404-410. doi: 10.1016/j.coi.2005.05.009

Law, H. K., Cheung, C. Y., Ng, H. Y., Sia, S. F., Chan, Y. O., Luk, W., . . . Lau, Y. L. (2005). Chemokine up-regulation in SARS-coronavirus-infected, monocyte-derived human dendritic cells. *Blood, 106*(7), 2366-2374. doi: 10.1182/blood-2004-10-4166

Lee, C., Lee, J. M., Lee, N. R., Jin, B. S., Jang, K. J., Kim, D. E., . . . Chong, Y. (2009). Aryl diketoacids (ADK) selectively inhibit duplex DNA-unwinding activity of SARS coronavirus NTPase/helicase. *Bioorg Med Chem Lett, 19*(6), 1636-1638. doi: 10.1016/j.bmcl.2009.02.010

Lee, N., Hui, D., Wu, A., Chan, P., Cameron, P., Joynt, G. M., . . . Sung, J. J. (2003). A major outbreak of severe acute respiratory syndrome in Hong Kong. *N Engl J Med, 348*(20), 1986-1994. doi: 10.1056/NEJMoa030685

Lee, S., & Lee, C. (2014). Outbreak-related porcine epidemic diarrhea virus strains similar to US strains, South Korea, 2013. *Emerg Infect Dis, 20*(7), 1223-1226. doi: 10.3201/eid2007.140294

Leparc-Goffart, I., Hingley, S. T., Chua, M. M., Jiang, X., Lavi, E., & Weiss, S. R. (1997). Altered pathogenesis of a mutant of the murine coronavirus MHV-A59 is associated with a Q159L amino acid substitution in the spike protein. *Virology, 239*(1), 1-10. doi: 10.1006/viro.1997.8877

Li, B. X., Ge, J. W., & Li, Y. J. (2007). Porcine aminopeptidase N is a functional receptor for the PEDV coronavirus. *Virology, 365*(1), 166-172. doi: 10.1016/j.virol.2007.03.031

Li, F. (2015). Receptor recognition mechanisms of coronaviruses: a decade of structural studies. *J Virol, 89*(4), 1954-1964. doi: 10.1128/JVI.02615-14

Li, F., Berardi, M., Li, W., Farzan, M., Dormitzer, P. R., & Harrison, S. C. (2006). Conformational states of the severe acute respiratory syndrome coronavirus spike protein ectodomain. *J Virol, 80*(14), 6794-6800. doi: 10.1128/JVI.02744-05

Li, J., & Yuan, J. (2008). Caspases in apoptosis and beyond. *Oncogene, 27*(48), 6194-6206. doi: 10.1038/onc.2008.297

Li, Q., Guan, X., Wu, P., Wang, X., Zhou, L., Tong, Y., . . . Feng, Z. (2020). Early Transmission Dynamics in Wuhan, China, of Novel Coronavirus–Infected Pneumonia. *New England Journal of Medicine*. doi: 10.1056/NEJMoa2001316

Li, W., Hulswit, R. J. G., Widjaja, I., Raj, V. S., McBride, R., Peng, W., . . . Bosch, B. J. (2017). Identification of sialic acid-binding function for the Middle East respiratory syndrome coronavirus spike glycoprotein. *Proc Natl Acad Sci U S A, 114*(40), E8508-E8517. doi: 10.1073/pnas.1712592114

Li, W., Li, H., Liu, Y., Pan, Y., Deng, F., Song, Y., . . . He, Q. (2012). New variants of porcine epidemic diarrhea virus, China, 2011. *Emerg Infect Dis, 18*(8), 1350-1353. doi: 10.3201/eid1808.120002

Li, W., Luo, R., He, Q., van Kuppeveld, F. J. M., Rottier, P. J. M., & Bosch, B. J. (2017). Aminopeptidase N is not required for porcine epidemic diarrhea virus cell entry. *Virus Res, 235*, 6-13. doi: 10.1016/j.virusres.2017.03.018

Li, W., Moore, M. J., Vasilieva, N., Sui, J., Wong, S. K., Berne, M. A., . . . Farzan, M. (2003). Angiotensin-converting enzyme 2 is a functional receptor for the SARS coronavirus. *Nature, 426*(6965), 450-454. doi: 10.1038/nature02145

Li, W., Shi, Z., Yu, M., Ren, W., Smith, C., Epstein, J. H., . . . Wang, L. F. (2005). Bats are natural reservoirs of SARS-like coronaviruses. *Science, 310*(5748), 676-679. doi: 10.1126/science.1118391

Li, W., van Kuppeveld, F. J. M., He, Q., Rottier, P. J. M., & Bosch, B. J. (2016). Cellular entry of the porcine epidemic diarrhea virus. *Virus Res, 226*, 117-127. doi: 10.1016/j.virusres.2016.05.031

Liang, P. H. (2006). Characterization and inhibition of SARS-coronavirus main protease. *Curr Top*

*Med Chem, 6*(4), 361-376. doi: 10.2174/156802606776287090

Lin, C. N., Chung, W. B., Chang, S. W., Wen, C. C., Liu, H., Chien, C. H., & Chiou, M. T. (2014). US-like strain of porcine epidemic diarrhea virus outbreaks in Taiwan, 2013-2014. *J Vet Med Sci, 76*(9), 1297-1299. doi: 10.1292/jvms.14-0098

Lin, H. X., Feng, Y., Wong, G., Wang, L., Li, B., Zhao, X., . . . Zhang, C. (2008). Identification of residues in the receptor-binding domain (RBD) of the spike protein of human coronavirus NL63 that are critical for the RBD-ACE2 receptor interaction. *J Gen Virol, 89*(Pt 4), 1015-1024. doi: 10.1099/vir.0.83331-0

Lin, Y. S., Lin, C. F., Fang, Y. T., Kuo, Y. M., Liao, P. C., Yeh, T. M., . . . Lei, H. Y. (2005). Antibody to severe acute respiratory syndrome (SARS)-associated coronavirus spike protein domain 2 cross-reacts with lung epithelial cells and causes cytotoxicity. *Clinical and experimental immunology, 141*(3), 500-508. doi: 10.1111/j.1365-2249.2005.02864.x

Lipsitch, M., Cohen, T., Cooper, B., Robins, J. M., Ma, S., James, L., . . . Murray, M. (2003). Transmission dynamics and control of severe acute respiratory syndrome. *Science, 300*(5627), 1966-1970. doi: 10.1126/science.1086616

Liu, C., Ma, Y., Yang, Y., Zheng, Y., Shang, J., Zhou, Y., . . . Li, F. (2016). Cell Entry of Porcine Epidemic Diarrhea Coronavirus Is Activated by Lysosomal Proteases. *J Biol Chem, 291*(47), 24779-24786. doi: 10.1074/jbc.M116.740746

Liu, C., Tang, J., Ma, Y., Liang, X., Yang, Y., Peng, G., . . . Li, F. (2015). Receptor Usage and Cell Entry of Porcine Epidemic Diarrhea Coronavirus. *Journal of Virology, 89*(11), 6121. doi: 10.1128/JVI.00430-15

Liu, C., Xu, H. Y., & Liu, D. X. (2001). Induction of caspase-dependent apoptosis in cultured cells by the avian coronavirus infectious bronchitis virus. *J Virol, 75*(14), 6402-6409. doi: 10.1128/JVI.75.14.6402-6409.2001

Liu, Y., Pu, Y., & Zhang, X. (2006). Role of the mitochondrial signaling pathway in murine coronavirus-induced oligodendrocyte apoptosis. *J Virol, 80*(1), 395-403. doi: 10.1128/JVI.80.1.395-403.2006

Locksley, R. M., Killeen, N., & Lenardo, M. J. (2001). The TNF and TNF receptor superfamilies: integrating mammalian biology. *Cell, 104*(4), 487-501. doi: 10.1016/s0092-8674(01)00237-9

Lopez-Montero, I., Monroy, F., Velez, M., & Devaux, P. F. (2010). Ceramide: from lateral segregation to mechanical stress. *Biochim Biophys Acta, 1798*(7), 1348-1356. doi: 10.1016/j.bbamem.2009.12.007

Lu, I. L., Mahindroo, N., Liang, P. H., Peng, Y. H., Kuo, C. J., Tsai, K. C., . . . Wu, S. Y. (2006). Structure-based drug design and structural biology study of novel nonpeptide inhibitors of severe acute respiratory syndrome coronavirus main protease. *J Med Chem, 49*(17), 5154-5161. doi: 10.1021/jm060207o

Mackay, I. M., & Arden, K. E. (2015). Middle East respiratory syndrome: An emerging coronavirus infection tracked by the crowd. *Virus Res, 202*, 60-88. doi: 10.1016/j.virusres.2015.01.021

Marchesini, N., & Hannun, Y. A. (2004). Acid and neutral sphingomyelinases: roles and mechanisms of regulation. *Biochem Cell Biol, 82*(1), 27-44. doi: 10.1139/o03-091

Marsden, P. A., Ning, Q., Fung, L. S., Luo, X., Chen, Y., Mendicino, M., . . . Levy, G. A. (2003). The Fgl2/fibroleukin prothrombinase contributes to immunologically mediated thrombosis in experimental and human viral hepatitis *J Clin Invest* (Vol. 112, pp. 58-66).

Marsh, M., & Helenius, A. (2006). Virus entry: open sesame. *Cell, 124*(4), 729-740. doi:

10.1016/j.cell.2006.02.007

Masters, P. S. (2006). The molecular biology of coronaviruses. *Adv Virus Res, 66*, 193-292. doi: 10.1016/S0065-3527(06)66005-3

Matsuyama, S., Nagata, N., Shirato, K., Kawase, M., Takeda, M., & Taguchi, F. (2010). Efficient activation of the severe acute respiratory syndrome coronavirus spike protein by the transmembrane protease TMPRSS2. *J Virol, 84*(24), 12658-12664. doi: 10.1128/JVI.01542-10

Matsuyama, S., Ujike, M., Morikawa, S., Tashiro, M., & Taguchi, F. (2005). Protease-mediated enhancement of severe acute respiratory syndrome coronavirus infection. *Proc Natl Acad Sci U S A, 102*(35), 12543-12547. doi: 10.1073/pnas.0503203102

Matsuyama, S., Ujike, M., Morikawa, S., Tashiro, M., & Taguchi, F. (2005). Protease-mediated enhancement of severe acute respiratory syndrome coronavirus infection. *Proceedings of the National Academy of Sciences of the United States of America, 102*(35), 12543-12547. doi: 10.1073/pnas.0503203102

McBride, R., van Zyl, M., & Fielding, B. C. (2014). The coronavirus nucleocapsid is a multifunctional protein. *Viruses, 6*(8), 2991-3018. doi: 10.3390/v6082991

McIlwain, D. R., Berger, T., & Mak, T. W. (2013). Caspase functions in cell death and disease. *Cold Spring Harb Perspect Biol, 5*(4), a008656. doi: 10.1101/cshperspect.a008656

McIntosh, K. (1974). Coronaviruses: a comparative review *Current Topics in Microbiology and Immunology/Ergebnisse der Mikrobiologie und Immunitätsforschung* (pp. 85-129): Springer.

McIntosh, K., Dees, J. H., Becker, W. B., Kapikian, A. Z., & Chanock, R. M. (1967). Recovery in tracheal organ cultures of novel viruses from patients with respiratory disease. *Proc Natl Acad Sci U S A, 57*(4), 933-940. doi: 10.1073/pnas.57.4.933

Miller, M. E., Adhikary, S., Kolokoltsov, A. A., & Davey, R. A. (2012). Ebolavirus requires acid sphingomyelinase activity and plasma membrane sphingomyelin for infection. *J Virol, 86*(14), 7473-7483. doi: 10.1128/JVI.00136-12

Millet, J. K., & Whittaker, G. R. (2015). Host cell proteases: Critical determinants of coronavirus tropism and pathogenesis. *Virus Res, 202*, 120-134. doi: 10.1016/j.virusres.2014.11.021

Molenkamp, R., & Spaan, W. J. (1997). Identification of a specific interaction between the coronavirus mouse hepatitis virus A59 nucleocapsid protein and packaging signal. *Virology, 239*(1), 78-86. doi: 10.1006/viro.1997.8867

Monto, A. S. (1974). Medical reviews. Coronaviruses. *Yale J Biol Med, 47*(4), 234-251.

Moody, C. A., & Laimins, L. A. (2009). Human papillomaviruses activate the ATM DNA damage pathway for viral genome amplification upon differentiation. *PLoS Pathog, 5*(10), e1000605. doi: 10.1371/journal.ppat.1000605

Morales, A., Lee, H., Goni, F. M., Kolesnick, R., & Fernandez-Checa, J. C. (2007). Sphingolipids and cell death. *Apoptosis, 12*(5), 923-939. doi: 10.1007/s10495-007-0721-0

Moyer, C. L., & Nemerow, G. R. (2011). Viral weapons of membrane destruction: variable modes of membrane penetration by non-enveloped viruses. *Curr Opin Virol, 1*(1), 44-49. doi: 10.1016/j.coviro.2011.05.002

Muller, M. A., Meyer, B., Corman, V. M., Al-Masri, M., Turkestani, A., Ritz, D., . . . Memish, Z. A. (2015). Presence of Middle East respiratory syndrome coronavirus antibodies in Saudi Arabia: a nationwide, cross-sectional, serological study. *Lancet Infect Dis, 15*(6), 629. doi: 10.1016/S1473-3099(15)00029-8

Muller, S., Dennemarker, J., & Reinheckel, T. (2012). Specific functions of lysosomal proteases

in endocytic and autophagic pathways. *Biochim Biophys Acta, 1824*(1), 34-43. doi: 10.1016/j.bbapap.2011.07.003

Nagy, B., Nagy, G., Meder, M., & Mocsari, E. (1996). Enterotoxigenic Escherichia coli, rotavirus, porcine epidemic diarrhoea virus, adenovirus and calici-like virus in porcine postweaning diarrhoea in Hungary. *Acta Vet Hung, 44*(1), 9-19.

Nal, B., Chan, C., Kien, F., Siu, L., Tse, J., Chu, K., . . . Altmeyer, R. (2005). Differential maturation and subcellular localization of severe acute respiratory syndrome coronavirus surface proteins S, M and E. *J Gen Virol, 86*(Pt 5), 1423-1434. doi: 10.1099/vir.0.80671-0

Narayanan, K., Maeda, A., Maeda, J., & Makino, S. (2000). Characterization of the coronavirus M protein and nucleocapsid interaction in infected cells. *J Virol, 74*(17), 8127-8134. doi: 10.1128/jvi.74.17.8127-8134.2000

Nelson, G. W., Stohlman, S. A., & Tahara, S. M. (2000). High affinity interaction between nucleocapsid protein and leader/intergenic sequence of mouse hepatitis virus RNA. *J Gen Virol, 81*(Pt 1), 181-188. doi: 10.1099/0022-1317-81-1-181

Neuman, B. W., Adair, B. D., Yoshioka, C., Quispe, J. D., Orca, G., Kuhn, P., . . . Buchmeier, M. J. (2006). Supramolecular architecture of severe acute respiratory syndrome coronavirus revealed by electron cryomicroscopy. *J Virol, 80*(16), 7918-7928. doi: 10.1128/JVI.00645-06

Neuman, B. W., Kiss, G., Kunding, A. H., Bhella, D., Baksh, M. F., Connelly, S., . . . Buchmeier, M. J. (2011). A structural analysis of M protein in coronavirus assembly and morphology. *J Struct Biol, 174*(1), 11-22. doi: 10.1016/j.jsb.2010.11.021

Newrzella, D., & Stoffel, W. (1996). Functional analysis of the glycosylation of murine acid sphingomyelinase. *J Biol Chem, 271*(50), 32089-32095. doi: 10.1074/jbc.271.50.32089

Nieto-Torres, J. L., DeDiego, M. L., Verdia-Baguena, C., Jimenez-Guardeno, J. M., Regla-Nava, J. A., Fernandez-Delgado, R., . . . Enjuanes, L. (2014). Severe acute respiratory syndrome coronavirus envelope protein ion channel activity promotes virus fitness and pathogenesis. *PLoS Pathog, 10*(5), e1004077. doi: 10.1371/journal.ppat.1004077

Ogretmen, B., & Hannun, Y. A. (2004). Biologically active sphingolipids in cancer pathogenesis and treatment. *Nat Rev Cancer, 4*(8), 604-616. doi: 10.1038/nrc1411

Oh, C., Kim, Y., & Chang, K. O. (2019). Proteases facilitate the endosomal escape of porcine epidemic diarrhea virus during entry into host cells. *Virus Res, 272*, 197730. doi: 10.1016/j.virusres.2019.197730

Ohnuma, K., Haagmans, B. L., Hatano, R., Raj, V. S., Mou, H., Iwata, S., . . . Morimoto, C. (2013). Inhibition of Middle East Respiratory Syndrome Coronavirus Infection by Anti-CD26 Monoclonal Antibody *J Virol* (Vol. 87, pp. 13892-13899).

Oka, T., Saif, L. J., Marthaler, D., Esseili, M. A., Meulia, T., Lin, C. M., . . . Wang, Q. (2014). Cell culture isolation and sequence analysis of genetically diverse US porcine epidemic diarrhea virus strains including a novel strain with a large deletion in the spike gene. *Vet Microbiol, 173*(3-4), 258-269. doi: 10.1016/j.vetmic.2014.08.012

Paarlberg, P. (2014). UPDATED ESTIMATED ECONOMIC WELFARE IMPACTS OF PORCINE EPIDEMIC DIARRHEA VIRUS (PEDV) *14-4*.

Padhan, K., Minakshi, R., Towheed, M. A., & Jameel, S. (2008). Severe acute respiratory syndrome coronavirus 3a protein activates the mitochondrial death pathway through p38 MAP kinase activation. *J Gen Virol, 89*(Pt 8), 1960-1969. doi: 10.1099/vir.0.83665-0

Paolini, C., De Francesco, R., & Gallinari, P. (2000). Enzymatic properties of hepatitis C virus NS3-associated helicase. *J Gen Virol, 81*(Pt 5), 1335-1345. doi: 10.1099/0022-1317-81-5-

1335

Paris, F., Fuks, Z., Kang, A., Capodieci, P., Juan, G., Ehleiter, D., . . . Kolesnick, R. (2001). Endothelial apoptosis as the primary lesion initiating intestinal radiation damage in mice. *Science, 293*(5528), 293-297. doi: 10.1126/science.1060191

Park, J. E., Cruz, D. J., & Shin, H. J. (2011). Receptor-bound porcine epidemic diarrhea virus spike protein cleaved by trypsin induces membrane fusion. *Arch Virol, 156*(10), 1749-1756. doi: 10.1007/s00705-011-1044-6

Park, J. E., Cruz, D. J., & Shin, H. J. (2014). Clathrin- and serine proteases-dependent uptake of porcine epidemic diarrhea virus into Vero cells. *Virus Res, 191*, 21-29. doi: 10.1016/j.virusres.2014.07.022

Park, J. E., Li, K., Barlan, A., Fehr, A. R., Perlman, S., McCray, P. B., Jr., & Gallagher, T. (2016). Proteolytic processing of Middle East respiratory syndrome coronavirus spikes expands virus tropism. *Proc Natl Acad Sci U S A, 113*(43), 12262-12267. doi: 10.1073/pnas.1608147113

Park, S. J., Song, D. S., & Park, B. K. (2013). Molecular epidemiology and phylogenetic analysis of porcine epidemic diarrhea virus (PEDV) field isolates in Korea. *Arch Virol, 158*(7), 1533-1541. doi: 10.1007/s00705-013-1651-5

Pasma, T., Furness, M. C., Alves, D., & Aubry, P. (2016). Outbreak investigation of porcine epidemic diarrhea in swine in Ontario. *Can Vet J, 57*(1), 84-89.

Paul, S. M., & Perlman, S. (2013). Coronaviridae *Fields Virology* (6th ed., pp. 825–858). Philadelphia, PA: Lippincot Williams & Willkins.

Paul, S. M., & Stanley, P. (2013). Coronaviridae (Sixth ed ed., Vol. 1, pp. 825-858). Philadelphia, PA: Lippincot Williams & Willkins.

Pedersen, N. C. (2009). A review of feline infectious peritonitis virus infection: 1963-2008. *J Feline Med Surg, 11*(4), 225-258. doi: 10.1016/j.jfms.2008.09.008

Peiris, J. S., Guan, Y., & Yuen, K. Y. (2004). Severe acute respiratory syndrome. *Nat Med, 10*(12 Suppl), S88-97. doi: 10.1038/nm1143

Pensaert, M., Haelterman, E. O., & Burnstein, T. (1970). Transmissible gastroenteritis of swine: virus-intestinal cell interactions. I. Immunofluorescence, histopathology and virus production in the small intestine through the course of infection. *Arch Gesamte Virusforsch, 31*(3), 321-334. doi: 10.1007/bf01253767

Pensaert, M. B., & de Bouck, P. (1978). A new coronavirus-like particle associated with diarrhea in swine. *Arch Virol, 58*(3), 243-247. doi: 10.1007/bf01317606

Peter, M. E., & Krammer, P. H. (1998). Mechanisms of CD95 (APO-1/Fas)-mediated apoptosis. *Curr Opin Immunol, 10*(5), 545-551. doi: 10.1016/s0952-7915(98)80222-7

Pfeiffer, A., Bottcher, A., Orso, E., Kapinsky, M., Nagy, P., Bodnar, A., . . . Schmitz, G. (2001). Lipopolysaccharide and ceramide docking to CD14 provokes ligand-specific receptor clustering in rafts. *Eur J Immunol, 31*(11), 3153-3164. doi: 10.1002/1521-4141(200111)31:11<3153::aid-immu3153>3.0.co;2-0

Pijpers, A., van Nieuwstadt, A. P., Terpstra, C., & Verheijden, J. H. (1993). Porcine epidemic diarrhoea virus as a cause of persistent diarrhoea in a herd of breeding and finishing pigs. *Vet Rec, 132*(6), 129-131. doi: 10.1136/vr.132.6.129

Pratelli, A., Tinelli, A., Decaro, N., Cirone, F., Elia, G., Roperto, S., . . . Buonavoglia, C. (2003). Efficacy of an inactivated canine coronavirus vaccine in pups. *New Microbiol, 26*(2), 151-155.

Pratelli, A., Tinelli, A., Decaro, N., Martella, V., Camero, M., Tempesta, M., . . . Buonavoglia, C.

(2004). Safety and efficacy of a modified-live canine coronavirus vaccine in dogs. *Vet Microbiol, 99*(1), 43-49. doi: 10.1016/j.vetmic.2003.07.009

Pritchard, G. C., Paton, D. J., Wibberley, G., & Ibata, G. (1999). Transmissible gastroenteritis and porcine epidemic diarrhoea in Britain. *Vet Rec, 144*(22), 616-618. doi: 10.1136/vr.144.22.616

Pritchett-Corning, K. R., Cosentino, J., & Clifford, C. B. (2009). Contemporary prevalence of infectious agents in laboratory mice and rats. *Lab Anim, 43*(2), 165-173. doi: 10.1258/la.2008.008009

ProMED-mail. (2020). ProMED-mail. from https://promedmail.org/promed-post/?id=6864153

Puranaveja, S., Poolperm, P., Lertwatcharasarakul, P., Kesdaengsakonwut, S., Boonsoongnern, A., Urairong, K., . . . Thanawongnuwech, R. (2009). Chinese-like strain of porcine epidemic diarrhea virus, Thailand. *Emerg Infect Dis, 15*(7), 1112-1115. doi: 10.3201/eid1507.081256

Pyrc, K., Berkhout, B., & van der Hoek, L. (2007). The novel human coronaviruses NL63 and HKU1. *J Virol, 81*(7), 3051-3057. doi: 10.1128/JVI.01466-06

Qiu, Z., Hingley, S. T., Simmons, G., Yu, C., Das Sarma, J., Bates, P., & Weiss, S. R. (2006). Endosomal proteolysis by cathepsins is necessary for murine coronavirus mouse hepatitis virus type 2 spike-mediated entry. *J Virol, 80*(12), 5768-5776. doi: 10.1128/JVI.00442-06

Raj, V. S., Mou, H., Smits, S. L., Dekkers, D. H., Muller, M. A., Dijkman, R., . . . Haagmans, B. L. (2013). Dipeptidyl peptidase 4 is a functional receptor for the emerging human coronavirus-EMC. *Nature, 495*(7440), 251-254. doi: 10.1038/nature12005

Ramajayam, R., Tan, K. P., & Liang, P. H. (2011). Recent development of 3C and 3CL protease inhibitors for anti-coronavirus and anti-picornavirus drug discovery. *Biochem Soc Trans, 39*(5), 1371-1375. doi: 10.1042/BST0391371

Reed, L. J., & Muench, H. (1938). A Simple Method of Estimating Fifty Per Cent Endpoints12. *American Journal of Epidemiology, 27*(3), 493-497. doi: 10.1093/oxfordjournals.aje.a118408

Regan, A. D., Ousterout, D. G., & Whittaker, G. R. (2010). Feline lectin activity is critical for the cellular entry of feline infectious peritonitis virus. *J Virol, 84*(15), 7917-7921. doi: 10.1128/JVI.00964-10

Regan, A. D., Shraybman, R., Cohen, R. D., & Whittaker, G. R. (2008). Differential role for low pH and cathepsin-mediated cleavage of the viral spike protein during entry of serotype II feline coronaviruses. *Vet Microbiol, 132*(3-4), 235-248. doi: 10.1016/j.vetmic.2008.05.019

Regan, A. D., & Whittaker, G. R. (2008). Utilization of DC-SIGN for entry of feline coronaviruses into host cells. *J Virol, 82*(23), 11992-11996. doi: 10.1128/JVI.01094-08

Ren, L., Yang, R., Guo, L., Qu, J., Wang, J., & Hung, T. (2005). Apoptosis induced by the SARS-associated coronavirus in Vero cells is replication-dependent and involves caspase. *DNA Cell Biol, 24*(8), 496-502. doi: 10.1089/dna.2005.24.496

Riley, S., Fraser, C., Donnelly, C. A., Ghani, A. C., Abu-Raddad, L. J., Hedley, A. J., . . . Anderson, R. M. (2003). Transmission dynamics of the etiological agent of SARS in Hong Kong: impact of public health interventions. *Science, 300*(5627), 1961-1966. doi: 10.1126/science.1086478

Roberts, A., Paddock, C., Vogel, L., Butler, E., Zaki, S., & Subbarao, K. (2005). Aged BALB/c mice as a model for increased severity of severe acute respiratory syndrome in elderly humans. *J Virol, 79*(9), 5833-5838. doi: 10.1128/JVI.79.9.5833-5838.2005

Rota, P. A., Oberste, M. S., Monroe, S. S., Nix, W. A., Campagnoli, R., Icenogle, J. P., . . . Bellini, W. J. (2003). Characterization of a novel coronavirus associated with severe acute

respiratory syndrome. *Science, 300*(5624), 1394-1399. doi: 10.1126/science.1085952

Rotolo, J. A., Zhang, J., Donepudi, M., Lee, H., Fuks, Z., & Kolesnick, R. (2005). Caspase-dependent and -independent activation of acid sphingomyelinase signaling. *J Biol Chem, 280*(28), 26425-26434. doi: 10.1074/jbc.M414569200

Rottier, P. J. M., Nakamura, K., Schellen, P., Volders, H., & Haijema, B. J. (2005). Acquisition of Macrophage Tropism during the Pathogenesis of Feline Infectious Peritonitis Is Determined by Mutations in the Feline Coronavirus Spike Protein *J Virol* (Vol. 79, pp. 14122-14130).

Rowland, R. R., Chauhan, V., Fang, Y., Pekosz, A., Kerrigan, M., & Burton, M. D. (2005). Intracellular localization of the severe acute respiratory syndrome coronavirus nucleocapsid protein: absence of nucleolar accumulation during infection and after expression as a recombinant protein in vero cells. *J Virol, 79*(17), 11507-11512. doi: 10.1128/JVI.79.17.11507-11512.2005

Rubio-Moscardo, F., Blesa, D., Mestre, C., Siebert, R., Balasas, T., Benito, A., . . . Martinez-Climent, J. A. (2005). Characterization of 8p21.3 chromosomal deletions in B-cell lymphoma: TRAIL-R1 and TRAIL-R2 as candidate dosage-dependent tumor suppressor genes. *Blood, 106*(9), 3214-3222. doi: 10.1182/blood-2005-05-2013

Ruch, T. R., & Machamer, C. E. (2012). The Coronavirus E Protein: Assembly and Beyond *Viruses* (Vol. 4, pp. 363-382).

Saelens, X., Festjens, N., Vande Walle, L., van Gurp, M., van Loo, G., & Vandenabeele, P. (2004). Toxic proteins released from mitochondria in cell death. *Oncogene, 23*(16), 2861-2874. doi: 10.1038/sj.onc.1207523

Santana, P., Pena, L. A., Haimovitz-Friedman, A., Martin, S., Green, D., McLoughlin, M., . . . Kolesnick, R. (1996). Acid sphingomyelinase-deficient human lymphoblasts and mice are defective in radiation-induced apoptosis. *Cell, 86*(2), 189-199. doi: 10.1016/s0092-8674(00)80091-4

Sanvicens, N., & Cotter, T. G. (2006). Ceramide is the key mediator of oxidative stress-induced apoptosis in retinal photoreceptor cells. *Journal of neurochemistry, 98*(5), 1432-1444. doi: 10.1111/j.1471-4159.2006.03977.x

Sato, T., Takeyama, N., Katsumata, A., Tuchiya, K., Kodama, T., & Kusanagi, K. (2011). Mutations in the spike gene of porcine epidemic diarrhea virus associated with growth adaptation in vitro and attenuation of virulence in vivo. *Virus genes, 43*(1), 72-78. doi: 10.1007/s11262-011-0617-5

Sawicki, S. G., Sawicki, D. L., & Siddell, S. G. (2007). A contemporary view of coronavirus transcription. *J Virol, 81*(1), 20-29. doi: 10.1128/JVI.01358-06

Schütze, S., Potthoff, K., Machleidt, T., Berkovic, D., Wiegmann, K., & Krönke, M. (1992). TNF activates NF-κB by phosphatidylcholine-specific phospholipase C-induced "Acidic" sphingomyelin breakdown. *Cell, 71*(5), 765-776. doi: 10.1016/0092-8674(92)90553-o

Schalk, A. F. a. H., M.C. (1931). An Apparently New Respiratory Disease of Baby Chicks. *J. Amer. Vet. Med. Ass, 78*, 413-423.

Schiff, L. A. (1998). Reovirus capsid proteins sigma 3 and mu 1: interactions that influence viral entry, assembly, and translational control. *Curr Top Microbiol Immunol, 233*(Pt 1), 167-183.

Schissel, S. L., Keesler, G. A., Schuchman, E. H., Williams, K. J., & Tabas, I. (1998). The cellular trafficking and zinc dependence of secretory and lysosomal sphingomyelinase, two products of the acid sphingomyelinase gene. *J Biol Chem, 273*(29), 18250-18259. doi:

10.1074/jbc.273.29.18250

Schneider, P. B., & Kennedy, E. P. (1967). Sphingomyelinase in normal human spleens and in spleens from subjects with Niemann-Pick disease. *J Lipid Res, 8*(3), 202-209.

Schultze, B., Gross, H. J., Brossmer, R., & Herrler, G. (1991). The S protein of bovine coronavirus is a hemagglutinin recognizing 9-O-acetylated sialic acid as a receptor determinant. *J Virol, 65*(11), 6232-6237.

Schultze, B., Krempl, C., Ballesteros, M. L., Shaw, L., Schauer, R., Enjuanes, L., & Herrler, G. (1996). Transmissible gastroenteritis coronavirus, but not the related porcine respiratory coronavirus, has a sialic acid (N-glycolylneuraminic acid) binding activity. *J Virol, 70*(8), 5634-5637.

Schulz, L. L., & Tonsor, G. T. (2015). Assessment of the economic impacts of porcine epidemic diarrhea virus in the United States. *J Anim Sci, 93*(11), 5111-5118. doi: 10.2527/jas.2015-9136

Schwandner, R., Wiegmann, K., Bernardo, K., Kreder, D., & Kronke, M. (1998). TNF receptor death domain-associated proteins TRADD and FADD signal activation of acid sphingomyelinase. *J Biol Chem, 273*(10), 5916-5922. doi: 10.1074/jbc.273.10.5916

Seidah, N. G., & Prat, A. (2012). The biology and therapeutic targeting of the proprotein convertases. *Nat Rev Drug Discov, 11*(5), 367-383. doi: 10.1038/nrd3699

Shi, D., Lv, M., Chen, J., Shi, H., Zhang, S., Zhang, X., & Feng, L. (2014). Molecular Characterizations of Subcellular Localization Signals in the Nucleocapsid Protein of Porcine Epidemic Diarrhea Virus *Viruses* (Vol. 6, pp. 1253-1273).

Shibata, I., Tsuda, T., Mori, M., Ono, M., Sueyoshi, M., & Uruno, K. (2000). Isolation of porcine epidemic diarrhea virus in porcine cell cultures and experimental infection of pigs of different ages. *Vet Microbiol, 72*(3-4), 173-182. doi: 10.1016/s0378-1135(99)00199-6

Shirato, K., Kanou, K., Kawase, M., & Matsuyama, S. (2017). Clinical Isolates of Human Coronavirus 229E Bypass the Endosome for Cell Entry. *J Virol, 91*(1). doi: 10.1128/JVI.01387-16

Shirato, K., Kawase, M., & Matsuyama, S. (2013). Middle East respiratory syndrome coronavirus infection mediated by the transmembrane serine protease TMPRSS2. *J Virol, 87*(23), 12552-12561. doi: 10.1128/JVI.01890-13

Shirato, K., Matsuyama, S., Ujike, M., & Taguchi, F. (2011). Role of proteases in the release of porcine epidemic diarrhea virus from infected cells. *J Virol, 85*(15), 7872-7880. doi: 10.1128/JVI.00464-11

Shivanna, V., Kim, Y., & Chang, K. O. (2014a). The crucial role of bile acids in the entry of porcine enteric calicivirus. *Virology, 456-457*, 268-278. doi: 10.1016/j.virol.2014.04.002

Shivanna, V., Kim, Y., & Chang, K. O. (2014b). Endosomal acidification and cathepsin L activity is required for calicivirus replication. *Virology, 464-465*, 287-295. doi: 10.1016/j.virol.2014.07.025

Shivanna, V., Kim, Y., & Chang, K. O. (2015). Ceramide formation mediated by acid sphingomyelinase facilitates endosomal escape of caliciviruses. *Virology, 483*, 218-228. doi: 10.1016/j.virol.2015.04.022

Shulla, A., Heald-Sargent, T., Subramanya, G., Zhao, J., Perlman, S., & Gallagher, T. (2011). A transmembrane serine protease is linked to the severe acute respiratory syndrome coronavirus receptor and activates virus entry. *J Virol, 85*(2), 873-882. doi: 10.1128/JVI.02062-10

Simmons, G., Gosalia, D. N., Rennekamp, A. J., Reeves, J. D., Diamond, S. L., & Bates, P. (2005).

Inhibitors of cathepsin L prevent severe acute respiratory syndrome coronavirus entry. *Proc Natl Acad Sci U S A, 102*(33), 11876-11881. doi: 10.1073/pnas.0505577102

Simmons, G., Reeves, J. D., Rennekamp, A. J., Amberg, S. M., Piefer, A. J., & Bates, P. (2004). Characterization of severe acute respiratory syndrome-associated coronavirus (SARS-CoV) spike glycoprotein-mediated viral entry. *Proceedings of the National Academy of Sciences, 101*(12), 4240-4245. doi: 10.1073/pnas.0306446101

Simmons, G., Zmora, P., Gierer, S., Heurich, A., & Pohlmann, S. (2013). Proteolytic activation of the SARS-coronavirus spike protein: cutting enzymes at the cutting edge of antiviral research. *Antiviral Res, 100*(3), 605-614. doi: 10.1016/j.antiviral.2013.09.028

Siu, Y. L., Teoh, K. T., Lo, J., Chan, C. M., Kien, F., Escriou, N., . . . Nal, B. (2008). The M, E, and N structural proteins of the severe acute respiratory syndrome coronavirus are required for efficient assembly, trafficking, and release of virus-like particles. *J Virol, 82*(22), 11318-11330. doi: 10.1128/JVI.01052-08

Snijder, E. J., Bredenbeek, P. J., Dobbe, J. C., Thiel, V., Ziebuhr, J., Poon, L. L., . . . Gorbalenya, A. E. (2003). Unique and conserved features of genome and proteome of SARS-coronavirus, an early split-off from the coronavirus group 2 lineage. *J Mol Biol, 331*(5), 991-1004. doi: 10.1016/s0022-2836(03)00865-9

Song, D., Moon, H., & Kang, B. (2015). Porcine epidemic diarrhea: a review of current epidemiology and available vaccines. *Clin Exp Vaccine Res, 4*(2), 166-176. doi: 10.7774/cevr.2015.4.2.166

Song, D. S., Oh, J. S., Kang, B. K., Yang, J. S., Moon, H. J., Yoo, H. S., . . . Park, B. K. (2007). Oral efficacy of Vero cell attenuated porcine epidemic diarrhea virus DR13 strain. *Res Vet Sci, 82*(1), 134-140. doi: 10.1016/j.rvsc.2006.03.007

Spiegel, M., Schneider, K., Weber, F., Weidmann, M., & Hufert, F. T. (2006). Interaction of severe acute respiratory syndrome-associated coronavirus with dendritic cells. *J Gen Virol, 87*(Pt 7), 1953-1960. doi: 10.1099/vir.0.81624-0

Stancevic, B., & Kolesnick, R. (2010). Ceramide-rich platforms in transmembrane signaling. *FEBS Lett, 584*(9), 1728-1740. doi: 10.1016/j.febslet.2010.02.026

Stennicke, H. R., & Salvesen, G. S. (1997). Biochemical characteristics of caspases-3, -6, -7, and -8. *J Biol Chem, 272*(41), 25719-25723. doi: 10.1074/jbc.272.41.25719

Stevenson, G. W., Hoang, H., Schwartz, K. J., Burrough, E. R., Sun, D., Madson, D., . . . Yoon, K. J. (2013). Emergence of Porcine epidemic diarrhea virus in the United States: clinical signs, lesions, and viral genomic sequences. *J Vet Diagn Invest, 25*(5), 649-654. doi: 10.1177/1040638713501675

Stockman, L. J., Bellamy, R., & Garner, P. (2006). SARS: systematic review of treatment effects. *PLoS medicine, 3*(9), e343. doi: 10.1371/journal.pmed.0030343

Stohlman, S. A., Baric, R. S., Nelson, G. N., Soe, L. H., Welter, L. M., & Deans, R. J. (1988). Specific interaction between coronavirus leader RNA and nucleocapsid protein. *J Virol, 62*(11), 4288-4295.

Stohr, K., & Coll, W. H. O. M. (2003). A multicentre collaboration to investigate the cause of severe acute respiratory syndrome. *Lancet, 361*(9370), 1730-1733. doi: Doi 10.1016/S0140-6736(03)13376-4

Stroher, U., DiCaro, A., Li, Y., Strong, J. E., Aoki, F., Plummer, F., . . . Feldmann, H. (2004). Severe acute respiratory syndrome-related coronavirus is inhibited by interferon- alpha. *J Infect Dis, 189*(7), 1164-1167. doi: 10.1086/382597

Sturman, L. S., Ricard, C. S., & Holmes, K. V. (1985). Proteolytic cleavage of the E2 glycoprotein

of murine coronavirus: activation of cell-fusing activity of virions by trypsin and separation of two different 90K cleavage fragments. *J Virol, 56*(3), 904-911.

Subbarao, K., McAuliffe, J., Vogel, L., Fahle, G., Fischer, S., Tatti, K., . . . Murphy, B. (2004). Prior infection and passive transfer of neutralizing antibody prevent replication of severe acute respiratory syndrome coronavirus in the respiratory tract of mice. *J Virol, 78*(7), 3572-3577. doi: 10.1128/jvi.78.7.3572-3577.2004

Sui, J., Li, W., Murakami, A., Tamin, A., Matthews, L. J., Wong, S. K., . . . Marasco, W. A. (2004). Potent neutralization of severe acute respiratory syndrome (SARS) coronavirus by a human mAb to S1 protein that blocks receptor association. *Proc Natl Acad Sci U S A, 101*(8), 2536-2541. doi: 10.1073/pnas.0307140101

Suliman, A., Lam, A., Datta, R., & Srivastava, R. K. (2001). Intracellular mechanisms of TRAIL: apoptosis through mitochondrial-dependent and -independent pathways. *Oncogene, 20*(17), 2122-2133. doi: 10.1038/sj.onc.1204282

Sun, D., Wang, X., Wei, S., Chen, J., & Feng, L. (2016). Epidemiology and vaccine of porcine epidemic diarrhea virus in China: a mini-review. *J Vet Med Sci, 78*(3), 355-363. doi: 10.1292/jvms.15-0446

Sun, R.-Q., Cai, R.-J., Chen, Y.-Q., Liang, P.-S., Chen, D.-K., & Song, C.-X. (2012). Outbreak of Porcine Epidemic Diarrhea in Suckling Piglets, China. *Emerging Infectious Diseases, 18*(1), 161-163. doi: 10.3201/eid1801.111259

Tai, W., Wang, Y., Fett, C. A., Zhao, G., Li, F., Perlman, S., . . . Du, L. (2017). Recombinant Receptor-Binding Domains of Multiple Middle East Respiratory Syndrome Coronaviruses (MERS-CoVs) Induce Cross-Neutralizing Antibodies against Divergent Human and Camel MERS-CoVs and Antibody Escape Mutants. *J Virol, 91*(1). doi: 10.1128/JVI.01651-16

Takahashi, K., Okada, K., & Ohshima, K. (1983). An outbreak of swine diarrhea of a new-type associated with coronavirus-like particles in Japan. *Nihon Juigaku Zasshi, 45*(6), 829-832. doi: 10.1292/jvms1939.45.829

Takano, T., Tomizawa, K., Morioka, H., Doki, T., & Hohdatsu, T. (2014). Evaluation of protective efficacy of the synthetic peptide vaccine containing the T-helper 1 epitope with CpG oligodeoxynucleotide against feline infectious peritonitis virus infection in cats. *Antivir Ther, 19*(7), 645-650. doi: 10.3851/IMP2735

Takasuka, N., Fujii, H., Takahashi, Y., Kasai, M., Morikawa, S., Itamura, S., . . . Tsunetsugu-Yokota, Y. (2004). A subcutaneously injected UV-inactivated SARS coronavirus vaccine elicits systemic humoral immunity in mice. *Int Immunol, 16*(10), 1423-1430. doi: 10.1093/intimm/dxh143

Tan, Y. J., Fielding, B. C., Goh, P. Y., Shen, S., Tan, T. H., Lim, S. G., & Hong, W. (2004). Overexpression of 7a, a protein specifically encoded by the severe acute respiratory syndrome coronavirus, induces apoptosis via a caspase-dependent pathway. *J Virol, 78*(24), 14043-14047. doi: 10.1128/JVI.78.24.14043-14047.2004

Tang, L., Zhu, Q., Qin, E., Yu, M., Ding, Z., Shi, H., . . . Chen, Z. (2004). Inactivated SARS-CoV vaccine prepared from whole virus induces a high level of neutralizing antibodies in BALB/c mice. *DNA Cell Biol, 23*(6), 391-394. doi: 10.1089/104454904323145272

Tani, H., Shiokawa, M., Kaname, Y., Kambara, H., Mori, Y., Abe, T., . . . Matsuura, Y. (2010). Involvement of ceramide in the propagation of Japanese encephalitis virus. *J Virol, 84*(6), 2798-2807. doi: 10.1128/JVI.02499-09

Tanner, J. A., Zheng, B. J., Zhou, J., Watt, R. M., Jiang, J. Q., Wong, K. L., . . . Huang, J. D. (2005). The adamantane-derived bananins are potent inhibitors of the helicase activities and

replication of SARS coronavirus. *Chem Biol, 12*(3), 303-311. doi: 10.1016/j.chembiol.2005.01.006

ter Meulen, J., Bakker, A. B. H., van den Brink, E. N., Weverling, G. J., Martina, B. E. E., Haagmans, B. L., . . . Osterhaus, A. D. M. E. (2004). Human monoclonal antibody as prophylaxis for SARS coronavirus infection in ferrets. *The Lancet, 363*(9427), 2139-2141. doi: 10.1016/s0140-6736(04)16506-9

Theuns, S., Conceicao-Neto, N., Christiaens, I., Zeller, M., Desmarets, L. M., Roukaerts, I. D., . . . Nauwynck, H. J. (2015). Complete genome sequence of a porcine epidemic diarrhea virus from a novel outbreak in belgium, january 2015. *Genome Announc, 3*(3), e00506-00515. doi: 10.1128/genomeA.00506-15

Thiel, V., Herold, J., Schelle, B., & Siddell, S. G. (2001). Viral replicase gene products suffice for coronavirus discontinuous transcription. *J Virol, 75*(14), 6676-6681. doi: 10.1128/JVI.75.14.6676-6681.2001

tian, k., Lv, C., Xiao, Y., & Li, X. (2016). Porcine epidemic diarrhea virus: current insights. *Virus Adaptation and Treatment, 8*, 1. doi: 10.2147/vaat.s107275

Tiew, K. C., He, G., Aravapalli, S., Mandadapu, S. R., Gunnam, M. R., Alliston, K. R., . . . Groutas, W. C. (2011). Design, synthesis, and evaluation of inhibitors of Norwalk virus 3C protease. *Bioorg Med Chem Lett, 21*(18), 5315-5319. doi: 10.1016/j.bmcl.2011.07.016

Tooze, J., Tooze, S., & Warren, G. (1984). Replication of coronavirus MHV-A59 in sac- cells: determination of the first site of budding of progeny virions. *Eur J Cell Biol, 33*(2), 281-293.

Traggiai, E., Becker, S., Subbarao, K., Kolesnikova, L., Uematsu, Y., Gismondo, M. R., . . . Lanzavecchia, A. (2004). An efficient method to make human monoclonal antibodies from memory B cells: potent neutralization of SARS coronavirus. *Nat Med, 10*(8), 871-875. doi: 10.1038/nm1080

Tripet, B., Howard, M. W., Jobling, M., Holmes, R. K., Holmes, K. V., & Hodges, R. S. (2004). Structural characterization of the SARS-coronavirus spike S fusion protein core. *J Biol Chem, 279*(20), 20836-20849. doi: 10.1074/jbc.M400759200

Tyrell, D. (1968). Coronaviruses. *Nature (Lond.), 220*, 650.

Tyrrell, D. A., Cohen, S., & Schlarb, J. E. (1993). Signs and symptoms in common colds. *Epidemiol Infect, 111*(1), 143-156. doi: 10.1017/s0950268800056764

Usami, Y., Yamaguchi, O., Kumanomido, K., & Matsumura, Y. (1998). Antibody Response of Pregnant Sows to Porcine Epidemic Diarrhea Virus Live Vaccine and Maternally-Derived Antibodies of the Piglets. *Journal of the Japan Veterinary Medical Association, 51*(11), 652-655. doi: 10.12935/jvma1951.51.652

Utermohlen, O., Herz, J., Schramm, M., & Kronke, M. (2008). Fusogenicity of membranes: the impact of acid sphingomyelinase on innate immune responses. *Immunobiology, 213*(3-4), 307-314. doi: 10.1016/j.imbio.2007.10.016

Utermohlen, O., Karow, U., Lohler, J., & Kronke, M. (2003). Severe impairment in early host defense against Listeria monocytogenes in mice deficient in acid sphingomyelinase. *J Immunol, 170*(5), 2621-2628. doi: 10.4049/jimmunol.170.5.2621

Van Diep, N., Norimine, J., Sueyoshi, M., Lan, N. T., Hirai, T., & Yamaguchi, R. (2015). US-like isolates of porcine epidemic diarrhea virus from Japanese outbreaks between 2013 and 2014. *SpringerPlus, 4*(1), 756. doi: 10.1186/s40064-015-1552-z

van Doremalen, N., Miazgowicz, K. L., Milne-Price, S., Bushmaker, T., Robertson, S., Scott, D., . . . Munster, V. J. (2014). Host species restriction of Middle East respiratory syndrome

coronavirus through its receptor, dipeptidyl peptidase 4. *J Virol, 88*(16), 9220-9232. doi: 10.1128/JVI.00676-14

Vasiljeva, O., Reinheckel, T., Peters, C., Turk, D., Turk, V., & Turk, B. (2007a). Emerging roles of cysteine cathepsins in disease and their potential as drug targets. *Current pharmaceutical design, 13*(4), 387-403. doi: Doi 10.2174/138161207780162962

Vasiljeva, O., Reinheckel, T., Peters, C., Turk, D., Turk, V., & Turk, B. (2007b). Emerging roles of cysteine cathepsins in disease and their potential as drug targets. *Curr Pharm Des, 13*(4), 387-403.

Vennema, H., de Groot, R. J., Harbour, D. A., Dalderup, M., Gruffydd-Jones, T., Horzinek, M. C., & Spaan, W. J. (1990). Early death after feline infectious peritonitis virus challenge due to recombinant vaccinia virus immunization. *J Virol, 64*(3), 1407-1409.

Vennema, H., Poland, A., Foley, J., & Pedersen, N. C. (1998). Feline infectious peritonitis viruses arise by mutation from endemic feline enteric coronaviruses. *Virology, 243*(1), 150-157. doi: 10.1006/viro.1998.9045

Verheij, M., Bose, R., Lin, X. H., Yao, B., Jarvis, W. D., Grant, S., . . . Kolesnick, R. N. (1996). Requirement for ceramide-initiated SAPK/JNK signalling in stress-induced apoptosis. *Nature, 380*(6569), 75-79. doi: 10.1038/380075a0

Verma, S., Bednar, V., Blount, A., & Hogue, B. G. (2006). Identification of functionally important negatively charged residues in the carboxy end of mouse hepatitis coronavirus A59 nucleocapsid protein. *J Virol, 80*(9), 4344-4355. doi: 10.1128/JVI.80.9.4344-4355.2006

Vincent, M. J., Bergeron, E., Benjannet, S., Erickson, B. R., Rollin, P. E., Ksiazek, T. G., . . . Nichol, S. T. (2005). Chloroquine is a potent inhibitor of SARS coronavirus infection and spread. *Virol J, 2*, 69. doi: 10.1186/1743-422X-2-69

Vlasak, R., Luytjes, W., Spaan, W., & Palese, P. (1988). Human and bovine coronaviruses recognize sialic acid-containing receptors similar to those of influenza C viruses. *Proc Natl Acad Sci U S A, 85*(12), 4526-4529. doi: 10.1073/pnas.85.12.4526

Vlasova, A. N., Marthaler, D., Wang, Q., Culhane, M. R., Rossow, K. D., Rovira, A., . . . Saif, L. J. (2014). Distinct characteristics and complex evolution of PEDV strains, North America, May 2013-February 2014. *Emerg Infect Dis, 20*(10), 1620-1628. doi: 10.3201/eid2010.140491

Walls, A. C., Tortorici, M. A., Snijder, J., Xiong, X., Bosch, B. J., Rey, F. A., & Veesler, D. (2017). Tectonic conformational changes of a coronavirus spike glycoprotein promote membrane fusion. *Proc Natl Acad Sci U S A, 114*(42), 11157-11162. doi: 10.1073/pnas.1708727114

Wang, H., Yang, P., Liu, K., Guo, F., Zhang, Y., Zhang, G., & Jiang, C. (2008). SARS coronavirus entry into host cells through a novel clathrin- and caveolae-independent endocytic pathway. *Cell Res, 18*(2), 290-301. doi: 10.1038/cr.2008.15

Wang, J., Zhao, P., Guo, L., Liu, Y., Du, Y., Ren, S., . . . Wu, J. (2013). Porcine epidemic diarrhea virus variants with high pathogenicity, China. *Emerg Infect Dis, 19*(12), 2048-2049. doi: 10.3201/eid1912.121088

Wang, L. H., Rothberg, K. G., & Anderson, R. G. (1993). Mis-assembly of clathrin lattices on endosomes reveals a regulatory switch for coated pit formation. *J Cell Biol, 123*(5), 1107-1117. doi: 10.1083/jcb.123.5.1107

Wei, L., Sun, S., Xu, C. H., Zhang, J., Xu, Y., Zhu, H., . . . Gu, J. (2007). Pathology of the thyroid in severe acute respiratory syndrome. *Hum Pathol, 38*(1), 95-102. doi: 10.1016/j.humpath.2006.06.011

Weiner, L. P. (1973). Pathogenesis of demyelination induced by a mouse hepatitis. *Arch Neurol,*

*28*(5), 298-303. doi: 10.1001/archneur.1973.00490230034003

Weingartl, H., Czub, M., Czub, S., Neufeld, J., Marszal, P., Gren, J., . . . Cao, J. (2004). Immunization with modified vaccinia virus Ankara-based recombinant vaccine against severe acute respiratory syndrome is associated with enhanced hepatitis in ferrets. *J Virol, 78*(22), 12672-12676. doi: 10.1128/JVI.78.22.12672-12676.2004

Weiss, R. C., & Scott, F. W. (1981). Antibody-mediated enhancement of disease in feline infectious peritonitis: comparisons with dengue hemorrhagic fever. *Comp Immunol Microbiol Infect Dis, 4*(2), 175-189. doi: 10.1016/0147-9571(81)90003-5

White, J. M., & Whittaker, G. R. (2016). Fusion of Enveloped Viruses in Endosomes. *Traffic, 17*(6), 593-614. doi: 10.1111/tra.12389

Whitworth, K. M., Rowland, R. R. R., Petrovan, V., Sheahan, M., Cino-Ozuna, A. G., Fang, Y., . . . Prather, R. S. (2019). Resistance to coronavirus infection in amino peptidase N-deficient pigs. *Transgenic Res, 28*(1), 21-32. doi: 10.1007/s11248-018-0100-3

WHO. (2004). Summary of probably SARS cases with onset of illness from 1 November 2002 to 31 July 2003. WHO. from http://www.who.int/csr/sars/country/table2004_04_21/en/

WHO. (2020). Novel Coronavirus - China. from https://www.who.int/csr/don/12-january-2020-novel-coronavirus-china/en/

Wicht, O., Li, W., Willems, L., Meuleman, T. J., Wubbolts, R. W., van Kuppeveld, F. J., . . . Bosch, B. J. (2014). Proteolytic activation of the porcine epidemic diarrhea coronavirus spike fusion protein by trypsin in cell culture. *J Virol, 88*(14), 7952-7961. doi: 10.1128/JVI.00297-14

Widjaja, I., Wang, C., van Haperen, R., Gutiérrez-Álvarez, J., van Dieren, B., Okba, N. M., . . . Bosch, B. J. (2019). Towards a solution to MERS: protective human monoclonal antibodies targeting different domains and functions of the MERS-coronavirus spike glycoprotein *Emerg Microbes Infect* (Vol. 8, pp. 516-530).

Williams, R. K., Jiang, G. S., & Holmes, K. V. (1991). Receptor for mouse hepatitis virus is a member of the carcinoembryonic antigen family of glycoproteins. *Proc Natl Acad Sci U S A, 88*(13), 5533-5536. doi: 10.1073/pnas.88.13.5533

Winter, C., Schwegmann-Wessels, C., Cavanagh, D., Neumann, U., & Herrler, G. (2006). Sialic acid is a receptor determinant for infection of cells by avian Infectious bronchitis virus. *J Gen Virol, 87*(Pt 5), 1209-1216. doi: 10.1099/vir.0.81651-0

Wong, M. C., Javornik Cregeen, S. J., Ajami, N. J., & Petrosino, J. F. (2020). Evidence of recombination in coronaviruses implicating pangolin origins of nCoV-2019. *bioRxiv*, 2020.2002.2007.939207. doi: 10.1101/2020.02.07.939207

Wong, S. K., Li, W., Moore, M. J., Choe, H., & Farzan, M. (2004). A 193-amino acid fragment of the SARS coronavirus S protein efficiently binds angiotensin-converting enzyme 2. *J Biol Chem, 279*(5), 3197-3201. doi: 10.1074/jbc.C300520200

Woo, P. C., Lau, S. K., Lam, C. S., Lau, C. C., Tsang, A. K., Lau, J. H., . . . Yuen, K. Y. (2012). Discovery of seven novel Mammalian and avian coronaviruses in the genus deltacoronavirus supports bat coronaviruses as the gene source of alphacoronavirus and betacoronavirus and avian coronaviruses as the gene source of gammacoronavirus and deltacoronavirus. *J Virol, 86*(7), 3995-4008. doi: 10.1128/JVI.06540-11

Wood, E. N. (1977). An apparently new syndrome of porcine epidemic diarrhoea. *Vet Rec, 100*(12), 243-244. doi: 10.1136/vr.100.12.243

Wrapp, D., Wang, N., Corbett, K. S., Goldsmith, J. A., Hsieh, C.-L., Abiona, O., . . . McLellan, J. S. (2020). Cryo-EM structure of the 2019-nCoV spike in the prefusion conformation.

*Science*, eabb2507. doi: 10.1126/science.abb2507

Wu, K., Li, W., Peng, G., & Li, F. (2009). Crystal structure of NL63 respiratory coronavirus receptor-binding domain complexed with its human receptor. *Proc Natl Acad Sci U S A, 106*(47), 19970-19974. doi: 10.1073/pnas.0908837106

Wurm, T., Chen, H., Hodgson, T., Britton, P., Brooks, G., & Hiscox, J. A. (2001). Localization to the nucleolus is a common feature of coronavirus nucleoproteins, and the protein may disrupt host cell division. *J Virol, 75*(19), 9345-9356. doi: 10.1128/JVI.75.19.9345-9356.2001

Xu, M., Xia, M., Li, X. X., Han, W. Q., Boini, K. M., Zhang, F., . . . Li, P. L. (2012). Requirement of translocated lysosomal V1 H(+)-ATPase for activation of membrane acid sphingomyelinase and raft clustering in coronary endothelial cells. *Mol Biol Cell, 23*(8), 1546-1557. doi: 10.1091/mbc.E11-09-0821

Xu, X., Zhang, H., Zhang, Q., Huang, Y., Dong, J., Liang, Y., . . . Tong, D. (2013). Porcine epidemic diarrhea virus N protein prolongs S-phase cell cycle, induces endoplasmic reticulum stress, and up-regulates interleukin-8 expression. *Vet Microbiol, 164*(3-4), 212-221. doi: 10.1016/j.vetmic.2013.01.034

Yamada, Y., & Liu, D. X. (2009). Proteolytic activation of the spike protein at a novel RRRR/S motif is implicated in furin-dependent entry, syncytium formation, and infectivity of coronavirus infectious bronchitis virus in cultured cells. *J Virol, 83*(17), 8744-8758. doi: 10.1128/JVI.00613-09

Yamauchi, Y., & Helenius, A. (2013). Virus entry at a glance. *J Cell Sci, 126*(Pt 6), 1289-1295. doi: 10.1242/jcs.119685

Yan, F., Xia, D., Lv, S., Qi, Y., & Xu, H. (2010). Functional analysis of the orf390 gene of the white spot syndrome virus. *Virus Res, 151*(1), 39-44. doi: 10.1016/j.virusres.2010.03.014

Yan, H., Xiao, G., Zhang, J., Hu, Y., Yuan, F., Cole, D. K., . . . Gao, G. F. (2004). SARS coronavirus induces apoptosis in Vero E6 cells. *Journal of medical virology, 73*(3), 323-331. doi: 10.1002/jmv.20094

Yang, D., & Leibowitz, J. L. (2015). The structure and functions of coronavirus genomic 3' and 5' ends. *Virus Res, 206*, 120-133. doi: 10.1016/j.virusres.2015.02.025

Yang, H., Xie, W., Xue, X., Yang, K., Ma, J., Liang, W., . . . Rao, Z. (2005). Design of wide-spectrum inhibitors targeting coronavirus main proteases. *PLoS Biol, 3*(10), e324. doi: 10.1371/journal.pbio.0030324

Yang, H., Yang, M., Ding, Y., Liu, Y., Lou, Z., Zhou, Z., . . . Rao, Z. (2003). The crystal structures of severe acute respiratory syndrome virus main protease and its complex with an inhibitor. *Proc Natl Acad Sci U S A, 100*(23), 13190-13195. doi: 10.1073/pnas.1835675100

Yang, Z. Y., Werner, H. C., Kong, W. P., Leung, K., Traggiai, E., Lanzavecchia, A., & Nabel, G. J. (2005). Evasion of antibody neutralization in emerging severe acute respiratory syndrome coronaviruses. *Proc Natl Acad Sci U S A, 102*(3), 797-801. doi: 10.1073/pnas.0409065102

Yeager, C. L., Ashmun, R. A., Williams, R. K., Cardellichio, C. B., Shapiro, L. H., Look, A. T., & Holmes, K. V. (1992). Human aminopeptidase N is a receptor for human coronavirus 229E. *Nature, 357*(6377), 420-422. doi: 10.1038/357420a0

Ying, T., Li, W., & Dimitrov, D. S. (2016). Discovery of T-Cell Infection and Apoptosis by Middle East Respiratory Syndrome Coronavirus *J Infect Dis* (Vol. 213, pp. 877-879). United States.

Zaki, A. M., van Boheemen, S., Bestebroer, T. M., Osterhaus, A. D., & Fouchier, R. A. (2012). Isolation of a novel coronavirus from a man with pneumonia in Saudi Arabia. *N Engl J Med, 367*(19), 1814-1820. doi: 10.1056/NEJMoa1211721

Zeng, F., Chow, K. Y., Hon, C. C., Law, K. M., Yip, C. W., Chan, K. H., . . . Leung, F. C. (2004). Characterization of humoral responses in mice immunized with plasmid DNAs encoding SARS-CoV spike gene fragments. *Biochem Biophys Res Commun, 315*(4), 1134-1139. doi: 10.1016/j.bbrc.2004.01.166

Zhang, C. H., Lu, J. H., Wang, Y. F., Zheng, H. Y., Xiong, S., Zhang, M. Y., . . . Zhang, B. (2005). Immune responses in Balb/c mice induced by a candidate SARS-CoV inactivated vaccine prepared from F69 strain. *Vaccine, 23*(24), 3196-3201. doi: 10.1016/j.vaccine.2004.11.073

Zhang, H., Wang, G., Li, J., Nie, Y., Shi, X., Lian, G., . . . Deng, H. (2004). Identification of an antigenic determinant on the S2 domain of the severe acute respiratory syndrome coronavirus spike glycoprotein capable of inducing neutralizing antibodies. *Journal of Virology, 78*(13), 6938-6945. doi: 10.1128/JVI.78.13.6938-6945.2004

Zhang, L., Wei, L., Jiang, D., Wang, J., Cong, X., & Fei, R. (2007). SARS-CoV nucleocapsid protein induced apoptosis of COS-1 mediated by the mitochondrial pathway. *Artif Cells Blood Substit Immobil Biotechnol, 35*(2), 237-253. doi: 10.1080/10731190601188422

Zhang, Y., Mattjus, P., Schmid, P. C., Dong, Z., Zhong, S., Ma, W. Y., . . . Dong, Z. (2001). Involvement of the acid sphingomyelinase pathway in uva-induced apoptosis. *J Biol Chem, 276*(15), 11775-11782. doi: 10.1074/jbc.M006000200

Zhang, Z., Shen, L., & Gu, X. (2016). Evolutionary Dynamics of MERS-CoV: Potential Recombination, Positive Selection and Transmission. *Sci Rep, 6*, 25049. doi: 10.1038/srep25049

Zhao, J., Li, K., Wohlford-Lenane, C., Agnihothram, S. S., Fett, C., Zhao, J., . . . Perlman, S. (2014). Rapid generation of a mouse model for Middle East respiratory syndrome. *Proc Natl Acad Sci U S A, 111*(13), 4970-4975. doi: 10.1073/pnas.1323279111

Zhao, J., Wohlford-Lenane, C., Zhao, J., Fleming, E., Lane, T. E., McCray, P. B., Jr., & Perlman, S. (2012). Intranasal treatment with poly(I*C) protects aged mice from lethal respiratory virus infections. *J Virol, 86*(21), 11416-11424. doi: 10.1128/JVI.01410-12

Zhao, L., Jha, B. K., Wu, A., Elliott, R., Ziebuhr, J., Gorbalenya, A. E., . . . Weiss, S. R. (2012). Antagonism of the interferon-induced OAS-RNase L pathway by murine coronavirus ns2 protein is required for virus replication and liver pathology. *Cell Host Microbe, 11*(6), 607-616. doi: 10.1016/j.chom.2012.04.011

Zhao, P., Ke, J. S., Qin, Z. L., Ren, H., Zhao, L. J., Yu, J. G., . . . Qi, Z. T. (2004). DNA vaccine of SARS-Cov S gene induces antibody response in mice. *Acta Biochim Biophys Sin (Shanghai), 36*(1), 37-41. doi: 10.1093/abbs/36.1.37

Zheng, W., Kollmeyer, J., Symolon, H., Momin, A., Munter, E., Wang, E., . . . Merrill, A. H., Jr. (2006). Ceramides and other bioactive sphingolipid backbones in health and disease: lipidomic analysis, metabolism and roles in membrane structure, dynamics, signaling and autophagy. *Biochim Biophys Acta, 1758*(12), 1864-1884. doi: 10.1016/j.bbamem.2006.08.009

Zhou, J., Chu, H., Chan, J. F., & Yuen, K. Y. (2015). Middle East respiratory syndrome coronavirus infection: virus-host cell interactions and implications on pathogenesis. *Virol J, 12*, 218. doi: 10.1186/s12985-015-0446-6

Zhou, N., Pan, T., Zhang, J., Li, Q., Zhang, X., Bai, C., . . . Zhang, H. (2016). Glycopeptide Antibiotics Potently Inhibit Cathepsin L in the Late Endosome/Lysosome and Block the Entry of Ebola Virus, Middle East Respiratory Syndrome Coronavirus (MERS-CoV), and Severe Acute Respiratory Syndrome Coronavirus (SARS-CoV). *J Biol Chem, 291*(17), 9218-9232. doi: 10.1074/jbc.M116.716100

Zhou, P., Yang, X.-L., Wang, X.-G., Hu, B., Zhang, L., Zhang, W., . . . Shi, Z.-L. (2020). A pneumonia outbreak associated with a new coronavirus of probable bat origin. *Nature*. doi: 10.1038/s41586-020-2012-7

Zhou, Y., Vedantham, P., Lu, K., Agudelo, J., Carrion, R., Jr., Nunneley, J. W., . . . Simmons, G. (2015). Protease inhibitors targeting coronavirus and filovirus entry. *Antiviral Res, 116*, 76-84. doi: 10.1016/j.antiviral.2015.01.011

Zhu, M. S., Pan, Y., Chen, H. Q., Shen, Y., Wang, X. C., Sun, Y. J., & Tao, K. H. (2004). Induction of SARS-nucleoprotein-specific immune response by use of DNA vaccine. *Immunol Lett, 92*(3), 237-243. doi: 10.1016/j.imlet.2004.01.001

Zhu, N., Zhang, D., Wang, W., Li, X., Yang, B., Song, J., . . . Research, T. (2020). A Novel Coronavirus from Patients with Pneumonia in China, 2019. *N Engl J Med*, 10.1056/NEJMoa2001017. doi: 10.1056/NEJMoa2001017

Ziebuhr, J., Snijder, E. J., & Gorbalenya, A. E. (2000). Virus-encoded proteinases and proteolytic processing in the Nidovirales. *J Gen Virol, 81*(Pt 4), 853-879. doi: 10.1099/0022-1317-81-4-853

Zumla, A., Chan, J. F., Azhar, E. I., Hui, D. S., & Yuen, K. Y. (2016). Coronaviruses - drug discovery and therapeutic options. *Nat Rev Drug Discov, 15*(5), 327-347. doi: 10.1038/nrd.2015.37

Zuniga, S., Cruz, J. L. G., Sola, I., Mateos-Gomez, P. A., Palacio, L., & Enjuanes, L. (2010). Coronavirus Nucleocapsid Protein Facilitates Template Switching and Is Required for Efficient Transcription. *Journal of Virology, 84*(4), 2169-2175. doi: 10.1128/JVI.02011-09

Zuniga, S., Sola, I., Moreno, J. L., Sabella, P., Plana-Duran, J., & Enjuanes, L. (2007). Coronavirus nucleocapsid protein is an RNA chaperone. *Virology, 357*(2), 215-227. doi: 10.1016/j.virol.2006.07.046